**UNIVERSIDADE FEDERAL RURAL DE PERNAMBUCO**
**PRÓ-REITORIA DE PESQUISA E PÓS-GRADUAÇÃO**
**PROGRAMA DE PÓS-GRADUAÇÃO EM RECURSOS PESQUEIROS E AQUICULTURA**

# ESTRUTURA ESPACIAL DO ESPADARTE E DISTRIBUIÇÃO ESPAÇO-TEMPORAL POR SEXO DO ESPADARTE E DA ALBACORA-BANDOLIM CAPTURADOS PELA FROTA BRASILEIRA DE ESPINHEL PELÁGICO NO ATLÂNTICO SUDOESTE

**Silvaneide Luzinete Rodrigues**

Tese apresentada ao Programa de Pós-Graduação em Recursos Pesqueiros e Aquicultura da Universidade Federal Rural de Pernambuco como exigência para obtenção do título de Doutor.

**Prof. Dr. Humber Agrelli de Andrade**
Orientador

**Recife,**
**Agosto/2024**

Dados Internacionais de Catalogação na Publicação
Sistema Integrado de Bibliotecas da UFRPE
Bibliotecário(a): Auxiliadora Cunha – CRB-4 1134

R696e Rodrigues, Silvaneide Luzinete.
Estrutura espacial do espadarte e distribuição espaço-temporal por sexo do Espadarte e da Albacora-bandolim capturados pela frota brasileira de espinhel pelágico no atlântico sudoeste / Silvaneide Luzinete Rodrigues. – Recife, 2024.
112 f.; il.

Orientador(a): Humber Agrelli de Andrade.

Tese (Doutorado) – Universidade Federal Rural de Pernambuco, Programa de Pós-Graduação em Recursos Pesqueiros e Aquicultura, Recife, BR-PE, 2024.

Inclui referências e anexo(s).

1. Atum . 2. Atum - Dinâmica populacional. 3. Geoestatística. 4. Autocorrelação Espacial 5. Peixes - Populações. I. Andrade, Humber Agrelli de, orient. II. Título

CDD 639.3

**UNIVERSIDADE FEDERAL RURAL DE PERNAMBUCO**
**PRÓ-REITORIA DE PESQUISA E PÓS-GRADUAÇÃO**
**PROGRAMA DE PÓS-GRADUAÇÃO EM RECURSOS PESQUEIROS E AQÜICULTURA**

ESTRUTURA ESPACIAL DO ESPADARTE E DISTRIBUIÇÃO ESPAÇO-TEMPORAL POR SEXO DO ESPADARTE E DA ALBACORA-BANDOLIM CAPTURADOS PELA FROTA BRASILEIRA DE ESPINHEL PELÁGICO NO ATLÂNTICO SUDOESTE

**Silvaneide Luzinete Rodrigues**

Tese julgada adequada para obtenção do título de doutor em Recursos Pesqueiros e Aquicultura. Defendida e aprovada em 26/08/2024 pela seguinte Banca Examinadora.

---

**Prof. Dr.Humber Agrelli de Andrade**
Orientador
Depaq/UFRPE

---

**Prof. Dr. Paulo Guilherme V. de Oliveira**
Membro interno
Depaq/UFRPE

---

**Profa. Dra. Ilka Siqueira Lima Branco Nunes**
Membro externo
Depaq/UFRPE

---

**Profa. Dra. Natalia Priscila Alves Bezerra**
Membro externo
CCHN / UFES

---

**Prof. Dr. Marcelo Francisco de Nóbrega**
Menbro externo
Docean /UFPE

# Dedicatória

Dedico esta tese a todos os visionários e incansáveis pesquisadores que, com paixão e determinação, se empenham na preservação dos recursos aquáticos. Que seu trabalho inspire gerações presentes e futuras a valorizar e proteger nosso patrimônio natural, garantindo um legado sustentável e próspero para todos.

## Agradecimentos

Primeiramente, agradeço a Deus, que iluminou meu caminho durante toda essa caminhada, permitindo que os obstáculos fossem superados e que eu alcançasse esta realização. Sua presença constante foi a fonte de minha força e perseverança.

À minha família, meu alicerce, sem a qual eu não teria tido a força para prosseguir nessa longa jornada. Em especial, agradeço à minha mãe, Luzinete Rodrigues, e ao meu pai, José Antônio Rodrigues (em memória), por seu amor incondicional e apoio inabalável. Vocês são minha inspiração diária. Agradeço também às minhas irmãs, Silvana Rodrigues e Suzana Silva, por sempre compartilharem das minhas aflições e celebrarem minhas superações. A união e o carinho de vocês foram fundamentais para a conclusão deste trabalho.

Sou profundamente grato a todos os professores que tiveram paciência e dedicação para me ajudar a concluir esta tese. Em especial, agradeço ao meu orientador, Humber Agrielli de Andrade, cuja competência e conhecimento guiaram-me pelo caminho da aprendizagem. Sua orientação foi crucial para o desenvolvimento deste trabalho.

Agradeço à coordenação do curso de Engenharia de Pesca, ao diretor do Departamento de Pesca e Aquicultura, e a todos os funcionários da Universidade Federal Rural de Pernambuco (UFRPE), que proporcionaram um ambiente propício para o meu crescimento acadêmico e profissional.

Minha gratidão se estende também aos amigos e colegas de laboratório, que me apoiaram e me deram força para concluir e defender esta tese. Entre eles, agradeço a Ana Júlia, Vivian, Matheus, Lucas, Vinícius, Marcela, Yury, Yasmim e Douglas. A amizade e o companheirismo de vocês foram inestimáveis, e pretendo levar esses laços preciosos para toda a vida.

Este trabalho é fruto de um esforço coletivo, e a todos que, de alguma forma, contribuíram para a realização deste sonho, deixo aqui o meu mais sincero agradecimento. Juntos, superamos desafios e celebramos conquistas, e por isso, sou eternamente grata.

## Resumo

A pesca de espécies marinhas altamente migratórias, como o espadarte (*Xiphias gladius*) e a albacora-bandolim (*Thunnus obesus*), apresenta desafios significativos para a conservação e gestão sustentável dos estoques pesqueiros. Estas espécies são ecologicamente essenciais nos ecossistemas marinhos e economicamente valiosas para a pesca comercial. No entanto, avaliar suas populações e implementar estratégias eficazes de manejo é complexo devido à natureza migratória dessas espécies, variabilidade ambiental e impacto das atividades de pesca. Nesta tese, investigamos a dinâmica espacial do espadarte e da albacora-bandolim utilizando dados de captura da frota brasileira de espinhel pelágico. A tese é dividida em dois artigos, cada um com objetivos específicos. No primeiro artigo, buscamos criar um índice de abundância para espécies migratórias. Desenvolvemos um protocolo de análise em três etapas: primeiro, modelar a taxa de captura considerando variáveis que afetam a capturabilidade; segundo analisar os resíduos para identificar autocorrelação; e terceiro, aplicar um algoritmo recursivo ponderado por área para considerar a autocorrelação espacial anual. Aplicamos este procedimento a dados de captura de espadarte pela frota brasileira de espinhel pelágico. Os resultados mostraram maiores valores de dependência espacial em 2005, 2008, 2012 e 2014 (456 km, 111 km, 80 km e 443 km, respectivamente) e menores em 2011 e 2013 (média de 15,45 km). Além disso, observamos uma tendência de declínio na abundância do espadarte entre 2010 e 2017, detectada antes pelos índices propostos do que pelos índices convencionais. Esses resultados sugerem que os índices alternativos oferecem uma visão potencialmente mais precisa da dinâmica populacional do espadarte no Atlântico Sul, enfatizando a importância de múltiplas abordagens na avaliação da abundância de espécies marinhas. O segundo capítulo investigou a distribuição espacial entre os sexos do espadarte e da albacora-bandolim, abordando uma lacuna crítica na conservação e gestão sustentável dos estoques pesqueiros. Utilizando dados da frota brasileira de espinhel pelágico (PROBORDO), analisou-se 272.048 registros de pesca entre 2005 e 2011. Os resultados indicam que as proporções de fêmeas de espadarte foram significativamente maiores no setor sul do Brasil, com a proporção geral de fêmeas atingindo 41,5%, enquanto os machos predominaram no setor equatorial oeste. O comprimento do espadarte variou de 150 cm em 2007 (o maior valor) a 137 cm em 2009, com uma tendência geral de maior presença de fêmeas nas classes de tamanho superior a 180 cm. Por outro lado, a albacora-bandolim apresentou uma predominância de capturas de machos ao longo de toda a área de estudo, com exceção de 2006, quando a proporção de fêmeas aumentou em regiões tropicais específicas. A variação média de comprimento da albacora-bandolim oscilou entre 200 cm e 250 cm, com uma proporção de fêmeas que variou de 25% a 87%, sendo predominante nas classes de comprimento em torno de 200 cm. Essas dinâmicas de captura refletem influências ecológicas e comportamentais, além de práticas de pesca específicas, ressaltando a necessidade de estratégias de gestão adaptadas para a sustentabilidade das populações na região. Ao integrar dados espaciais e temporais com abordagens analíticas múltiplas, os resultados deste estudo fornecem informações valiosas para a conservação e manejo dessas importantes espécies marinhas, contribuindo para a implementação de estratégias de gestão mais eficazes e sustentáveis.


**Palavras-chave:** Atum e Espécies Afins**,** Dinâmica Populacional, Geoestatística, Autocorrelação Espacial, Conservação Marinha, Estratificação Sexual.

## Abstract

Fishing for highly migratory marine species, such as swordfish (*Xiphias gladius*) and bigeye tuna (*Thunnus obesus*), presents significant challenges for the conservation and sustainable management of fish stocks. These species are ecologically essential in marine ecosystems and economically valuable for commercial fishing. However, assessing their populations and implementing effective management strategies is complex due to the migratory nature of these species, environmental variability, and the impact of fishing activities. In this thesis, we investigate the spatial dynamics of swordfish and bigeye tuna using catch data from the Brazilian pelagic longline fleet. The thesis is divided into two articles, each with specific objectives. In the first article, we aim to create an abundance index for migratory species. We developed a three-step analysis protocol: first, model the catch rate considering variables that affect catchability; second, analyze the residuals to identify autocorrelation; and third, apply a recursive area-weighted algorithm to account for annual spatial autocorrelation. We applied this procedure to swordfish catch data from the Brazilian pelagic longline fleet. The results showed higher values of spatial dependence in 2005, 2008, 2012, and 2014 (456 km, 111 km, 80 km, and 443 km, respectively) and lower values in 2011 and 2013 (average of 15.45 km). Additionally, we observed a declining trend in swordfish abundance between 2010 and 2017, detected earlier by the proposed indices than by conventional indices. These results suggest that alternative indices offer a potentially more accurate view of the population dynamics of swordfish in the South Atlantic, emphasizing the importance of multiple approaches in assessing the abundance of marine species. The second chapter investigated the spatial distribution between the sexes of swordfish and bigeye tuna, addressing a critical gap in the conservation and sustainable management of fish stocks. Using data from the Brazilian pelagic longline fleet (PROBORDO), we analyzed 272,048 fishing records between 2005 and 2011. The results indicate that the proportions of female swordfish were significantly higher in the southern sector of Brazil, with the overall proportion of females reaching 41.5% (95% CI: 39.7% to 43.5%), while males predominated in the western equatorial sector. Swordfish median fork length ranged from 150 cm in 2007 (the highest value) to 137 cm in 2009, with a general trend of a greater presence of females in size classes above 180 cm. On the other hand, bigeye tuna showed a predominance of males throughout the study area, except in 2006, when the proportion of females increased in specific tropical regions. The average length of bigeye tuna ranged between 200 cm and 250 cm, with the proportion of females varying from 25% to 87%, predominantly in the length classes around 200 cm. These capture dynamics reflect ecological and behavioral influences, as well as specific fishing practices, highlighting the need for adapted management strategies for population sustainability in the region. By integrating spatial and temporal data with multiple analytical approaches, the results of this study provide valuable information for the conservation and management of these important marine species, contributing to the implementation of more effective and sustainable management strategies.

**Keywords**: Tuna and Related Species, Population Dynamics, Geostatistics, Spatial Autocorrelation, Marine Conservation, Sexual Stratification.

## Lista de figuras



## Artigo 1



## Artigo 2

## Lista de tabelas

### Artigo 1 Página



### Artigo 2

## Sumário

# 1. INTRODUÇÃO

A avaliação de estoque de espécies marinhas é uma ferramenta fundamental para o manejo sustentável dos recursos pesqueiros. Trata-se de um processo científico que visa estimar o tamanho e a dinâmica populacional de uma determinada espécie, considerando fatores como taxa de mortalidade, recrutamento, crescimento, estrutura espacial do estoque, esfoço de pesca  e captura (HILBORN & WALTERS, 1992; QUINN, 1999; HADDON, 2001; GEBREMEDHIN et al., 2021). Através dessa abordagem, é possível determinar a saúde e a capacidade de recuperação do estoque, além de identificar se a exploração atual está dentro de limites sustentáveis(GEBREMEDHIN et al., 2021; RAZA et al., , 2013). A importância da avaliação de estoque reside na sua capacidade de fornecer subsídios técnicos para a implementação de medidas de manejo que garantam a exploração responsável dos recursos marinhos, prevenindo o colapso de populações e assegurando a disponibilidade do recurso para gerações futuras (RAZA et al., , 2013).

Na maioria das avaliações de estoques convencionais, são utilizados modelos baseados em dados de captura e esforço da pesca comercial (HILBORN & WALTERS, 1992; CAMPBELL, 2016; XU et al., 2018). Para a execução desses modelos, é necessário o uso de um índice de abundância relativa, como Captura por Unidade de Esforço (CPUE). Esses índices são gerados por meio de ferramentas estatísticas, como os Modelos Lineares Generalizados (GLM) e suas variantes, incluindo modelos lineares generalizados de efeitos mistos, árvores de regressão e modelos aditivos generalizados (MCCULLAGH & NELDER, 1989; MAUNDER & PUNT, 2004; THORSON et al., 2016; PUNT et al., 2019).

As avaliações de estoque são utilizadas em uma ampla gama de unidades de gestão pesqueira (CADRIN, 2020), geralmente sob a suposição de que os organismos estão distribuídos no espaço de forma homogênea e sem conectividade com outras populações ou estoques. No entanto, essa suposição não se aplica à maioria dos animais aquáticos (THORSON et al., 2016; CAMPBELL, 2016; BERGER et al., 2017; CADRIN et al., 2020). Além disso, a concentração de embarcações pesqueiras nas mesmas áreas de pesca ocasiona autocorrelação nos dados disponíveis para a estimação dos índices de abundância relativa, comprometendo, assim, boa parte dos modelos de avaliações de estoques (MAUNDER & PUNT, 2004; WANG et al., 2015; CAMPBELL, 2016; XU et al., 2018).

A distribuição espacial de uma espécie e como ela muda ao longo do tempo pode

ser particularmente informativa sobre como a população responde à pressão pesqueira e às condições ambientais (BERGER et al., 2017; CADRIN et al., 2020). Além disso, o conhecimento sobre interações interespecíficas, como a co-ocorrência ou repulsão de espécies obtido com base na análise de suas distribuições espaciais, pode ajudar a entender os processos de competição e auxiliar na implementação de medidas de manejo ecossistêmico (MORFIN et al., 2012; SARAUX et al., 2014). Embora muitos trabalhos sobre pesca se concentrem em uma única espécie, há uma crescente percepção de que o manejo deve incluir considerações sobre interações entre espécies e entre essas espécies e seu ambiente (JENSEN et al., 2012).

As estruturas espaciais dos estoques pesqueiros, principalmente de espécies oceânicas migratórias, são atualmente uma das maiores fontes de incerteza, sendo consideradas um grande desafio nas avaliações de estoques (BERGER et al., 2017; CADRIN et al., 2020). Ignorar ou especificar inadequadamente a estrutura espacial da população nos modelos de avaliação e na gestão da pesca pode resultar em sobrepesca ou colapso do estoque (CADRIN et al., 2020). Portanto, são recomendados estudos que visem o desenvolvimento de métodos que possam melhorar e possibilitar a integração da representação do escopo espacial aos modelos de avaliação (CADRIN, 2020).

A dinâmica espaço-temporal das espécies pode ser investigada por meio da utilização de indicadores espaciais e de geoestatística, que permitem avaliar como as espécies ocupam o espaço, o que está relacionado à abundância. A relação entre índices de ocupação e de abundância é amplamente utilizada em estudos de macroecologia (Reuchlin-Hugenholtz, 2015; Rufino et al., 2018, 2019), mas é pouco frequente no manejo de espécies oceânicas migratórias, incluindo as de interesse comercial (HURTADO-FERRO et al., 2014). Exemplos incluem o espadarte (*Xiphias gladius*) e a albacora-bandolim (*Thunnus obesus*) (BORNATOWSKI et al., 2018; ERAUSKIN-EXTRAMIANA et al., 2019), espécies cujos estoques estão em grande parte sobrepescados ou explorados em seu limite máximo sustentável (ICCAT, 2024; FAO, 2022).

Diante do exposto, no presente trabalho se propõe investigar a estrutura espacial do espadarte e da albacora-bandolim, para os quais se dispões de dados da pesca de espinhel pelágico no Sudoeste do Atlântico. A tese é dividida em dois artigos, cada um com objetivos específicos e abordagens metodológicas distintas. O primeiro artigo tem como objetivo desenvolver um protocolo de análise em três etapas para estimar índices relativos de abundância do espadarte a partir de dados comerciais de pesca. Em adição, o índice de

abundância alternativo com base na autocorrelação especial será comparado com os índices oficiais fornecido pelo governo brasileiro a International Commission for the Conservation of Atlantic Tunas-ICCAT. O entendimento da distribuição e da variabilidade espaço-temporal de adensamentos dos exemplares destes estoques deve ajudar na interpretação dos dados de pesca comercial, e consequentemente nas futuras tomadas de decisões, contribuindo, desta forma, para o manejo adequado destes estoques e de pescarias a eles relacionadas.

O segundo artigo visa analisar os padrões de distribuição espacial entre os sexos do espadarte e da albacora-bandolim, com foco nas diferenças de distribuição sexual e suas implicações para a gestão das pescarias. A tese visa fornecer uma compreensão detalhada das dinâmicas espaciais do espadarte e da albacora-bandolim no Atlântico Sudoeste, contribuindo para a implementação de estratégias de gestão mais eficazes e sustentáveis. Ao considerar múltiplas abordagens analíticas e integrar dados espaciais e temporais, espera-se que os resultados deste estudo ofereçam informações valiosas para a conservação e manejo dessas importantes espécies marinhas.

## 1.1. OBJETIVOS

### *1.1.1. Objetivo geral*

Analisar a dinâmica espaço-temporal dos adensamentos e fragmentações dos estoques do espadarte e da albacora-bandolim capturados pela frota brasileira de espinhel pelágico no Sudoeste do Atlântico.

### *1.1.2. Objetivos específicos*

Artigo 1:

- Analisar a relação de dependência espacial dos dados de CPUE oriundos da frota comercial de espinhel pelágico;
- Investigar variações nos padrões de distribuições espaciais dos adensamentos ao longo dos anos;
- Quantificar e medir o número de adensamentos de espadarte ao longo da área de estudo;
- Avaliar a possibilidade de estimar índices anuais de abundância relativa, com base em análise do número e tamanho de adensamentos;
- Comparar a taxa de captura padronizada alternativa do espadarte, com os índices de abundâncias oficiais do governo brasileiro, enviados a ICCAT.

Artigo 2:

- Examinar a distribuição espacial de machos e fêmeas de espadarte e albacora-bandolim;
- Avaliar a sobreposição espacial entre as duas espécies investigadas;
- Avaliar como esses padrões de distribuição espacial podem influenciar as estratégias de manejo e conservação.

## 1.2. REFERENCIAL TEORICO

### *1.2.1 Espinhel pelágico*

O espinhel é um dispositivo de pesca projetado para capturar peixes pelágicos ou demersais (MONTEALEGRE-QUIJANO, 2011). Desenvolvido no século XX, logo após a Segunda Guerra Mundial (ÁVILA-DA-SILVA & VAZ-DOS-SANTOS, 2000), este equipamento de pesca consiste geralmente de uma linha principal da qual partem várias linhas secundárias, cada uma equipada com anzóis em suas extremidades. Ao tentar se alimentar da isca, os animais são fisgados ou ficam em suas linhas (WATSON & KERSTETTER, 2006). O espinhel pode ser classificado quanto à sua estrutura como fixo ou de deriva, e quanto à sua posição em vertical ou horizontal, bem como em relação à profundidade, superficial ou de fundo (MONTEALEGRE-QUIJANO, 2011).

A pesca com espinhel horizontal é voltada principalmente para a captura de espécies como os atuns, espadarte e tubarões (POISSON et al., 2019), utilizando uma linha principal de mono e polifilamento que pode se estender por até 110km, dependendo do tipo de embarcação. Por outro lado, o espinhel vertical se diferencia do horizontal por possuir um flutuador com sinalizador em uma extremidade da linha principal e um peso na outra extremidade, responsável por manter a linha principal esticada verticalmente (COLUCHI et al., 2005; MONTEALEGRE-QUIJANO, 2011). Este tipo de arte de pesca é indicado para a captura de peixes recifais, como pargo e garoupa (MONTEALEGRE-QUIJANO, 2011).

No Brasil, o modelo de espinhel pelágico utilizado pela frota é caracterizado por sua profundidade operacional e técnicas de pesca específicas, adaptadas para capturar uma diversidade de espécies. Operando predominantemente no Atlântico Sudoeste, essa prática visa atingir espécies como atuns, espadarte e tubarões em profundidades que variam de acordo com as espécies-alvo e a temperatura da água, otimizando as taxas de captura (MAFRA et al., 2019).

<u>Tipos de Espinhel Pelágico no Brasil</u>

1. **Espinhel Pelágico Chinês**: Comum nas frotas de Recife/PE, caracteriza-se por uma linha principal composta por cabos de monofilamento e multifilamentares. Linhas secundárias,

boias e radio-boias são adicionadas a cada 5 a 6 linhas secundárias, com espaçamento de aproximadamente 30 metros entre elas, totalizando comprimentos de 20 a 25 metros. O anzol utilizado é o tipo "tuna hook" e as principais iscas são o *milk-fish* e a cavalinha (*Scomber japonicus*). A operação de imersão ocorre durante o dia, com o recolhimento à noite (COLUCHI et al., 2005).

2. **Espinhel Pelágico Modelo Itaipava**: Utilizado principalmente para a captura do dourado, apresenta uma linha principal de nylon multifilamentar que pode alcançar até 5 milhas náuticas de comprimento. As boias de isopor, sem cabos de sustentação, suportam anzóis do tipo J, com iscas compostas por fragmentos de peixes. Todo o ciclo de imersão e emersão ocorre durante o dia (COLUCHI et al., 2005).
3. **Espinhel Pelágico Americano Norte e Nordeste**: Direcionado principalmente para atuns, espadarte e tubarões, este modelo utiliza uma linha principal de nylon monofilamentar, com até 65 milhas náuticas de comprimento, operada por um tambor hidráulico. As boias são dispostas entre 4 e 8 linhas secundárias, espaçadas em cerca de 60 metros. A isca predominante é a lula, e as operações se iniciam à noite, prolongando-se até a manhã seguinte (COLUCHI et al., 2005).
4. **Espinhel Pelágico Americano Sul-Sudeste**: Semelhante ao modelo anterior, diferencia-se pela diversidade de iscas, incluindo lulas e outros peixes, e pelo tipo de anzol usado, que é do tipo J 9/0. Essa modalidade é adaptada para capturas em diferentes profundidades e espécies (COLUCHI et al., 2005).

### *1.2.2 Desenvolvimento da Pesca de Espinhel Pelágico no Brasil*

A pesca de espinhel pelágico teve seu início no Brasil em 1956, por pescadores de navios asiáticos baseados no porto do Recife, nordeste do país (HAZIN et al., 1998; MENESES DE LIMA et al., 2000). Operando com cabos principais de nylon multifilamento, as primeiras incursões pesqueiras entre junho e julho daquele ano resultaram em capturas por unidade de esforço médias de 7,7 peixes por 100 anzóis, predominando albacora laje e albacora branca, o que evidenciou um considerável potencial pesqueiro (LEE, 1957). No entanto, em 1964, motivos de ordem econômica levaram à interrupção das atividades da frota, resultando em um declínio na captura de atuns e espécies associadas (MENESES DE LIMA et. al., 2000).

A retomada da pesca com espinhel pelágico no Brasil ocorreu em 1967, com a entrada em operação dos primeiros navios nacionais, em paralelo ao arrendamento de embarcações estrangeiras (SUDEPE, 1983). Inicialmente centradas no porto de Santos, as embarcações nacionais logo migraram para o Rio de Janeiro, refletindo uma tendência de concentração geográfica da atividade pesqueira (IBAMA, 1985). A década de 1980 testemunhou a expansão da pesca de espinhel pelágico, com o surgimento de embarcações menores no nordeste do Brasil, as

quais adotaram tecnologias adaptadas das embarcações japonesas arrendadas (HAZIN et al., 1998; MENEZES DE LIMA et. al., 2000).

Um marco significativo ocorreu na metade da década de 1990, com o arrendamento de uma embarcação norte-americana, que desencadeou mudanças substanciais na frota nacional. Houve a transição do uso do espinhel pelágico de multifilamento japonês para o monofilamento, além da adoção de atratores luminosos (HAZIN et al., 2002). Essas transformações resultaram em uma mudança no alvo principal da pesca, deslocando-se dos atuns para o espadarte (ARFELLI, 1996; HAZIN et al., 2002).

Concomitantemente ao desenvolvimento da frota nacional, ocorreram arrendamentos de embarcações de diversas bandeiras, com períodos de permanência e atuação variáveis. A composição da frota, os alvos de pesca e as tecnologias empregadas demonstraram grande variabilidade ao longo das décadas (MOURATO, 2007; MOURATO et al., 2011; RODRIGUES et al., 2020). Os registros históricos revelam um cenário complexo, caracterizado por uma diversidade de bandeiras, espécies-alvo, tecnologias e estratégias de pesca sendo empregadas pela frota brasileira.

Em síntese, o desenvolvimento da pesca de espinhel pelágico no Brasil foi marcado por uma série de transformações influenciadas por fatores econômicos, tecnológicos e ambientais. O panorama atual reflete a capacidade adaptativa da indústria pesqueira brasileira diante das exigências do mercado e das regulamentações governamentais, visando garantir a sustentabilidade a longo prazo dessa atividade crucial.

### *1.2.3 Espardate (Xiphias gladius)*

O espadarte (Figura 1) é uns dos principais recursos pesqueiros, junto com os atuns e tubarões (FAO, 2022; ERAUSKIN-EXTRAMIANA et al., 2019). Tal espécies faz parte da ordem dos perciliformes, sendo o único organismo da família xiphiidae a fazer parte do grupo econômico dos atuns e afins. Esses animais são cosmopolítica, habitando as zonas tropical e temperada dos oceanos atlântico, índico e pacíficos, além dos mares tropicais e temperado do planeta (Mar Báltico, Mar Mediterrâneo, Mar de Mármara, Mar Negro, Mar de Azov e Mar Vermelho) (NAKAMURA,1985**)**.

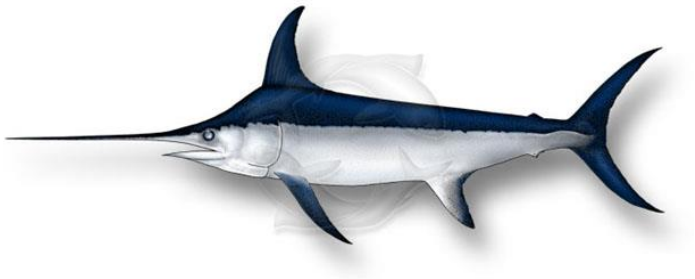

Figura 1. *Xiphias gladius* by Fishpics

Conhecidos também como Swordfish (nome popular em inglês) se deferência dos demais agulhões, pelo seu alto poder de osmorregulação térmica, tolerando faixas de temperatura entre 5°C-27°C (NAKAMURA,1985**)** e profundidade em torno de 0-800m (COLLETTE, 1995**)**. Essa ampla tolerância a diferentes temperaturas, possibilitaram habitar águas oceânicas do mundo inteiro (cosmopolita) e também é responsável pelo seu deslocamento vertical (GARCÍA, 2007). No entanto são geralmente encontrados em faixa de temperaturas acima de 18° C e profundidades inferiores a 550m **(**NAKAMURA,1985**),** sendo mais abundante entre os primeiros 100m durante a noite e 510m de profundidade no período diurno (HAZIN, 2006).

A temperatura oceanográfica desempenha papel importantíssimo na distribuição e migrações dos *X. gladius* (REY, 1988; PALKO et al., 1981 , AROCHA, 1997 , MEJUTO & GARCÍA-CORTÉS, 2014 ), Segundo García (2007) apesar desses animais fisiologicamente manterem a temperatura corporal superior ao ambiente externo, seu sistema de compensação térmica não é tão eficiente quantos os dos tunídeos, fazendo com que ester apresente uma distribuição espaço-temporal fortemente influência pelos fatores físicos químicos das massas d´aguas que o rodeiam. Essa dependência é fortemente associada aos níveis de biomassa dos indivíduos, ou seja, quanto menor o peso corporal maior o nível de dependência (GARCÍA, 2007). Em outras palavras, animais menores tendem a permanecerem em águas mais quente, enquanto os maiores possuem probabilidade de migração mais elevadas em águas com temperaturas menores.

Com relação idade e crescimento, há uma diferencia significativa entre os sexos, sendo em geral, as fêmeas com maiores valores de comprimento em relação aos machos (TAYLOR E MURPHY, 1992; TSERPES et al., 2008; SUN et al., 2002; ABID et al., 2019), os machos geralmente atingem a maturidade sexual em aproximadamente 2 a 3 anos de idade, correspondendo a um comprimento total de cerca de 95 cm (ABID et al., 2019). Em contraste, as fêmeas amadurecem mais tarde, em torno de 4 a 5 anos, em

comprimentos de aproximadamente 170 cm (ABID et al., 2019; ALIÇLI et al., 2012). A temporada de desova do espadarte ocorre de junho a setembro, com as fêmeas produzindo cerca de 17,5 milhões de ovos anualmente (HATZONIKOLAKIS et al., 2020). Essas características colaboram com a hipótese de dependência desses animais com a variáveis ambientais, no qual se nota que geralmente os grandes migradores são compostos por fêmeas que fazem grandes deslocamento durante a época de reprodução quanto na busca de alimento já os machos menos ativos, preferindo zonas mais quentes.

Outra característica importante refere-se a sua alimentação, esta é extremamente variada e pouco seletiva quanto o tamanho da presa, composta basicamente de pequenos peixes pelágicos, como carapau, barracudinha, pescada preta, cantarrilo, arenque, etc (NAKAMURA,1985; TIBBO et al., 1961; STILLWELL & KOHLER, 1985). Além de invertebrados, como crustáceos e cefalópodes, as lulas se destacam como as principais iscas utilizadas na captura do Xiphiidae nas regiões tropicais e equatoriais do Atlântico (AMORIM et al., 2015; GILMAN et al., 2020).

### *1.2.4 Albacora-Bandolim(Thunnus obesus)*

A albacora-bandolim (Figura 2) é uma espécie de atum altamente valorizada tanto comercial quanto ecologicamente nos oceanos ao redor do mundo (FAO, 2022; Erauskin-Extramiana et al., 2019). Pertencente à família Scombridae, esta espécie distingue-se dos outros atuns por seu corpo robusto, fusiforme e ligeiramente comprimido lateralmente. Segundo Collette (1995), O primeiro arco branquial possui entre 23 e 31 rastros branquiais. As barbatanas dorsais são separadas por um estreito espaço, com a segunda dorsal seguida por 8 a 10 pequenas barbatanas, enquanto a barbatana anal é acompanhada por 7 a 10 barbatanas. As nadadeiras peitorais são moderadamente longas, representando de 22 a 31% do comprimento furcal em exemplares grandes, podendo ser tão longas quanto as de *Thunnus alalunga* em exemplares menores. Entre as nadadeiras pélvicas, há dois processos interpélvicos. As escamas do corpo são muito pequenas, com um espartilho de escamas maiores e mais grossas, embora não muito distinto. O pedúnculo caudal é delgado, com uma quilha lateral forte entre duas quilhas menores. A superfície ventral do fígado é estriada e a espécie possui bexiga natatória (COLLETTE, 2001, 1995).

Em termos de coloração, o dorso da albacora-bandolim é azul escuro metálico, enquanto as laterais inferiores e o ventre são esbranquiçados (MIYAKE, 1990). Em espécimes vivos, uma faixa lateral azul iridescente percorre os lados do corpo. A primeira

barbatana dorsal é de um amarelo profundo, enquanto a segunda barbatana dorsal e a anal são de um amarelo claro. As demais barbatanas são de um amarelo brilhante, com bordas pretas (COLLETTE, 2001).

Figura 2. *Thunnus obesus* , *by CAFS*

A espécie possui uma distribuição ampla em todos os oceanos entre 45º N e 40º S, podendo atingir até 230 cm de comprimento e 250 kg de peso (COLLETTE & NAUEN, 1983; CAYRÉ et al., 1993). Habita águas quentes dos oceanos Atlântico, Índico e Pacífico, sendo altamente valorizada no mercado asiático, onde é consumida fresca como sashimi (HANAMOTO, 1987; SUN et al., 2001).

Os padrões de maturação variam entre os sexos e conforme a localização geográfica (SU et al., 2001; SCHAEFER et al., 2005). O tamanho em que 50% dos indivíduos atingem a maturidade sexual (L50) varia entre 94 cm e 139,92 cm, com diferenças entre regiões que refletem as pressões ambientais e de pesca. No Oceano Pacífico Oriental, as fêmeas amadurecem em comprimentos entre 102 cm e 125 cm, com um L50 estimado em 124,08 cm (GUOPING et al., 2011). No Oceano Atlântico Tropical, onde a frota brasileira opera, as fêmeas atingem a maturidade sexual em torno de 117,7 cm (GUOPING et al., 2011). No Oceano Índico Centro-Ocidental, a maturidade é observada em 110 cm, enquanto no Oceano Pacífico Tropical, o comprimento mínimo registrado é de 94 cm, com L50 de 107,8 cm (ZHU et al., 2010). Além disso, a albacora-bandolim possui um padrão reprodutivo caracterizado por uma temporada de desova prolongada, ocorrendo de março a novembro, com as fêmeas apresentando múltiplas desovas e uma fecundidade de lote considerável, variando de 0,84 a 8,56 milhões de ovos (SUN et al., 2013).

Em relação à alimentação, a albacora-bandolim é um predador oportunista, se alimentando principalmente de peixes pelágicos, como sardinhas, cavalas e lulas(COLLETTE, 1995; CAMPELLO et al., 2022). Sua dieta varia sazonalmente e geograficamente, dependendo da disponibilidade de presas em diferentes regiões de seu habitat (COLLETTE, 1995).

### *1.2.5 Estoque Pesqueiro do Espadarte e da Albacora-Bandolim*

A gestão dos estoques pesqueiros de espadarte e albacora-bandolim é frequentemente conduzida por Organizações Regionais de Gestão Pesqueira (ORGP), devido à natureza cosmopolita dessas espécies e sua ampla distribuição oceânica (CULLIS-SUZUKI & PAULY, 2010; HAAS et al., 2020). Em geral, essas organizações visam estabelecer medidas de conservação e manejo sustentável da pesca (MOONEY-SEUS & ROSENBERG, 2007). Atualmente, existem 18 ORGPs com mandatos para estabelecer tais medidas, cobrindo quase todo o alto-mar (CULLIS-SUZUKI & PAULY, 2010; HAAS et al., 2020). Essas entidades colaboram com governos, cientistas, a indústria pesqueira e outras partes interessadas para desenvolver e implementar estratégias de gestão eficazes(ARMITAGE et al., 2009; HAAS et al., 2020).

Essa gestão envolve uma abordagem integrada, considerando tanto as características biológicas das espécies quanto os aspectos socioeconômicos da pesca. As estratégias incluem a definição de limites de captura, tamanhos mínimos de desembarque, áreas de proteção marinha e períodos de defeso para a reprodução (CULLIS-SUZUKI & PAULY, 2010; HAAS et al., 2020). Além disso, programas de monitoramento e pesquisa são essenciais para avaliar o estado dos estoques e fundamentar decisões de manejo.

No Oceano Atlântico, a gestão de espécies marinhas migratórias, incluindo os atuns e espécies associadas, é realizada pela Comissão Internacional para a Conservação dos Atuns do Atlântico (ICCAT)( HAAS et al., 2020). Para fins de gestão, é adotada a hipótese de que no Atlântico há dois estoques distintos de espadarte, um estoque no Atlântico Norte e outro no Atlântico Sul separados em 5° N e um estoque único para a albacora-bandolim (ICCAT, 2024).

De acordo com a última avaliação formal, a biomassa do estoque de espadarte no Atlântico Norte, em 2020 (B2020), estava acima da Biomassa no Nível Máximo de Produção Sustentável (*Biomass at Maximum Sustainable Yield* - BMSY), com uma mediana de B2020/BMSY = 1,08. Além disso, a mortalidade por pesca (F2020) estava abaixo do Nível Máximo de Produção Sustentável (*Fishing Mortality at Maximum Sustainable Yield* - FMSY), com uma mediana de F2020/FMSY = 0,80. O Rendimento Máximo Sustentável (*Maximum Sustainable Yield* - MSY) mediano foi estimado em 12.819 toneladas, com um IC de 95% variando entre 10.864 e 15.289 toneladas.

Por outro lado, para o estoque de espadarte no Atlântico Sul, indicou que a biomassa de 2020 (B2020) estava abaixo do BMSY, com uma mediana de 0,77. Já a mortalidade

por pesca em 2020 (F2020) estava ligeiramente acima do FMSY, com uma mediana de 1,03. O MSY foi estimado em 11.481 toneladas, sinalizando que a biomassa do estoque de espadarte do Atlântico Sul está sobreexplorada e a sobrepesca continua ocorrendo. A avaliação do cenário-base sugere uma probabilidade de 56% de que o estoque se encontra no quadrante vermelho do gráfico de Kobe (ICCAT, 2022, 2024), indicando uma situação preocupante de sobrepesca e necessidade de medidas de manejo urgentes.

Com relação ao estoque da albacora-bandolim do Oceano Atlântico, a ultima avaliação, realizada em 2019, indicou que o estoque está sobreexplorado, com uma mediana SSB2019/SSBMSY de 0,94. No entanto, o estoque não está sofrendo sobrepesca, conforme a mediana F2019/FMSY igual a 1,00. A média do Rendimento Máximo Sustentável foi estimada em 86.833 toneladas, com um IC de 80% entre 72.210 e 106.440 toneladas (ICCAT, 2024).

De modo geral, ao longo das últimas décadas, observou-se uma tendência de declínio na biomassa do estoque de espadarte e da albacora-bamdolim no Atlântico Sul. Os dados coletados indicam uma redução gradual da abundância da espécie, com variações regionais consideráveis. Isso pode ser atribuído à pesca intensiva e à exploração não sustentável dos recursos pesqueiros(ICCAT, 2024; RODRIGUES et al., 2020).

A CPUE do espadarte e da albarora-bamdolim também apresentou flutuações significativas ao longo dos anos. Inicialmente, houve um aumento na CPUE devido ao aumento da capacidade tecnológica da pesca, com a introdução de métodos mais eficientes de captura (RODRIGUES et al., 2020). No entanto, essa tendência se reverteu nas últimas décadas, com uma diminuição constante da CPUE. Isso indica que a pesca está se tornando menos produtiva e que os estoques de espadarte e de albaroa-bamdolim estão sendo esgotados (ICCAT, 2024; RODRIGUES et al., 2020).

Em resumo, as flutuações e o declínio nas capturas anuais, juntamente com a sobre-exploração observada, indicam a necessidade urgente de medidas de gestão mais rigorosas para evitar a sobrepesca e garantir a sustentabilidade dos estoques. Os resultados das avaliações formais recomendam a implementação de limites de captura e outras medidas de controle de esforço de pesca (ICCA, 2024). Essas ações são essenciais para assegurar que as populações de espadarte e albacora-bandolim sejam mantidas dentro de níveis sustentáveis, permitindo a continuidade das atividades pesqueiras e a preservação dos ecossistemas marinhos.

# 2. Artigo Científico 1: Unveiling New Insights: A Geostatistical Approach to Accurately Estimate South Atlantic Swordfish Abundance Using Commercial Catch Data

Silvaneide Luzinete Rodrigues[1]*, Humber Agrelli Andrade[2]

[1] Laboratory of Applied Statistical Modeling – MOE, Department of Fisheries and Aquaculture, Federal Rural University of Pernambuco.Rua Dom Manuel de Medeiros, s/n, Dois-Irmãos, Recife-PE, Brasil. ORCID: http://orcid.org/0000-0002-1204-5818. E-mail: silvaneide.pescaufrpe@gmail.com

[2] Laboratory of Applied Statistical Modeling – MOE, Department of Fisheries and Aquaculture, Federal Rural University of Pernambuco. Rua Dom Manuel de Medeiros, s/n, Dois-Irmãos, Recife-PE, Brasil. ORCID: http://orcid.org/0000-0002-4221-8441. E-mail: humber.andrade@ufrpe.br

**Abstract:** The present study addresses challenges to estimate the relative abundance indices recorded for highly migratory marine species based on commercial fishing data. The aim of this research is to develop a three-step analysis protocol. The first step regards modeling catch rate based on variables capable of affecting this rate to rule out the effects of catchability-related factors. Subsequently, residuals were analyzed to identify autocorrelation. Finally, an area-weighed recursive algorithm was applied by taking into consideration the specific spatial autocorrelation recorded for each year within the assessed period-of-time. This procedure was applied to the analysis of commercial South Atlantic swordfish (*Xiphias gladius*) catch data of the Brazilian pelagic longline fleet. Overall, swordfish accounted for the highest spatial dependence values (in terms of distance) in 2005, 2008, 2012 and 2014: 456 km, 111 km, 80 km and 443 km, respectively, as well as for the lowest values of it in 2011 and 2013: 15.45 km, on average. In addition, according to the results, there was general downward trend in species' abundance between 2010 and 2017. This outcome was detected few years earlier than conventional standardization indices. Therefore, it was possible inferring that the proposed indices are an alternative and a potentially more accurate perspective of swordfish population dynamics in the South Atlantic. This finding highlights the need of taking into account multiple approaches to assess the abundance of marine species.

**Keywords:** Autocorrelation, Fishery dependente, Fishery resources, Generalized Linear Model (GLM), Migratory marine species, Sustainability.

## 1. Introduction

Fishery stock assessment has been taken as ultimate excellence standard to provide management guidance for commercial fishery (Maunder et al., 2020). Models based on catch data and commercial fishing effort are often used to generate relative abundance indices, such as the case of the Catch Per Unit Effort (CPUE) (Hilborn & Walters, 1992; Campbell, 2016; Xu et al., 2018; Cadrin, 2020). However, CPUE can be affected by factors unrelated to species abundance, such as changes in target species, and variations in both fishing strategies and activity fields (He et al., 1997; Campbel, 2004; Xu et al., 2018; Maunder & Punt, 2004; Maunder et al., 2020). Therefore, the process called CPUE standardization is often applied to rule out or reduce the effect

of factors that are not directly related to species' abundance (Maunder & Punt, 2004; Hoyle et al., 2024).

CPUE standardization is carried out through statistical techniques, such as Generalized Linear Models (GLM) (Mccullagh & Nelder, 1989; Maunder & Punt, 2004; Thorson et al., 2016; Punt, 2019). However, it is challenging applying models for this purpose. Among these challenges one finds fishery-dependent CPUE, which can be affected by sampling spatial or temporal biases or anomalies (data deviations or irregularities) (Yu et al., 2013; Crespo et al., 2018; Maunder et al., 2020). The non-random nature of fish spatial distributions can lead to preferential sampling (Conn et al., 2017; Maunder et al., 2020; Ducharme-Barth et al., 2022), i.e., sampling can be influenced by certain non-random factors, such as choosing fishing areas based on the prior knowledge of, or on locations, where catch is likely to happen. Sampling anomalies can lead to disconnection between stock abundance trajectories and standardized CPUE time series, a fact that results in biased relative abundance indices (Reuchlin-Hugenholtz et al., 2015; Ducharme-Barth et al., 2022; Hoyle et al., 2024).

Several studies have been carried out to improve CPUE standardization by incorporating the spatial and temporal heterogeneity of fishing resources' distribution and sampling designs in statistical models. Thorson et al. (2016) proposed the use of mixed linear generalized models (MLG) to standardize CPUE by taking into account spatial and temporal autocorrelation. Maunder & Punt (2004) and Punt et al. (2019) used regression trees and generalized additive models (GAM), respectively, to add spatial structure imputation techniques to the models. Ducharme-Barth et al. (2022) highlighted the importance of taking preferential sampling and spatial variability to standardize CPUE by using spatiotemporal delta-GLMM models applied to commercial fishing data.

Using spatial indicators and geostatistics to investigate species' spatial-temporal dynamics has become a growing research field. Some studies have assessed the association between occupancy and abundance indices of commercial-interest species (Morfin et al., 2012; Yu et al., 2013; Saraux et al., 2014; Reuchlin-Hugenholtz et al., 2015). Woillez et al. (2009) proposed an algorithm to identify and model spatial and spatiotemporal autocorrelation structures based on migratory fish-density data. However, the high costs linked to the collection of independent fishing samples impair the application of techniques to migratory oceanic species presenting wide spatial distribution.

Caught tuna and similar species presenting wide spatial distribution, and species with great global socioeconomic and ecological relevance, stand out among the stocks of migratory species that have no independent data of commercial fishing. The pelagic longline fishery of the South Atlantic Ocean swordfish stock (*Xiphias gladius* Linnaeus, 1758) has been the subject of recent assessments conducted by the International Commission for the Conservation of Atlantic Tunas (ICCAT), specifically in 2017 and 2022. According to the results, there is strong downward trend

in stock yield, although the stock remains classified as overexploited and subjected to overfishing. Nevertheless, catches from the last 5 years were below the Total Allowable Catch (TAC) established by the International Commission for the Conservation of Atlantic Tunas (ICCAT), which is the intergovernmental body responsible for tuna and tuna-like species conservation in the Atlantic Ocean and adjacent seas (ICCAT, 2022). There was also significant uncertainty regarding the reliability of the provided data, as well as inconsistency in the time series of standardized CPUE indices calculated by scientific commissions of ICCAT member countries (ICCAT, 2014, 2022).

Brazil plays important role in fishing South Atlantic Swordfish Stock – SASS, since it accounts for one of the largest fishing fleets in the Southwest Atlantic (ICCAT, 2014, 2017, 2022). The 2017 series was divided into two parts for standardization purposes, namely: before (1978-2004) and after (2005-2012) the monitoring program had started - including onboard observers for charted vessels, at late 2004 (Carneiro et al., 2017). This division was carried out due to the huge difference in the scale set for CPUE values and to data dispersion between the two assessed periods. In addition, the standardized CPUE series of the first assessed period (1978-2004) was conflicting to other CPUE indices that were calculated based on data of other fleets also operating SASS. After all, only the second part of the Brazilian CPUE series (2005-2012) was used in the stock assessment model of the Regional Fisheries Management Organizations (RFMOs) (ICCAT, 2017). Subsequently, one part of the CPUE series presenting high dispersion and any up- or downward trend (1978-1993) was removed from the stock assessment; however, the 1994-2020 time series was used for stock assessment purposes (Mourato et al., 2022).

Data in the aforementioned paperwork were weighted by area, but equal weight was adopted for each spatial square (5°x5° latitude by longitude). This approach allowed assuming that the sampling was representative for all spatial grid points of squares, including those with poor sampling and limited region representation - which is unlikely to happen in extensive spatial strata. This scenario demands using spatial-temporal modeling methods that embody information from neighboring locations, and from grids presenting higher spatial resolution, to enable getting more accurate and reliable relative abundance index estimates (Maunder et al., 2020).

This study aimed to conduct a fine-scale geostatistical investigation of the spatial dynamics of swordfish catches and fishing effort by the Brazilian pelagic longline fleet in the Southwestern South Atlantic (SASS). By incorporating spatial structure into CPUE standardization models, the research addresses a critical need for more accurate assessments of overfished populations. The results were compared to previously established findings, highlighting the importance of considering spatial structure in fisheries data analysis. The observed differences enhance our understanding of the stock's spatial distribution and its implications for abundance estimates. Ultimately, this paper contributes to a more precise scientific understanding of South Atlantic swordfish stocks, which have recently been classified as overfished, and supports improved

decision-making and management strategies within the SASS framework.

## 2. Materials and methods

### *2.1 Data*

Information about the Brazilian commercial fleet available at the National Tuna and Related Fishing Data Bank, also known as BNDA, by the Ministry of Fisheries and Aquaculture (MPA), was analyzed. This database holds information on pelagic longline fishery provided by onboard maps plotted by fishing masters from commercial vessels. This program covers a fraction of the undertaken commercial trips. Therefore, data available at BNDA regard a sample of longline fishing operations in the Brazilian Exclusive Economic Zone (EEZ) and in adjacent international waters.

The database contains over 106,647 records of fishing sets conducted between 1978 and 2020 by both Brazilian national boats and leased boats from 19 different foreign countries. Variables recorded in the database include the name and flag of the boats, geographical location (longitude and latitude), dates of longline deployment and retrieval, number of hooks, and catch per species (or group of species) expressed either in number or weight. Additionally, for some fishing sets, there are records of Sea Surface Temperature (SST) and type of bait used, although these variables are often incomplete. For this study, the following data were used from the BNDA: boat flag of origin (national or foreign), geographical coordinates (longitude and latitude), number of swordfish caught per fishing set, dates of the fishing sets (deployment), number of hooks deployed, and number of hooks per basket. Due to the lack of consistent records for SST and type of bait, these variables were not included in the present analysis.

### *2.2 Data review and filtering*

Firstly, fishing records presenting coarse spatial resolution, such as data aggregated in resolution latitude and longitude quadrants (1º by 1º or 5º by 5º), were ruled out. Only fishing records of bids with indicated coordinates and fine resolution with degree indication and the least minutes when the fishing bid was made were kept. Data from 2004, and from years prior to it, were not included in the analyses, since the fishing hauls recorded in BNDA were mostly reported in aggregate form up to this same year.

Clearly wrong data were also ruled out, such as records of hauls located in open fields and unreliable data like records of fishing hauls presenting less than 800 hooks – this number is not the standard set for the Brazilian fleet (Lira et al., 2017). Data that did not meet the proposition by Carneiro et al (2017) and Mourato et al (2022), at ICCAT scope, were also ruled out. Therefore, data of vessels missing swordfish catch records that have fished for less than 6 months or that have reported less than 50 fishing trips were disregarded. Only vessels with lease flags were taken into consideration, since there was a relatively large number of fishing records corresponding to

at least 2% of the total data.

The number of hooks per basket (HPB) is one of the variables of interest given its relevance as proxy for the intended target in the fishing haul. Bid records that missed information were also ruled out. Consequently, the time interval between 2018 and 2020 was not included in the analysis, since most of their bid records did not present HPB information.

Finally, after all the filtering, 23,068 fishing trips of national vessels (BRA-BRA) and of chartered vessels from Spain (BRA-ESP), Honduras (BRA-HND), Morocco (BRA-MAR) and Panama (BRA-PAN), carried out between 2005 and 2017 (Table 1) were selected, and distributed between latitude 10°N and 40°S, and longitude 20° and 55°W (Figure 1). The analysis allowed comparisons to the study carried out by Carneiro et al. (2017) and Mourato et al. (2022), from 2005 to 2017, after the filter was applied.

Table 1. Number of fishing set records and active flags per year. Vessels: National (BRA) and leased vessels from Spain (BRA-ESP), Honduras (BRA-HND), Morocco (BRA-MAR) and Panama (BRA-PAN).

| YEAR | BRA-BRA | BRA-ESP | BRA-HND | BRA-MAR | BRA-PAN | TOTAL |
|---|---|---|---|---|---|---|
| 2005 | 2,193 | 864 | 306 | 91 | 332 | 3,786 |
| 2006 | 1,489 | 540 | 315 | 305 | 238 | 2,887 |
| 2007 | 2,068 | 585 | 146 | 271 | 183 | 3,253 |
| 2008 | 885 | 160 | 133 | 98 | - | 1,276 |
| 2009 | 880 | 342 | 132 | 44 | - | 1,398 |
| 2010 | 622 | 479 | - | 27 | - | 1,128 |
| 2011 | 657 | 378 | - | - | - | 1,035 |
| 2012 | 1,855 | 160 | - | - | - | 2,015 |
| 2013 | 759 | - | - | - | - | 759 |
| 2014 | 725 | - | - | - | - | 725 |
| 2015 | 1,221 | - | - | - | - | 1,221 |
| 2016 | 2,302 | - | - | - | - | 2,302 |
| 2017 | 1,283 | - | - | - | - | 1,283 |
| **TOTAL** | 16,939 | 3,508 | 1,032 | 836 | 753 | 23,068 |

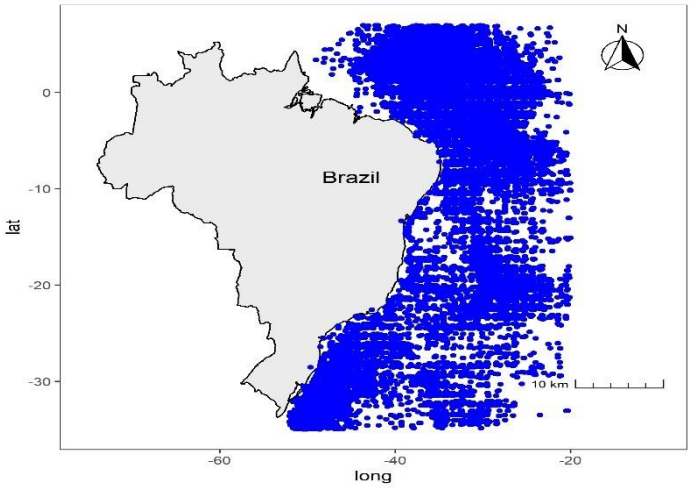


Figure 1.Study site location. The blue points indicate the distribution of longline fishing operations conducted by the Brazilian pelagic longline fleet from 2005 to 2017.

### *2.3 Data modeling process stages*

A relative abundance index set for swordfish was generated based on three steps as presented below, and further in the text. The first step of the method involved using a GLM to remove factors unrelated to abundance from the CPUE estimates. Spatial autocorrelation in standardized CPUE residuals was assessed at the second step through the application of geostatistical techniques. The recursive algorithm developed by Woillez et al. (2009), which takes into consideration the specific spatial autocorrelation set for each assessed element, was addressed at the third step (Figure 2).

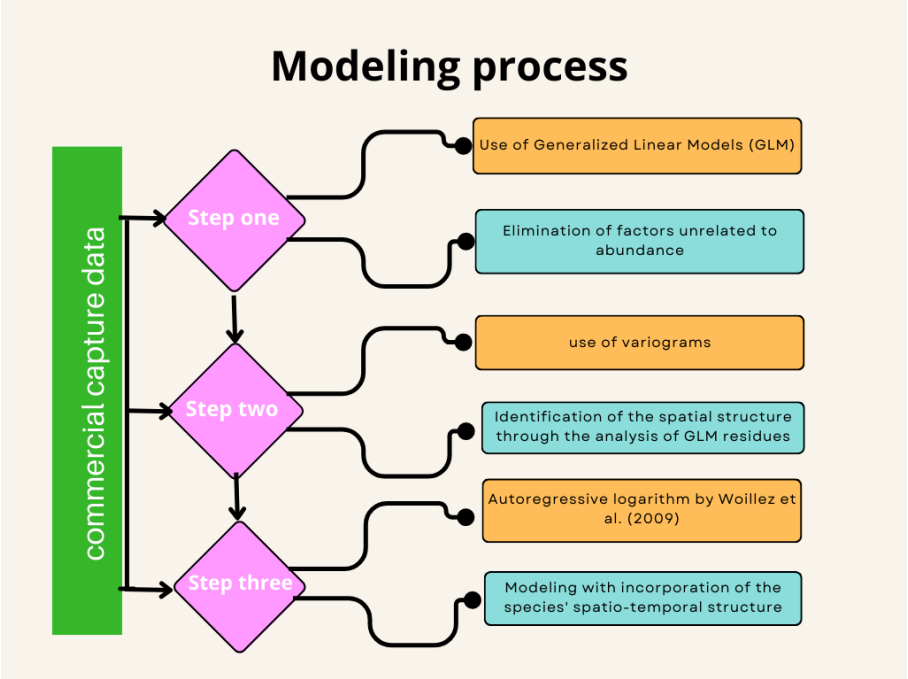


Figure 2. Diagram illustrating the modeling process applied to generate the relative abundance index of commercial fishery recorded for ocean species based on GLMs and spatial analysis.

*2.3.1 Standardizing catch per effort unit*

The first step of the procedure regards standardizing fishing data through MLGs. Catch expressed by number of copies was the response variable, which is the most frequent recording strategy. The adopted explanatory variables are shown in Table 2. The flag variable must be assessed because fishing strategies are different depending on the fleet (Rodrigues et al., 2020). As aforementioned, the HPB variable is also potentially relevant since it has been often used as fleet-direction indicator. Fishing effort is measured by the number of hooks. These variables were also used in previous studies, at ICCAT scope (i.e. Carneiro et al., 2017; Mourato et al., 2022). However, the present study significantly differs from previous studies, since the explanatory variables associated with space and time were herein taken into consideration. Fishing trips were aggregated in 5°x5°-degree squares, in previous studies, whereas data presenting maximum resolution were used in the current research, including positioning in degrees and the minutes of each fishing trip. The explanatory variable ‘month’ was included in the model to capture finer intra-annual cycles in swordfish catch rates. In contrast to previous research, which grouped data into three-month intervals (quarters) for analysis (e.g., Carneiro et al., 2017; Mourato et al., 2022), this study uses the monthly data directly. This approach allows for a more granular level of analysis, potentially revealing smaller-scale temporal variations. As for the present study, ‘year” was not included in the models; consequently, it is possible assuming that the residues carried information about relative variation in abundance, over the years. Residues became of interest at

the time to estimate relative abundance indices. In essence, this is the difference between the herein adopted approach and other approaches used in previous research.

Table 2. Variables analyzed to develop generalized linear models.

| Variable | Classification | Range | Description |
|---|---|---|---|
| SWO | Numeric | 0-50 | Swordfish catch |
| Month | Categorical | 1–12 | Months of the year |
| Latitude | Numeric | 10°N–35°S | Geographic coordinates |
| Longitude | Numeric | 15°W–55°W | Geographic coordinates |
| Flags | Categorical | 1–5 | National vessels (BRA-BRA) and chartered vessels from Spain (BRA-ESP), Honduras (BRA-HND), Morocco (BRA-MAR), and Panama (PAN). |
| HPB | Numeric | 3–14 | Number of hooks per basket (HPB) |
| Effort | Numeric | 800-1,691 | Number of hooks |

The general formulation of a generalized linear model is given by $g(\mu) = \beta_0 + \beta_1 X_{1+} \beta_2 X_{2+} \ldots + \beta_p X_p$; wherein, $g(\mu)$ is the ligation function, which describes the association between the mean recorded for the response variable ($\mu$) and the linear predictor. $\beta_0, \beta_1, \beta_2, \ldots, \beta_p$ are the model coefficients, which represent the effect of explanatory variables $X1, X2, \ldots, Xp$ on the mean recorded for the response variable (McCullagh & Nelder, 1989; Zeileis et al., 2008).

Response variable (catch) is measured based on number of fish; therefore, exponential-family probability distributions were taken into consideration for discrete variables, including adjustments made to deal with excess zero, such as zero-inflated and barrier models. The applied models and the respective connection functions used for each assessed case are shown in Table 3. Fishing effort was included as offset in the modeling process. Details and theoretical foundations set for generalized linear models can be found in McCullagh & Nelder (1989), Dobson (2008), and in Zeileis et al. (2008), Mullahy (1986) and Lambert (1992), when it comes to extensions made to deal with cases of excess zero.

Table 3. Summary of Generalized Linear Models (GLMs) used in data analysis applied to catch data provided by the Brazilian Pelagic Longline Swordfish Fisheries. Wherein, "$\mu$" represents the mean count of swordfish caught per effort unit and "$\theta$" represents the dispersion parameter used to calculate over-dispersion in the count data. Function "g" represents the link function used to relate mean "$\mu$" to the linear predictor in the models.

| Model | Link Function |
|---|---|
| Poisson (P) | $g(\mu) = log(\mu)$ |
| Negative Binomial (NB) | $g(\mu) = log(\mu/(\mu + \theta))$ |
| Zero-Inflated Poisson (ZIP) | $g(\mu) = log(\mu)$ |

| | | | |
|---|---|---|---|
| Zero-Inflated Negative Binomial (ZINB) | | | $g(\mu) = log(\mu/(\mu + \theta))$ |
| Hurdle with Negative Binomial (HNB) | | | $g(\mu) = log(\mu/(\mu + \theta))$ |

The selection of relevant explanatory variables and their inclusion order, as main factor in the model, were carried out based on Akaike Information Criterion (AIC) (Akaike, 1974). Balance between bias and estimates' variance is taken into account to seek a more parsimonious model when this criterion is used (Burnham & Anderson, 2004). The first-order interactions of explanatory variables were added to the model after the main factors were included in it, as long as they led to AIC reduction.

Conventional descriptive residuals were diagnosed to assess the quality of adjustments made in the models. Tests were carried out to assess patterns, including spatial/temporal autocorrelation, normality and over-dispersion, by using the same procedure adopted by Hartig (2022). AIC and diagnosis of residuals were the criteria took into consideration to select the final models. Deviance analyses were carried out to investigate whether the inclusion of each explanatory variable would end up reducing the significance of the deviance after models' selection.

### 2.3.2 Spatial structure

The swordfish spatial distribution structure was investigated based on the spatial autocorrelation analysis applied to residuals of the generalized linear model, which was adjusted in the previous step. Most residual data are free from factors that mask changes in organisms' population density, and this process allows identifying local positive or negative irregularities in fish density (Vignaux, 1996; Kleisner et al., 2010). The analysis was conducted based on spatial dimensions (latitude and longitude) for each given year, as well as the distances between fishing sets carried out within the same time intervals. Dependency associations between residuals and distances between these fishing sets were calculated using variograms, following the procedure outlined by Kleisner et al. (2010) and Saul et al. (2013). This approach aimed to estimate the distances at which the aggregations of *X. gladius* no longer exhibit a contagious aggregation pattern.

The semi-variogram function was mathematically expressed as $\gamma(h) = \frac{1}{2N(h)}\sum_{i=1}^{n(h)}[z(xi) - z(xi+h)]^2$, wherein $\gamma(h)$ is the estimated semi-variance between pairs of points separated by a distance $h$, $N(h)$ is the number of pairs of measured values, $z(xi)$ and $z(xi+h)$ are values of the $i$-$^{th}$ observation of the regionalized variable, which was collected at points $xi$ and $xi+h$ $(i = 1,\ldots,n)$, apart from vector $h$. Distance $h$ between consecutive launches in the space was measured in kilometers. The empirical variogram was modeled based on using functions presenting known exponential, spherical and Gaussian calculations. The

function better minimizing the square root of the error was chosen to adjust the data (Chang et al., 2017). Parameters involved in models' adjustments are reach or range (a), which corresponds to variable's influence; nugget (C0), semi-variance at distance 0; plateau (C+C0), asymptote that stabilizes the function in a random field; and sill (C), distance between nugget and plateau, which corresponds to the maximum semi-variance found in the analyzed data set (Kleisner et al., 2010).

The maximum distance of $h$ was adjusted for each case until stabilizing $\gamma(h)$, for calculation purposes. Results deriving from the semi-variogram function allowed detecting spatial aggregations or densifications in the investigated fish populations. Thus, if the spatial dependence value resulting from the semi-variogram persists for maximum distance of 10 km, this measurement would estimate the fish-density diameter.

The degree of spatial dependence ($GDE$) was calculated as the ratio between sill and the threshold $GDE = \frac{C}{C0+C}$, and classified as low spatial dependence for $GDE$ < 25%, as mild for 25% < $GDE$ < 75% and as strong for $GDE$ > 75%, according Zimback (2001).

*2.3.3 Density estimates*

Spatial density was calculated through the recursive algorithm developed by Woillez et al. (2009). This algorithm starts from the value of the largest residue (maximum zi), which is the starting mark of the first aggregation structure. The closest launches are aggregated to the patch, if the distance between them and the gravity center ($CG$) does not exceed the densification limit distance. The limit distance represents the sample's spatial dependence value in the current year, which is determined by the range recorded through the autocorrelation analyses applied to GLM residuals; otherwise, the current value of the sample would define a new patch.

*2.3.4 Relative abundance indices based on density estimates*

The relative abundance index expressed in number of individuals was estimated through the discrete sum related to sample locations $xi$ $(i = 1, \dots, n)$, which were weighed based on influence sites around the samples (determined in the set space). The $Si = \sum_{i=1}^{n} wizi$ formula refers to influence range and $zi$ is the standardized catch value recorded for swordfish at point $xi$ (latitude and longitude), as proposed by Woillez et al. (2007, 2009). The herein used influence range was defined based on the range value collected from the variograms calculated at the previous step.

*2.3.5 Spatial distributions of population density*

Swordfish relative abundance distribution mapping was prepared based on the ordinary kriging (KO) method, which was chosen for being one of the best methods for the linear prediction of regionalized variables. It is highly recommended to spatially assess autocorrelated data (Chen

et al., 2016; Chang et al., 2017). Furthermore, it was seen as suitable to estimate density indices set for fish populations (Yu et al., 2013). The general formula for KO prediction is $z(ho) = \sum_{i=1}^{n} \lambda_i z(hi)$, wherein $h0$ is the place of prediction, $z(h0)$ is the predicted value, $z(hi)$ is the value measured at the i-$^{th}$ location, $\lambda i$ is the unknown weight of the measured value at the i-$^{th}$ location, besides being the total amount of measured values. Weight $\lambda i$ is determined by the semi-variogram. Yearly animal density maps were plotted by using kriging observations in the study site.

All analyses at this, and other, aforementioned steps were carried out in R software, version 4.2.0 (R Core Team, 2022), in the Mass (Venables & Ripley, 2002), pscl (Zeileis et al., 2008), lmtest (Achim & Torsten, 2002), DHARMa (Hartig, 2022), Gstat (Gräler et al., 2016) and RGeostats (Armines, 2022) packages. Spatial data were available at the coordinate system World Geodetic System, which was launched in 1984 (WGS84).

## 3. Results

Results in Table 4 summarize the different Generalized Linear Models applied to model swordfish catch data (SWO) between 2005 and 2017. Poisson model (P) presented extremely high AIC (277439425.0) and log likelihood of -138719606. This finding points out poor adjustment to swordfish catch data. In comparative terms, the Negative Binomial (NB) model had significant AIC reduction (180832375.6) and improved log likelihood (-90416080) at Chi-Square value of 9.6607e+07.

Models considering zero inflation (ZIP and ZINB) and the Hurdle model (HNB) proved to be even more suitable for data modeling due to their significantly lower AICs. The ZIP model recorded AIC equal to 208035.7 and log likelihood of -103907, with extremely high Chi-Square: 1.8062e+08 ($p < 2.2e-16$). This finding highlights significant improvement in the adjustments made to catching data in comparison to the Poisson and Negative Binomial models.

The ZINB model accounted for the best adjustment to swordfish catch among all models, since it recorded the lowest AIC (150615.2) and the highest log likelihood (-75196). This model presented Chi-Square value equal to 5.7423e+04 ($p < 2.2e-16$); therefore, it stood out as the most effective approach to catch SWO data distribution, which includes many zeros. The HNB model, although similar to ZINB in complexity, recorded slightly higher AIC (151104.5) and log likelihood of -75440, at Chi-Square value equal to 4.8933e+02 ($p < 2.2e-16$).

Table 4. Summary of Generalized Linear Models (GLMs): Poisson (P), Negative Binomial (NB), Zero-Inflated Poisson (ZIP), Zero-Inflated Negative Binomial (ZINB) and Hurdle with Negative Binomial (HNB) applied to swordfish (SWO) catch data modeling between 2005 and 2017; wherein K corresponds to the number of estimated parameters, AIC is the Akaike Information Criterion, logLik corresponds to the log likelihood, Chi-square. **T**he explanatory variables

included in the models were flags (F), month (M), latitude (LAT), longitude (LON), and Number of hooks per basket (HPB).

| **GLM** | **Formula** | **K** | **AIC** | **logLik** | **Chisq** | **p-Valor (Pr(>Chisq))** |
|---|---|---|---|---|---|---|
| P | SWO ~ (F + M + HPB + LAT + LON)^2-F:HPB | 107 | 277439425.0 | -138719606 | - | - |
| NB | SWO ~ (F + M + HPB + LAT + LON)^2-F:HPB | 108 | 180832375.6 | -90416080 | 9.6607e+07 | < 2.2e-16 |
| ZIP | SWO ~ (F + M + HPB + LAT + LON)^2- LAT:LON\| 1 | 111 | 208035.7 | -103907 | 1.8062e+08 | < 2.2e-16 |
| ZINB | SWO ~ (F + M + HPB + LAT + LON)^2- LAT:LON \| 1 | 112 | 150615.2 | -75196 | 5.7423e+04 | < 2.2e-16 |
| HND | SWO ~ (F + M + HPB + LAT + LON)^2-F: LAT:LON \| 1 | 112 | 151104.5 | -75440 | 4.8933e+02 | < 2.2e-16 |

Note: Significance code: 0 ‘’ 0.001 ‘’ 0.01 ‘’ 0.05 ‘.’ 0.1 ‘ ’ 1

The analysis applied to adjusted models’ residuals showed that the P and NB distributions presented significant data over-dispersion (p-value < 0.001) around the model’s straight line (Figure 3, panel to the right). In addition, the quantile graphs suggest that the distributions of P, NB and ZIP models’ residuals present marked deviations from normality (Figure 3, panel to the center), but the distributions are homoscedastic (Figure 3, panel to the left).

Accordingly, the Zero Inflated Negative Binomial model was selected for analyses relating the species’ spatial-temporal structure, since it presented better performance in swordfish catch data modeling. More details on swordfish catch per effort unit (CPUE) standardization are available in the appendices.

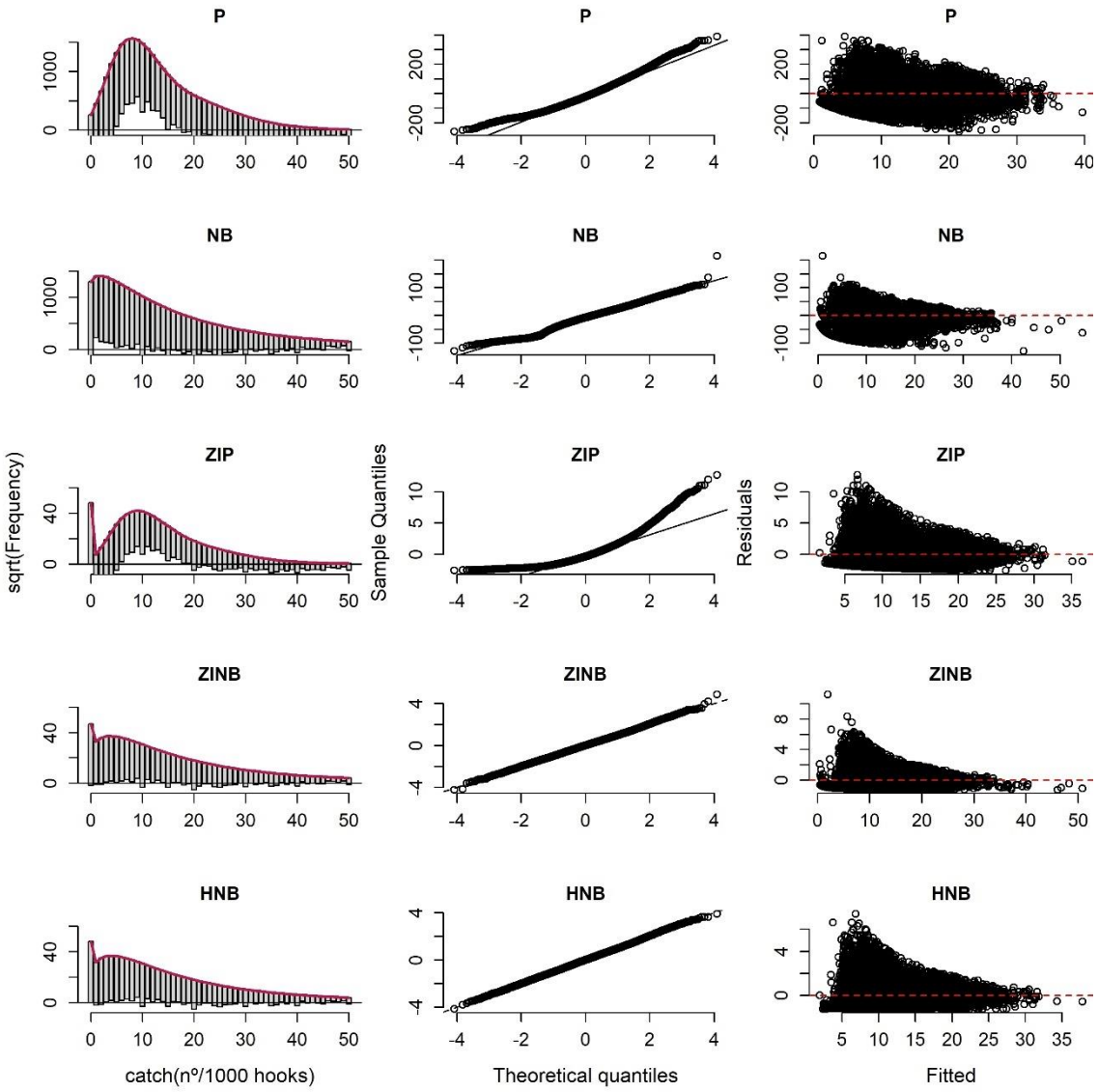


Figure 3. Residual diagnosis of the assembled models according to the following approaches: Poisson (P), Negative Binomial (NB), Zero Inflated Poisson (ZIP), Zero Inflated Negative Binomial (ZINB) and Hurdle with Negative Binomial (HNB) by testing the residuals for homogeneity (right), normality (center) and dispersion (right). The plots on the right represent the expected values estimated from the constructed abundance index, while the plots in the center and on the left display the residual diagnostics for normality and homogeneity.

*Spatial structure and population densities*

In almost all assessed years, variograms were modeled using a spherical function (Figure 4 end Table 5). The variogram structures indicated a non-random spatial distribution. Specifically, the variance of the residuals increased with distance, suggesting that fishing operations at closer points tended to show more similar catch values compared to operations at more distant locations. The year of 2017 was an exception, when there was stationary trend in all directions (Figure 4 C). This finding suggests lack of spatial covariance structure. Overall, swordfish showed spatial dependence on longer distances in 2005, 2008, 2012 and 2014 (456 km, 111 km, 80 km and 443 km, respectively), and on shorter ones in 2011 and 2013 (15.45 km, on average). The maximum

variability value (sill) found in the analyzed data set was close to 1.60, in 2005, whereas these values ranged from 0.6 to 1.25, in the other years.

The nugget effect changed over the years in the described analysis. It showed higher values from the early years until 2007, and at the end of the 2012-2017 time series. This finding points out that data from these years accounted for higher degree of randomness and uncorrelated variability, which cannot be explained by spatial dependence or structure. A likely explanation for this variation lies on the influence of environmental factors that affect fish distribution. Finally, measurement error, sampling bias or modeling assumptions may have contributed to the observed variation in the nugget effect and it should be taken into consideration for results' interpretation.

Table 5. Root Mean Square Error (RMSE) and Variogram Coefficients (Nugget, Sill, Range) for Exponential, Spherical, and Gaussian Models.

| Year | Model | Nug | Psill | Range | RMSE |
|---|---|---|---|---|---|
| 2005 | Exponential | 0.5871177 | 0.2294502 | 456.2496 | 0.0581968 |
| | Spherical | 0.5935643 | 0.3100106 | 381.2804 | 0.0589451 |
| | Gaussian | 0.6069332 | 0.1698149 | 161.6764 | 0.0833326 |
| 2006 | Exponential | 0.7700745 | 0.3385086 | 70.88975 | 0.0962230 |
| | Spherical | 0.6602636 | 0.3757943 | 55.40500 | 0.0939694 |
| | Gaussian | 0.8247302 | 0.2474120 | 62.34459 | 0.0970390 |
| 2007 | Exponential | 0.6324657 | 0.5668379 | 18.11345 | 0.1166296 |
| | Spherical | 0.748331 | 0.3757943 | 55.40500 | 0.1146615 |
| | Gaussian | 0.8778352 | 0.3195405 | 22.08381 | 0.1179874 |
| 2008 | Exponential | 0.5325103 | 0.1610858 | 145.8102 | 0.2261372 |
| | Spherical | 0.5019047 | 0.1788234 | 83.51951 | 0.2262089 |
| | Gaussian | 0.5194744 | 0.1738320 | 40.50709 | 0.2326158 |
| 2009 | Exponential | 0.2104055 | 1.8421995 | 54.49860 | 0.1053251 |
| | Spherical | 0.2298305 | 0.3994724 | 21.10590 | 0.1038872 |
| | Gaussian | 0.253633 | 0.3878560 | 33.84560 | 0.1084614 |
| 2010 | Exponential | 0.8029752 | 1.7768950 | 36.86932 | 0.0781005 |
| | Spherical | 0.5246268 | 0.2307274 | 20.87067 | 0.0742279 |
| | Gaussian | 0.8545097 | 0.0000000 | 61.00000 | 0.0781948 |
| 2011 | Exponential | 0.3231659 | 34.061213 | 20.49019 | 0.3009558 |
| | Spherical | 0.3268840 | 0.4550845 | 16.53124 | 0.3002644 |
| | Gaussian | 0.32566103 | 0.3676007 | 15.30370 | 0.3107718 |
| 2012 | Exponential | 0.8133979 | 0.4962069 | 80.68094 | 0.2049446 |
| | Spherical | 0.6564213 | 0.6471364 | 55.04485 | 0.2048162 |
| | Gaussian | 0.7794934 | 0.5234405 | 20.82551 | 0.2054072 |
| 2013 | Exponential | 1.19247773 | 0.0124117 | 86.83184 | 0.5833212 |
| | Spherical | 1.0123746 | 0.1980791 | 17.08973 | 0.5256968 |
| | Gaussian | 1.0806496 | 0.0810542 | 17.94548 | 0.7034721 |
| 2014 | Exponential | 0.689474 | 0.8321503 | 432.7498 | 0.1541471 |
| | Spherical | 0.666576 | 0.8408734 | 403.2877 | 0.1656090 |
| | Gaussian | 0.7026692 | 0.6459057 | 125.5581 | 0.1702270 |
| 2015 | Exponential | 1.1743224 | 0.0000000 | 61.00000 | 0.3274924 |
| | Spherical | 0.8997726 | 0.2180359 | 22.13723 | 0.3236263 |
| | Gaussian | 1.138972 | 0.0000000 | 61.00000 | 0.3917916 |
| 2016 | Exponential | 00.00 | 0.7629446 | 36.00200 | 0.0800507 |
| | Spherical | 0.7066477 | 0.4654543 | 55.80923 | 0.0719551 |

| | | | | | |
|---|---|---|---|---|---|
| | Gaussian | 0.549811 | 0.1834192 | 15.92292 | 0.0758002 |
| 2017 | Exponential | 0.66741130 | 0.0000000 | 61.00000 | 0.2640437 |
| | Spherical | 0.6721993 | 0.0000000 | 61.00000 | 0.2621665 |
| | Gaussian | 0.6873072 | 0.0000000 | 61.00000 | 0.2732188 |

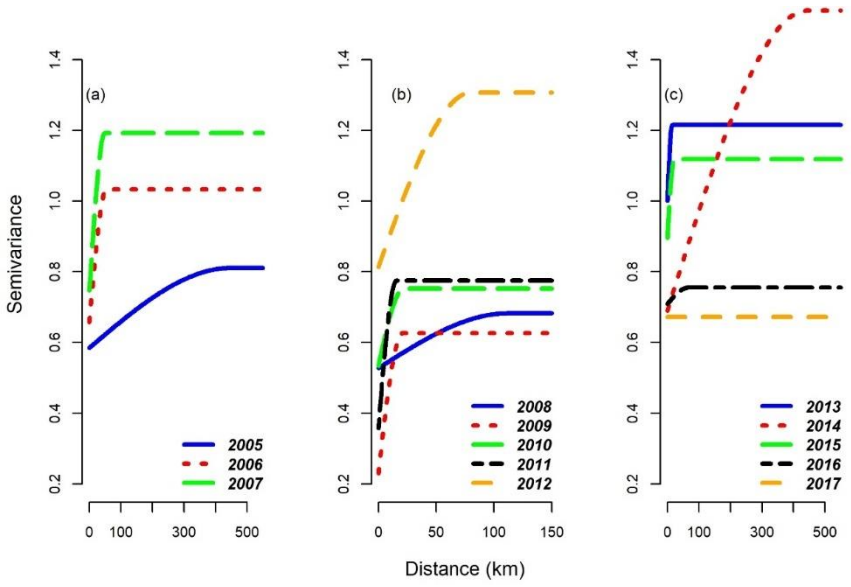


Figure 4.Yearly variograms of residues recorded for swordfish GLM catch by the Brazilian pelagic longline fleet. The time period 2005 to 2007 is represented in (A), 2008 to 2012 in (B) and 2013 to 2017 in (C).

The number of aggregations per year ranged from 16 and 546 (Table 6). Overall, the number of spots was larger than 174, except for 2005, 2008, 2014, which recorded aggregations lower than 100. Degree of spatial dependence was classified according to Zimback (2001) and it showed moderate autocorrelation in Swordfish fishing data, except for 2008, 2013, 2015 and 2017, when autocorrelations were weak.

Table 6. Number of aggregations and degree of spatial dependence (DSD) classification of swordfish caught by the Brazilian pelagic longline fleet between 2005 and 2017.

| Year | Aggregation (n°) | $DSD$ (%) | Classification ($DSD$) |
|---|---|---|---|
| 2005 | 26 | 28.18 | Moderate |
| 2006 | 353 | 36.27 | Moderate |
| 2007 | 475 | 37.48 | Moderate |
| 2008 | 98 | 23.22 | Low |
| 2009 | 546 | 63.47 | Moderate |
| 2010 | 422 | 30.54 | Moderate |
| 2011 | 499 | 58.19 | Moderate |
| 2012 | 170 | 37.88 | Moderate |
| 2013 | 274 | 16.36 | Low |
| 2014 | 16 | 54.67 | Moderate |
| 2015 | 356 | 19.50 | Low |
| 2016 | 247 | 39.71 | Moderate |
| 2017 | 204 | 0.02 | Low |

*Interannual distribution of fish densities with autocorrelation imputation*

The spatial-temporal variation of relative fish abundance index recorded from 2005 to 2017 highlighted high interannual variability (Figure 5). Despite data limitation recorded for some years (e.g. 2010, 2014 and 2017) and low geographic coverage, mainly in the central part of the study site (Figure 1 and 2, Appendix), this method can be used to predict fish aggregation by assuming its correlation to neighboring locations, i.e. catches are not independent.

The number of spots with density higher than 20 fish from 2005 to 2007 was relatively small if fish was distributed in oceanic regions close to longitudes -20° to -30° W. However, the highest densities were recorded in 2008, 2009 and 2012, in the central region of the study site (between latitudes -5°S and -35°S and longitude -30° W). In addition, despite the reduced analyzed fishing area in 2010 and 2011, results have pointed to increased density of specimens (>20 fish) in places presenting low density in previous years, except for oceanic regions close to Southern Brazil (latitudes below -30°S).

From 2013 onwards, fish density decreased (< 15 fish) in homogeneous distribution throughout the fishing area, except for 2014 and 2017, when there was sharp reduction in the predicted fishing area, mainly in regions considered suitable for high degree swordfish density.

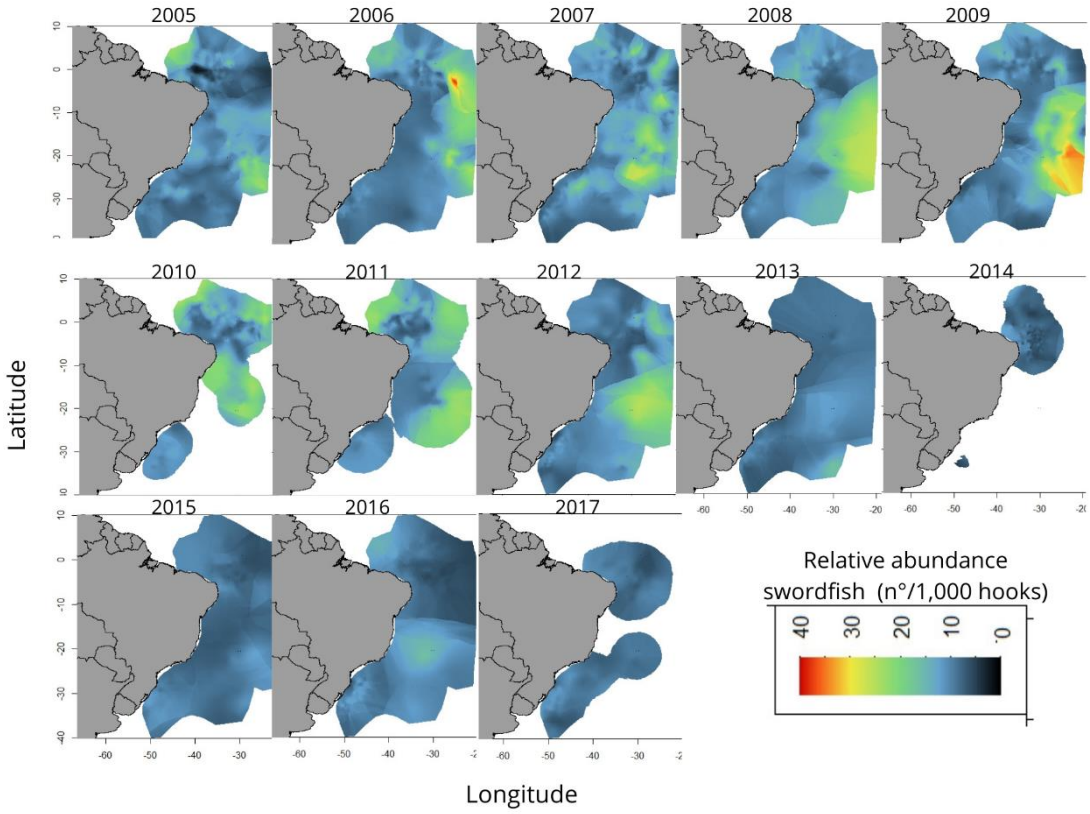


Figure 5. Space-time distribution of the relative abundance recorded for swordfish caught by the Brazilian pelagic longline fleet, between 2005 and 2017.

*Comparison of Relative Abundance Index*

Trends in Brazil's official standardized CPUE series and the herein estimated relative abundance set for South Atlantic swordfish are shown in Figure 6. The approach presented in 2022 accounted for high values at the beginning of the assessed period-of-time – the peak was reached in 1996 (1.581) -, and it was followed by downward trend until 2002 (0.901). There was slight increase in CPUE after this period, which remained relatively stable until 2015. From 2016 onwards, there was sharp drop in this value, which led to the lowest value ever recorded (0.628), in 2020 (Mourato et al., 2022). This result was similar to the trend found in the 2017 official swordfish standardization in comparison to the time when there was data overlapping (Carneiro et al., 2017).

The proposed indices showed consistently higher value than the official series between 2005 and 2010. In 2010, the proposed index value (1.2666) was significantly higher than that of the official series (1.06 and 1.11, respectively). After 2010, the proposed indices showed more significant downward trend than the official series. In 2013, the proposed index was 0.7965, whereas the official series reported 0.871. This divergence remained up to 2017.

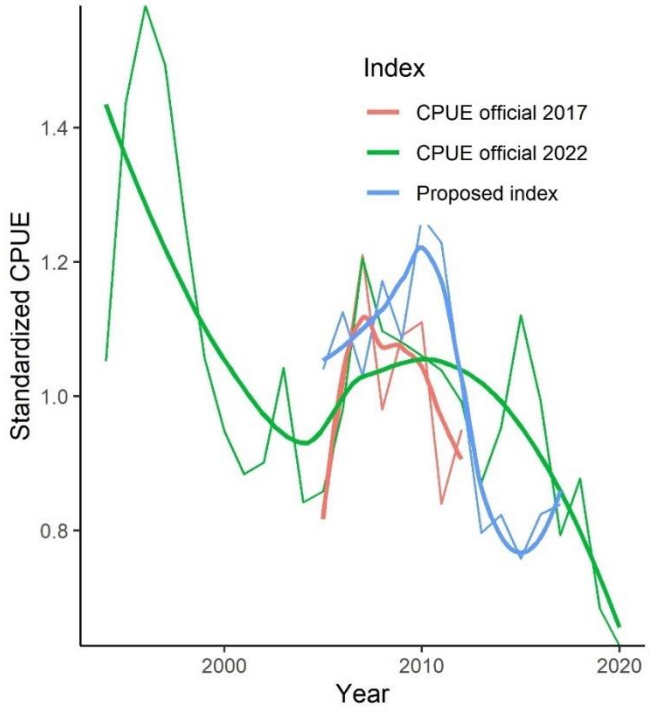


Figure 6. Abundance index expressed in number of individuals calculated by weighting the area of influence (Alternative index, blue) and the standardized catch rate - official CPUE 2017 (green) and official CPUE 2022 (orange-red) for swordfish caught by the Brazilian pelagic longline fleet. The thicker lines represent the smoothed trends of standardized CPUE over the years, while the thinner lines show the observed values of the proposed indices without smoothing.

## 4. Discussion

Heterogeneity of fishing data is one of the main challenges to standardize swordfish CPUE based on commercial fleet catch and effort (Maunder et al., 2020). Fishing effort spatial and temporal distribution, as well as vessels and fishing equipment features can significantly change over time and between regions (Maunder & Punt, 2004; Thorson, 2019). These factors can lead to CPUE under- or overestimation; consequently, they can affect the accuracy of calculated abundance indices. Additionally, spatial autocorrelation—such as the correlation between CPUE values across different locations or between travel times—further complicates accurate assessments (Berger et al., 2017; Jiao, et al., 2016, Hsu et al., 2022). Our study addresses these issues by applying geostatistical methods that incorporate spatial structure into CPUE standardization, thereby improving the reliability of abundance estimates.

Scientific data scarcity is another challenge to standardize CPUE of highly migratory marine species. Overall, fishing data are collected by fishers and can be influenced by factors such as the type of equipment used, fishing location, and the skills of the fishers (Maunder & Punt, 2004). In some cases, these data can be complemented by scientific data (Pinto et al., 2019;

Alglave et al., 2022), such as specimen sightings or captured-fish sampling. However, these scientific data are often scarce and they may not be enough to properly standardize CPUE (Thorson, 2019; Maunder et al., 2020; Alglave et al., 2022). Thus, optimizing fishery data analysis is essential to get reliable information about fish populations and to sustainably manage fishery resources.

An analysis protocol divided into three steps was herein developed to minimize several factors inherent to fishing-dependent data that directly or indirectly affect the efficiency of relative abundance indices based on catch per effort unit. The first step of the present study showed that the adopted pelagic longline catch data presented excess of zeros, so it was best modeled by MLGs with ZINB or HND distribution. Pelagic longline catch data may have presented excess of zeros due to several factors. Lack of fish in some areas or at some time of the year is a common factor resulting in zero catches on certain fishing lines (Walters, 2003). In addition, excess zeros can also result from inefficient fishing techniques, such as short fishing lines or inappropriate equipment. Other factors that may have contributed to over-zero include illegal fishing or under-reporting of catches (Thorson, 2019).

Analyses of residues modeled with ZINB carried out at the second step indicated that catches were not independent, since there were variations in the spatial distribution patterns of densities, over the years. Variogram parameters, mainly range, sill and nugget, showed significant variations throughout the study time, and this finding pointed towards the presence of spatial autocorrelation in the fishing data. This outcome has significant implications for conventional CPUE modeling and it can have several impacts on the accuracy of abundance indices, including the correlation between CPUE values at different locations or between temporal variations in fishing trajectories, between these locations (Thorson, 2019b). Identifying this year-specific spatial autocorrelation, as herein evidenced, is the way to emphasize the need of taking into consideration temporal variations in spatial autocorrelation at data analysis time (Ducharme-Barth et al., 2022).

The range parameter (a), which measures the distance over which spatial correlation persists before variance stabilizes, is critical for understanding the spatial distribution and aggregation patterns of swordfish. Studying variations in this parameter is essential for accurately interpreting changes in stock dynamics. Swordfish, like many highly migratory species, exhibit varying degrees of spatial dependence across years (Chang et al., 2012). In this study, the significant changes in range observed—such as the longer distances in 2005, 2008, 2012, and 2014 (ranging from 80 km to 456 km) and the shorter distances in 2011 and 2013 (averaging 15.45 km)—reflect shifts in the species' aggregation over time.

Incorporating these spatial dynamics into abundance indices is crucial, as it provides a more nuanced understanding of stock status (Hoyle et al., 2024). Without accounting for these variations, conventional abundance indices may overlook important spatial patterns, leading to

inaccurate estimates of population size and trends (Campbell, 2016; Ducharme-Barth et al., 2022). By integrating the range parameter into CPUE standardization models, we can better capture the complexity of swordfish spatial behavior, resulting in more precise and reliable stock assessments. This, in turn, supports more informed decision-making and management strategies for the conservation and sustainable exploitation of swordfish populations in the South Atlantic.

The analysis evidenced that the nugget effect changed over the years, and it showed more expressive values from the initial years until 2007, and at the end of the 2012-2017 time series. This variation highlights that data from these years showed higher degree of randomness and uncorrelated variability, which were not explainable by spatial dependence or structure. A likely explanation for this variation lies on the influence of environmental factors that affect swordfish distribution. Species' distribution can be significantly influenced by oceanographic conditions, such as temperature, currents and water masses, which account for yearly fluctuations and have impact on swordfish distribution and abundance (Chang et al., 2012; Elepathage et al., 2019). Changes in fishing practices, equipment and regulations may also have contributed to the observed variability in the nugget effect.

*Interannual distribution in fish densities with autocorrelation imputation*

According to the results, there was increase and decrease in fish density, in specific regions. Increase in the density of larger fish was observed in the central region of the study site between 2010 and 2011, except for oceanic areas close to Southern Brazil. However, from 2013 onwards, there was general decrease in the density of the analyzed fish, except for 2014 and 2017, when there was even higher reduction in the predicted fishing area, mainly in regions seen as suitable for high degree of swordfish fish density.

The herein used disaggregated latitude and longitude in swordfish fishing data allowed better representing these data's spatial distribution and identifying areas accounting for the highest concentration of fish. This finding is essential to assess the impact of fishing on fish communities and on marine habitats (Mauder et al., 2020).

This species' behavior can influence its spatial distribution in the South Atlantic. Studies have shown that swordfish shows spatial aggregation patterns that can change, overtime (Chang et al., 2012). Furthermore, this species may present different spatial distribution patterns at different life stages and in different geographic regions (Reuchlin-Hugenholtz, 2015); therefore, it is important taking these factors into consideration to analyze swordfish spatial distribution in the South Atlantic.

*Comparison of Relative Abundance Index*

According to ICCAT, the CPUE series set for swordfish in the South Atlantic showed varying trends, overtime (ICCAT, 2022). Some series show downward trends, as observed in

Brazil (Mourato et al., 2022), whereas others show discrete upward trend (Spain) (Ramos-Cartelle, et al., 2021) or stability (China Taipei and South Africa) (ICCAT, 2022). It is important considering these different trends to assess swordfish stocks and to plan fishery management applied to this species.

Discrepancies in CPUE data of South Atlantic swordfish can be largely attributed to factors related to the species' spatial distribution, as well as to environmental factors. The most recent South Atlantic swordfish stock assessment report recommended using PSAT (Pop-up Satellite Archival Tag) data at maximum spatial resolution (1° x 1° latitude and longitude) to get detailed information on swordfish spatial dynamics, stock distribution, as well as to assess alternatives to include these variables in stock assessment processes (ICCAT, 2023). This approach is expected to significantly reduce conflicting abundance indices related to temperature and tropical regions, thereby contributing to more accurate stock assessments. However, the scarcity of reliable data in many member countries makes it difficult to conduct studies in this crucial field (ICCAT, 2023). Therefore, it is essential to explore alternative approaches that use data of commercial fleets and that take into account the species' spatial distribution structure. The combination of spatially explicit statistical methods, such as that proposed by Woillez et al. (2009), in association with other standardization techniques may be a viable strategy for improving the accuracy of stock assessments and enhancing our understanding of the species' population dynamics.

Over the past 20 years, Brazil has worked to improve and develop a standardized CPUE series for swordfish species. However, it is important to emphasize that most of these standardized series were not included in models aimed at assessing swordfish stocks in the South Atlantic due to high interannual variability and divergences to other South Atlantic swordfish abundance indices (ICCAT, 2010, 2014, 2017). In summary, this series presented assessments carried out in 2010 and 2014, and showed significant fluctuations, overtime, with upward trend from the 2000s onwards (Hazin et al., 2010; Hazin et al., 2014). Assumingly, the observed patterns were the reflection of the Brazilian fleet's heterogeneous composition. The Brazilian fleet has experienced technological improvements, increased fishing effort and changes in the fishing target to catch swordfish and blue shark, to the detriment of the species' biomass trend (Rodrigues, et al., 2020; Hazin et al., 2010; ICCAT, 2010; 2014).

In 2017, the CPUE series was divided into two parts, namely: before and after the Onboard Observer Program for chartered vessels, as reported by Carneiro et al. (2017). This division proved necessary due to the high variability observed in the first part of the Brazilian CPUE series (from 1978 to 2004), which did not present clear temporal trend and was conflicting to other assessment indices presented to the stock management body (ICCAT, 2017). Accordingly, only the second part of the Brazilian CPUE series (from 2005 to 2012) was used in the stock assessment model.

In 2022, there was improvement in the Brazilian swordfish data standardization. It was the

first time a more extensive time series (1994 to 2020) was included in the stock assessment model, as mentioned by Mourato et al. (2022). Results showed that the swordfish CPUE remained relatively stable until 2015, and it decreased steadily until the end of the 2020 time series. Despite the observed advancements, discrepancies and questions related to the quality of data provided to managers remain.

The swordfish abundance index presented here showed a sharp decline in fish density from 2010 onwards. Overall, the proposed index indicated a decline in swordfish abundance before that detected 497 by the official CPUE. This finding is consistent with other CPUE series submitted by ICCAT member countries for swordfish stock assessment, but differs from the official results presented by Brazil to the commission.

The discrepancy found between the abundance estimation model proposed in the present study and Brazil's official catch rate from 2022 may be the result of lack of disaggregated data, such as latitude and longitude. Mourato et al. (2022) used aggregated coordinates (coordinates with 5º small area data) in the last CPUE standardization of the Brazilian Fleet Swordfish reported to ICCAT and it can lead to CPUE index under- and over-estimation because it does not take into account the spatial variation in small-area data (Mauder et al., 2020). Using the long but low-resolution standardized CPUE series can provide information about general trends of fish populations, over time. However, it can limit the understanding of more detailed spatial and temporal variations capable of mitigating short-term changes in abundances and of affecting the decision-making and management of these populations (Cadrin, 2020; Mauder et al., 2020). The statistical methods presented in this study revealed a general downward trend in swordfish abundance, detected earlier than with conventional approaches. These indices provide a potentially more accurate perspective on swordfish population dynamics in the South Atlantic, underscoring the importance of employing multiple methodologies to assess the abundance of marine species more effectively.

## 5. Conclusions

In conclusion, both analyzed series indicated a reduction in swordfish abundance over time. This negative trend suggests a likely imminent stock depletion, which could have significant ecological and socioeconomic consequences. However, there are major challenges in managing the Brazilian fleet, including the need for refined data, such as reliable information sources made up of environmental variables and more accurate details of equipment and fishing strategies used in each trip. In addition to improving data collection, the recent analyses have shown a significant reduction in HPB data, which impairs the ability to estimate more robust abundance indices.

## 6. References


Akaike, H. (1973). Information theory and an extension of the maximum likelihood principle. In Petrov, B.N., Csaki, F. (Eds.), Proceedings of the 2nd International Symposium on Information Theory. Publishing House of the Hungarian Academy of Sciences, Budapest, p. 268–281.

Achim, Z., Torsten, H. (2002). Diagnostic Checking in Regression Relationships. R News 2(3), 7-10. URLhttps://CRAN.R-project.org/doc/Rnews/.

Alglave, B., Rivot, E., Etienne, M. P., Woillez, M., Thorson, J. T., & Vermard, Y. (2022). Combining scientific survey and commercial catch data to map fish distribution. ICES Journal of Marine Science, 79(4), 1133-1149. https://doi.org/10.1093/icesjms/fsac032

Armines. (2022). RGeostats: The Geostatistical R Package. Version: 14.0.5. Free download from:http://cg.ensmp.fr/rgeostats.

Berger, A. M., et al. (2017). Space oddity: the mission for spatial integration. Canadian journal of fisheries and aquatic sciences, 74(11), 1698-1716. https://doi.org/10.1139/cjfas-2017-0150.

Burnham, K. P., & Anderson, D. R. (2004). Multimodel Inference: Understanding AIC and BIC in Model Selection. *Sociological Methods & Research, 33*(2), 261–304. https://doi.org/10.1177/0049124104268644.

Cadrin, S. X. (2020). Defining spatial structure for fishery stock assessment. Fisheries Research, 221, 105397. https://doi.org/10.1016/j.fishres.2019.105397.

Campbell, R.A. (2004). CPUE standardization and the construction of indices of stock abundance in a spatially varying fishery using general linear models. Fisheries Research, 70(2-3), 209-227. https://doi.org/10.1016/j.fishres.2004.08.026.

Campbell, R. A. (2016). A new spatial framework incorporating uncertain stock and fleet dynamics for estimating fish abundance. Fish and Fisheries, 17(1), 56-77. https://doi.org/10.1111/faf.12091

Carneiro, V. G., Rodrigues, S.L., Oliveira, E.S.C., & Andrade, H.A. (2017). Updated standardized catch rate of swordfish (xiphias gladius) caught in the south atlantic by the brazilian fleet. Collect. Vol. Sci. Pap. ICCAT, 74(3), 1050-1069.

Chang, Yi-Jay et al. (2012). Habitat suitability analysis and identification of potential fishing grounds for swordfish, Xiphias gladius, in the South Atlantic Ocean. International journal of remote sensing, 33(23), 7523-7541. https://doi.org/10.1080/01431161.2012.685980.

Chang, J., Shank, B.V., & Hart, D. R. (2017). A comparison of methods to estimate abundance and biomass from belt transect surveys. Limnology and Oceanography: Methods, 15(5), 480-494. https://doi.org/10.1002/lom3.10174

Chen, Y. et al. (2016). A comparative study of spatial interpolation methods for determining fishery resources density in the Yellow Sea. Acta Oceanologica Sinica, 35, 65-72. https://doi.org/10.1007/s13131-016-0966-y

Conn, P. B., Thorson, J. T., & Johnson, D.S. (2017). Confronting preferential sampling when analysing population distributions: diagnosis and model-based triage. Methods in Ecology and Evolution, 8(11), 1535-1546. https://doi.org/10.1111/2041-210X.12803

Crespo, G. O., Dunn, D. C., Reygondeau, G., Boerder, K., Worm, B., Cheung, W., Tittensor, D. P., & Halpin, P. N. (2018). The environmental niche of the global high seas pelagic longline fleet. Science Advances, 4(8), eaat3681. https://doi.org/10.1126/sciadv.aat3681

Dobson, A.J., Barnett, A. An introduction to generalized linear models. CRC press, 2008.

Ducharme-Barth, N. D., Grüss, A., Vincent, M. T., Kiyofuji, H., Aoki, Y., Pilling, G., ... & Thorson, J. T. (2022). Impacts of fisheries-dependent spatial sampling patterns on catch-per-unit-effort standardization: a simulation study and fishery application. Fisheries Research, 246, 106169. https://doi.org/10.1016/j.fishres.2021.106169

Elepathage, T. S. M., Tang, D., & Oey, L. (2019). The pelagic habitat of swordfish (Xiphias gladius) in the changing environment of the North Indian Ocean. Sustainability, 11(24), 7070. https://doi.org/10.3390/su11247070

Gräler, B., Pebesma, E., & Heuvelink, G. (2016). Spatio-Temporal Interpolation using gstat. The R Journal, 8(1), 204-218.

Hartig, F. (2022). DHARMa: Residual Diagnostics for Hierarchical (Multi-Level / Mixed) Regression Models. R package version 0.4.6. https://CRAN.R-project.org/package=DHARMa

Hazin, H.G., Minte-Vera, C.V., Hazin, F., Travassos, P., Carvalho,F. , Mourato, B.(2010). Standardized Cpue Series Of Swordfish, Xiphias Gladius, Caught By Brazilian Tuna Fisheries In The Southwestern Atlantic Ocean. Collect. Vol. Sci. Pap. ICCAT, 65(1): 274-284.

Hazin, H . G., Hazin, F.H.V., Mourato, B., Carvalho, F. and Frédou, T. (2014). Standardized catch rates of swordfish (Xiphias gladius) caught by the Brazilian fleet (1978- 2012) using Generalized Linear Mixed Models (GLMM) using Delta log approach. Collect. Vol. Sci. Pap. ICCAT, 70(4): 1875-1884.

He, X., Bigelow, K. A., & Boggs, C. H. (1997). Cluster analysis of longline sets and fishing strategies within the Hawaii-based fishery. Fisheries Research, 31(1), 147-158. https://doi.org/10.1016/S0165-7836(96)00564-4

Hilborn, R., & Walters, C. J. (1992). Quantitative fisheries stock assessment: choice, dynamics and uncertainty. London: Chapman and Hall.

Hoyle, S. D., Campbell, R. A., Ducharme-Barth, N. D., Grüss, A., Moore, B. R., Thorson, J. T., ... & Maunder, M. N. (2024). Catch per unit effort modelling for stock assessment: A summary of good practices. *Fisheries Research*, *269*, 106860.

Hsu, J., Chang, Y. J., & Ducharme-Barth, N. D. (2022). Evaluation of the influence of spatial treatments on catch-per-unit-effort standardization: A fishery application and simulation study of Pacific saury in the Northwestern Pacific Ocean. Fisheries Research, 255, 106440. https://doi.org/10.1016/j.fishres.2022.106440

ICCAT. (2010). Report of the 2009 ICCAT- Atlantic swordfish data preparatory session. Collect. Vol. Sci. Pap. ICCAT, 65(1): 1-123.

ICCAT. (2014). Report of the 2013 ICCAT- Atlantic swordfish data preparatory session. Collect. Vol. Sci. Pap. ICCAT, 70(4): 1365-1483.

ICCAT. (2017). Report of the 2017 ICCAT- Atlantic swordfish data preparatory session. Collect. Vol. Sci. Pap. ICCAT, 74(3): 841-967.

ICCAT. (2022). Report of the 2022 ICCAT- Atlantic swordfish data preparatory session. Collect. Vol. Sci. Pap. ICCAT, 79(2), 001-133.

ICCAT. (2023). Report for the Biennial Period, 2022-2023, Part I (2022). SCRS PLENARY SESSIONS 1 – 9.4 , Madrid, Spain.

Jiao, Y., O'Reilly, R., Smith, E., & Orth, D. (2016). Integrating spatial synchrony/asynchrony of population distribution into stock assessment models: a spatial hierarchical Bayesian statistical catch-at-age approach. ICES Journal of Marine Science: Journal du Conseil, 73, 1725-1738. https://doi.org/10.1093/icesjms/fsw036.

Kleisner, K. M., Walter, J. F., Diamond, S. L., & Die, D. J. (2010). Modeling the spatial autocorrelation of pelagic fish abundance. Marine Ecology Progress Series, 411, 203–213. https://doi.org/10.3354/meps08667

Lambert, D. (1992). Zero-inflated Poisson regression, with an application to defects in manufacturing. Technometrics, 34(1),1-14.

Lira, M. G., de Nóbrega, M. F., Oliveira, J. E. L (2017). Caracterização da pescaria industrialde espinhel-de-superfície no Rio Grande do Norte. Boletim do Instituto de Pesca, 43(3), 446-458. Doi: 10.20950/1678-2305.2017v43n3p446

McCullagh, P., & Nelder, J. A. (1989). Generalized linear models. London: Chapman and Hall.

Maunder, M. N., & Punt, A. E. (2004). Standardizing catch and effort data: a review of recent approaches. Fisheries Research, 70(2), 141-159.

https://doi.org/10.1016/j.fishres.2004.08.002

Maunder, M. N., Thorson, J. T., Xu, H., Oliveros-Ramos, R., Hoyle, S. D., Tremblay-Boyer, L., ... & Piner, K. R. (2020). The need for spatio-temporal modeling to determine catch-per-unit effort based indices of abundance and associated composition data for inclusion in stock assessment models. Fisheries Research, 229, 105594. https://doi.org/10.1016/j.fishres.2020.105594

Morfin, M., Fromentin, J. N., Jadaud, A., & Bez, N. (2012). Spatio-Temporal Patterns of Key Exploited Marine Species in the Northwestern Mediterranean Sea. PLoS one, 7(5), e37907. doi: 10.1371/journal.pone.0037907.

Mourato, B., Sant'ana, R., Gustavo Cardoso, L., & Travassos, P. (2022). Catch rates of swordfish from Brazilian longline Fisheries in the South Atlantic (1994-2020). Collect. Vol. Sci. Pap. ICCAT, 79(2), 335-346.

Mullahy, J. (1986). Specification and testing of some modified count data models. Journal of econometrics, 33(3), 341-365.

Pinto, C., Travers-Trolet, M., Macdonald, J. I., Rivot, E., & Vermard, Y. (2019). Combining multiple data sets to unravel the spatiotemporal dynamics of a data-limited fish stock. Canadian Journal of Fisheries and Aquatic Sciences, 76(8), 1338-1349. https://doi.org/10.1139/cjfas-2018-0149

Punt, A. E. (2019). Spatial stock assessment methods: A viewpoint on current issues and assumptions. Fisheries Research, 213, 132-143. https://doi.org/10.1016/j.fishres.2019.01.014

Ramos-Cartelle, A., Fernández-Costa, J., García-Cortés, B., & Mejuto-García, J. (2021). Updated standardized catch rates for south atlantic stock of Swordfish (xiphias gladius) from the spanish longline fleet for the Period 1989-2019. Collect. Vol. Sci. Pap. ICCAT, 78(7), 111-121.

R Core Team (2022). R: A language and environment for statistical computing. R Foundation for Statistical Computing, Vienna, Austria. URL https://www.R-project.org/.

Reuchlin-Hugenholtz, E., Shackell, N. L., & Hutchings, J.A. (2015). The potential for spatial distribution indices to signal thresholds in marine fish biomass. PLoS One, 10(3), e0120500. https://doi.org/10.1371/journal.pone.0120500.

Rodrigues, S. L., Carneiro, V. G. O., de FREITAS, A. J. R., & de ANDRADE, H. A. (2020). Spatiotemporal variability of target-species in tuna and tuna-like fishing in Brazil. Boletim do Instituto de Pesca, 46(2): e587. https://doi.org/10.20950/1678-2305.2020.46.2.587

Saraux, C., Fromentin, J. M., Bigot, J. L., Bourdeix, J. H., Morfin, M., Roos, D., Beveren, E. V., & Bez, N. (2014). Spatial Structure and Distribution of Small Pelagic Fish in the Northwestern Mediterranean Sea. PloS one, 9(11), e111211. https://doi.org/10.1371/journal.pone.0111211.

Saul, S.E., Walter, S. F., Die, D. J., Naar, D.F., & Donahue, B.T. (2013). Modeling the spatial distribution of commercially important reef fishes on the West Florida Shelf. Fisheries Research, 143, 12–20. https://doi.org/10.1016/j.fishres.2013.01.002.

Thorson, J. T., Rindorf, A., Gao, J., Hanselman, D. H., & Winker, H. (2016). Density-dependent changes in effective area occupied for sea-bottom-associated marine fishes. Proceedings of the Royal Society B: Biological Sciences, 283(1840), 20161853. https://doi.org/10.1098/rspb.2016.1853

Thorson, J. T. (2019) Guidance for decisions using the Vector Autoregressive Spatio-Temporal (VAST) package in stock, ecosystem, habitat and climate assessments. Fisheries Research, 210, 143-161. https://doi.org/10.1016/j.fishres.2018.10.013

Thorson, J.T. (2019b) Measuring the impact of oceanographic indices on species distribution shifts: The spatially varying effect of cold-pool extent in the eastern Bering Sea. Limnology and Oceanography, 64(6), 2632-2645. https://doi.org/10.1002/lno.11238. https://onlinelibrary.wiley.com/doi/abs/10.1002/lno.11238〉.

Thorson, J. T., Adams, C. F., Brooks, E. N., Eisner, L. B., Kimmel, D. G., Legault, C. M.,

... & Yasumiishi, E. M. (2020). Seasonal and interannual variation in spatio-temporal models for index standardization and phenology studies. ICES Journal of Marine Science, 77(5), 1879-1892. https://doi.org/10.1093/icesjms/fsaa074.

Venables, W. N., & Ripley, B. D. (2002) Modern Applied Statistics with S. Fourth Edition. Springer, New York. ISBN 0-387-95457-0.

Vignaux, M. (1996) Analysis of spatial structure in fish distribution using commercial catch and effort data from the New Zealand hoki fishery. Canadian Journal of Fisheries and Aquatic Sciences, 53, 963-973. https://doi.org/10.1139/f96-035

Xu, L., Chen, X., Guan, W., Tian, S., & Chen, Y. (2018). The impact of spatial autocorrelation on CPUE standardization between two different fisheries. Journal of Oceanology and Limnology, 36(3), 973-980. https://doi.org/10.1007/s00343-018-6294-7

Walters, Carl. (2003). Folly and fantasy in the analysis of spatial catch rate data. Canadian Journal of Fisheries and Aquatic Sciences, 60(12), 1433-1436. https://doi.org/10.1139/f03-15

Woillez, M. et al. (2007). Indices for capturing spatial patterns and their evolution in time, with application to European hake (Merluccius merluccius) in the Bay of Biscay. ICES Journal of Marine Science, 64, 537-550. https://doi.org/10.1093/icesjms/fsm025

Woillez, M., Rivoirard, J., & Petitgas, P. (2009). Notes on survey-based spatial indicators for monitoring fish populations. Aquatic Living Resources, 22(2), 155-164. https://doi.org/10.1051/alr/2009017

Yu, H., Jiao, Y., & Carstensen, L. W. (2013). Performance comparison between spatial interpolation and GLM/GAM in estimating relative abundance indices through a simulation study. Fisheries Research, 147, 186-195. https://doi.org/10.1016/j.fishres.2013.06.002

Zeileis, A. et al. (2008). Regression models for count data in R. Journal of Statistical Software, 27(8). http://www.jstatsoft.org/v27/i08/

Zimback, C.R.L. (2001). Análise espacial de atributos químicos de solos para fins de mapeamento da fertilidade do solo. Tese (Livre-Docência) - Faculdade de Ciências Agronômicas, Universidade Estadual Paulista, Botucatu.

## 3. ARTIGO CIENTÍFICO 2: Spatial sexual segregation of migratory marine species: implications for the sustainable management of swordfish and bigeye tuna in the Southwest Atlantic Ocean

Silvaneide Luzinete Rodrigues*, Lucas Vinícius Santos Silva, Humber Agrelli de Andrade

Universidade Federal Rural de Pernambuco. Departamento de Pesca e Aquicultura, Programa de Pós-graduação em Recursos Pesqueiros e Aquicultura, Recife – PE, Brasil.

*corresponding author: silvaneide.pescaufrpe@gmail.com

E-mail
Silvaneide L. Rodrigues: silvaneide.pescaufrpe@gmail.com
Lucas V. S. Silva: contatolucassantoss@gmail.com
Humber A. Andrade: humber.andrade@gmail.com

ORCID
Silvaneide L. Rodrigues: http://orcid.org/0000-0002-1204-5818
Lucas V. S. Silva: https://orcid.org/0000-0003-0291-9793
Humber A. Andrade: https://orcid.org/0000-0002-4221-8441

## Abstract

Gender differences in spatial organization and resource utilization constitute a fundamental area of investigation in species ecology and conservation. However, delving into this topic concerning migratory marine species, such as tunas and related species, has been hampered by the significant challenges associated with the high cost of research. This study aims to analyze the spatial distribution patterns between the sexes of the swordfish (*Xiphias gladius*) and bigeye tuna (*Thunnus obesus*) in the Southwestern Atlantic Ocean, filling a crucial knowledge gap for the conservation and sustainable management of fishery stocks. Using data from the fishing operations of the Brazilian pelagic longline fleet, contained in the Brazil Onboard Observer Program (PROBORDO), we analyzed 232,887 swordfish fishing sets and 39,161 for bigeye tuna, from 2005 to 2011. The results indicate that the proportions of female swordfish were significantly higher in the southern sector of Brazil, with the overall proportion of females reaching 41.5% (95% CI: 39.7% to 43.5%), while males predominated in the western equatorial sector. Swordfish median fork length ranged from 150 cm in 2007 (the highest value) to 137 cm in 2009, with a general trend of a greater presence of females in size classes above 180 cm. On the other hand, bigeye tuna showed a predominance of males throughout the study area, except in 2006, when the proportion of females increased in specific tropical regions. The average length of bigeye tuna ranged between 200 cm and 250 cm, with the proportion of females varying from 25% to 87%, predominantly in the length classes around 200 cm. This peculiarity in bigeye tuna catch dynamics suggests the influence of unique ecological and behavioral factors, as well as specific fishing practices in the study area. These findings highlight the importance of a detailed understanding of species interactions in mixed fisheries and the need to consider management strategies adapted to this complex dynamic to ensure the sustainability of bigeye tuna and swordfish populations in the studied region.

**Keywords:** tuna, conservation, spatial distribution, sexual segregation.

## 1. INTRODUCTION

Sexual segregation in species occurs when individuals of different sexes exhibit distinct patterns of spatial distribution and resource use, occupying specific areas during certain periods or life stages (Wearmouth & Sims, 2008). This phenomenon is common across various aquatic taxa, including sharks (Mucientes et al., 2009; Vandeperre et al., 2014; Fujinami et al., 2022), marine mammals (Ruckstuhl & Neuhaus, 2002; Leung et al., 2012; Baylis et al., 2016; Hawkins et al., 2020), sea turtles (Van Dam et al., 2008; Beal et al., 2022), and seabirds (Orgeret et al., 2021). Sexual differences in body size, behavior, nutritional needs, and habitat selection (Wearmouth & Sims, 2008) can influence population dynamics, genetic structure, and the resilience of marine species (Leung et al., 2012; Lombal et al., 2020). Therefore, understanding these patterns and the mechanisms relying sexual segregation is essential for implementing appropriate management strategies and conserving fishery stocks.

Despite the study of sexual segregation in aquatic species gaining attention in recent decades, there remains a significant knowledge gap regarding spatial sexual segregation in many marine species, especially those with high migratory capacity, such as tunas and related species (ICCAT, 2017; Mejuto, 2018). While some studies have investigated the spatial distribution of these species across various regions, differentiated behavior by size and sex has not been adequately documented. This is partly due to limitations in obtaining data with broad geographic coverage, the difficulty associated with capturing, handling, and dissecting large fish, as well as the scarcity of laboratory samples, often due to the high cost per fish unit (ICCAT, 2017; Mejuto, 2018; Alglave et al., 2022).

Among tuna and related species, whose gender patterns in spatial organization are poorly understood, swordfish (*Xiphias gladius*) and bigeye tuna (*Thunnus obesus*) stand out. These cosmopolitan species hold significant global ecological, economic, and social relevance (Erauskin-Extramiana et al., 2019; FAO, 2022). They play key roles as top predators in the marine food chain, controlling prey populations (Casini et al., 2009; Estes et al., 2011). Moreover, both swordfish and bigeye tuna are important targets for commercial and sport fishing, contributing substantially to local and regional economies (Hazin & Travassos, 2007; Lira et al., 2017; Rodrigues et al., 2020; Mourato et al., 2022).

Considering their economic importance, many stocks of tuna and related species are at alarmingly low levels of sustainability. The latest assessment by the International Commission for the Conservation of Atlantic Tunas (ICCAT) indicates that swordfish and bigeye tuna are nearing the reference points for maximum sustainable yields (MSY)

(ICCAT, 2024). This situation is further worsened by their status on the IUCN Red List, which classifies these species as near threatened and vulnerable, respectively (Collette et al., 2021; Collette et al., 2022). The lack of data on their biology and population dynamics, such as spatial distribution by size and sex, hinders effective decision-making for stock management and threatens the long-term survival of these species.

In the South Atlantic, Brazil encompasses the largest Exclusive Economic Zone (EEZ) and is responsible for the highest catches of swordfish and tuna in the southwestern portion (ICCAT, 2022). The Brazilian fleet, developed domestically, also included leased vessels from various flags, operating for different time periods. This heterogeneous fleet composition resulted in significant variability in fishing targets and technologies used over the decades (Rodrigues et al., 2020). To provide essential information for conservation and fisheries management, Brazil implemented the Brazil Onboard Observer Program (PROBORDO) between 2005 and 2011. The program aimed to collect detailed data on fishing activities and monitor the compliance of leased vessels with both national and international regulations.

Given the scarcity of scientific data obtained through fish sampling during scientific cruises (Pinto et al., 2019; Alglave et al., 2022), it becomes essential to investigate spatial distribution and differentiated resource use by sex using commercial fishing data to better understand the population dynamics and behavioral patterns of aquatic species. Based on this need, the present study aims to investigate the spatial sexual segregation of swordfish and bigeye tuna in the southwestern Atlantic region, using data from PROBORDO. The research seeks to identify potential areas of overlap and sexual segregation, with the goal of providing critical information for the development of sustainable management strategies. From the results obtained, we hope to contribute to the improvement of conservation and management measures, emphasizing the importance of continuous monitoring and adapting fishing strategies to the specific characteristics of each species.

## 2. METHODOLOGY

*Data*

The data used in the analyses, which pertains to fishing operations conducted by the Brazilian pelagic longline fleet, comes from the national onboard observer program (PROBORDO), maintained by the Secretariat of Aquaculture and Fisheries (SAP) within the Ministry of Fisheries and Aquaculture (MPA). PROBORDO exclusively monitored

leased foreign-flagged vessels operating under Brazilian agreements and was in effect to monitor these vessels between late 2005 and 2011. This program covered a portion of the fishing trips, resulting in a vast source of data on target species catches and fishing strategies.

The database contains information related to fish lengths, sex, vessel name, flag, geographical location (latitude and longitude), as well as the date and time of longline setting and retrieval. PROBORDO includes 626,241 fishing set records, distributed between latitudes 10º N and 40º S. In the present study, 232,887 fishing set records for swordfish and 39,161 for bigeye tuna were analyzed (Table 1).

*Table 1. Annual number (n) of fishing set records for swordfish (SWO) and bigeye tuna (BET).*

| Year | SWO (n) | BET (n) |
|---|---|---|
| 2005 | 11,958 | 4,414 |
| 2006 | 35,644 | 9,122 |
| 2007 | 123,857 | 4,221 |
| 2008 | 24,003 | 9,833 |
| 2009 | 1,734 | 1,920 |
| 2010 | 24,690 | 5,430 |
| 2011 | 11,001 | 4,221 |
| Total | 232,887 | 39,161 |

*Modelling*

For the analysis of the variation in lower jaw length to fork length (LJFL) of swordfish and fork length (FL) of bigeye tuna, analyses were conducted on data grouped by year, month, flag, and sex. Subsequently, a generalized linear model (GLM) was employed to study the relationship between length and the explanatory variables “year,” “flag,” “month,” and “sex” (considered as factors), as well as latitude, longitude, and the interaction between these continuous variables. The initial structure of the model was defined as:

$$length \sim (lat^2 + sex + year + month + lon^2)$$

which “length” is the continuous response variable. The model was fitted using the Gaussian family and the identity link.

Sex ratios were evaluated for the data grouped overall, by year, and by month. For this variation, maps were also constructed in 5°x5° squares (latitude x longitude). The binomial test (Hollander & Wolfe, 1973) was used to assess the hypothesis that the proportions of females and males were equal. A Generalized Linear Model (GLM) was employed to study the relationship between sex ratio, year, lengths, month, flag, and the geographical position where the longline was deployed in the water. The sex of the fish (female or male) was the response variable. The number of successes (e.g., female) and failures (e.g., male) were modeled following a binomial distribution. The explanatory variables “year,” “flag,” and “month” were all considered categorical (factors), while lengths, latitude, and longitude were included in the models as continuous variables (covariates). The structure of the initial full model, incorporating all available explanatory variables from PROBORDO, was selected to allow for the calculation of joint effects of year, flag, month, latitude, and longitude, including interactions. Preliminary analyses indicated that the relationship between sex ratio and latitude and longitude was not linear; therefore, the square of latitude ($lat^2$) and longitude ($lon^2$) were also considered as explanatory variables to account for non-linear effects. The initial model for swordfish and bigeye tuna fitted to the data was:

$$(ns, nf) \sim (year + length + month + lat^2 + lon^2)$$

which $ns$ e $nf$ represent the number of successes (females) and the number of failures (males). The link function was logit. After fitting the model, a backward approach based on the Akaike Information Criterion (Akaike, 1974) was used to select the variables and the final model for both the length models and the sex ratio models.

Spatial distribution of length

Maps in 5°x5° squares (latitude x longitude) were created to represent the spatial distribution of fish lengths. Lengths were classified into three categories: 'small,' 'intermediate,' and 'large,' using the quantiles of the length distribution of captured fish. The boundaries between these categories were defined based on the quantile values, dividing the sample into thirds. The first third of the distribution corresponded to the 'small' category, the intermediate third to the 'intermediate' category, and the upper third

to the 'large' category. The proportions of fish in each length range were represented by pie charts in each spatial cell, reflecting the percentages of individuals in each category. This approach allows for a clear visualization of the spatial variation in the size structure of the studied species, with data derived from the PROBORDO database.

Spatial distribution of male and female proportion

To visualize the distribution of male and female proportions, contour maps (5°x5° squares) were generated annually, monthly, and by flag, with each map representing the average predictions of sex ratio (prop) for the combinations of year, month, flag, latitude, and longitude. The proportion values were represented by a color scale, ranging from blue (female dominance) to red (male dominance), with the color transitions indicating the spatial and temporal variation in sexual composition. The contour lines over the colored representations clearly delineate the proportion of females in the population, allowing for a precise visualization of the variation in sexual composition over time and space. All analyses were conducted using R software (version 4.4.1, R Core Team, 2024).

## 3. **RESULTS**

Most of the sampled fish were captured west of the 20° W meridian in the equatorial region or in the area between 10–25° S and 25–30° W (Figure 1). In the extreme south, the sample size in the area located between the limits of 25–30° S and 40–45° W was relatively high for swordfish (Figure 1a) but extremely low for bigeye tuna (Figure 1b).

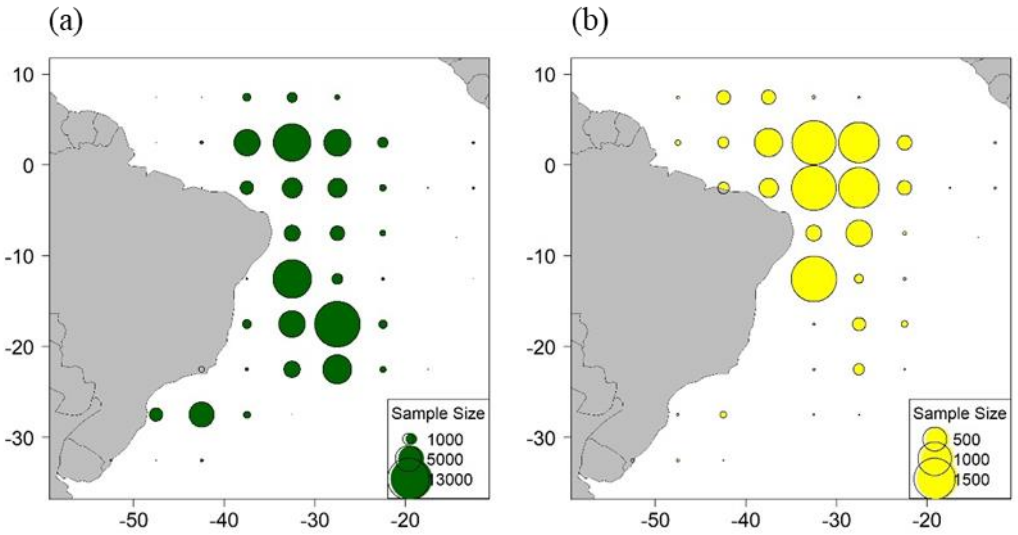


*Figure 1. Distribution of swordfish (a) and bigeye tuna (b) sampled by the Brazilian pelagic longline fleet between 2005 and 2011.*

There are data related to the catch captured by fishermen from chartered vessels from Spain, Honduras, Japan, Morocco, Panama, Portugal, Saint Kitts and Nevis, and the Republic of Vanuatu, for both swordfish and bigeye tuna (Figure 2). Furthermore, most samples were collected during trips of Spanish chartered vessels conducted in 2007, 2008, and 2010.

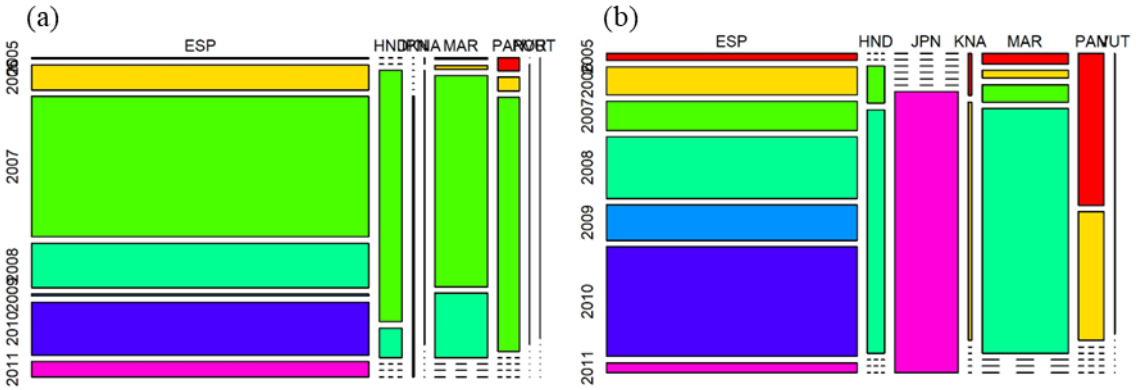


*Figure 2.* Mosaic plot for the data balance at the levels of year and flag for chartered vessels from Spain (ESP), Honduras (HND), Morocco (MAR), Panama (PAN), Japan (JPN), Saint Kitts and Nevis (KNA), and the Republic of Vanuatu (VUT), for *s*wordfish (a) and *b*igeye *t*una (b) sampled by the Brazilian pelagic longline fleet between 2005 and 2011. Each year in the figure is represented with a distinct color.

*Length analysis*

The swordfish showed its highest median length in 2007, at approximately 150 cm, while the lowest median was recorded in 2009, at around 137 cm (Figure 3a). The means for these years followed a similar pattern, with values close to 153 cm and 140 cm, respectively. For bigeye tuna, the median remained relatively constant over the years, around 148 cm (Figure 3b), suggesting little significant annual variation. Analyzing by flag, it was observed that swordfish captured by Spain and Japan exhibited greater length variation, with maximum values exceeding 250 cm, while Vanuatu recorded the shortest lengths, with medians around 120 cm (Figure 3c). For bigeye tuna, the flags also influenced lengths, with the highest medians observed in Spain, at about 160 cm, and the lowest in Vanuatu, at approximately 130 cm (Figure 3d). Regarding the months, swordfish showed a trend of increasing median lengths from April to July, reaching up to 160 cm (Figure 3e), while bigeye tuna maintained relatively stable lengths throughout the year, with medians around 140-150 cm (Figure 3f). These results suggest that, although there is some spatial and temporal variation in lengths, the differences are not pronounced, except for certain flags and specific months.

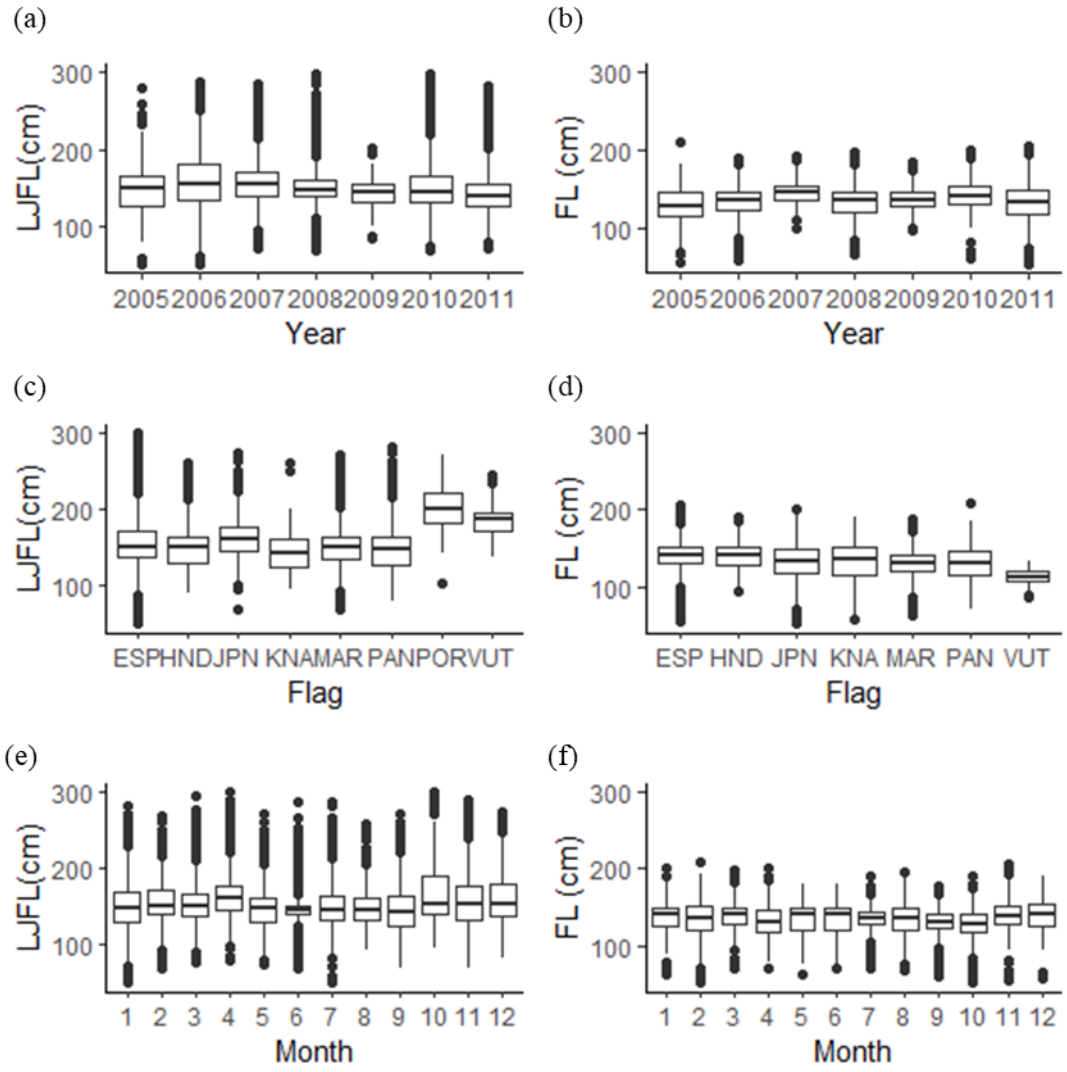


Figure 3. Quartiles for the Lower Jaw Fork Length (LJFL) of swordfish captured by year (a), flag (c), and month (e) and Fork Length (FL) of bigeye tuna, captured by year (b), flag (d), and month (f) by the foreign-flagged pelagic longline fleet chartered to Brazil, from 2005 to 2011.

The distribution of sex ratio by size class for swordfish ranged from 0.14 to 0.92 (Table 2). A predominance of females was observed in size classes above 180 cm, while males were more frequently seen in smaller size classes. For bigeye tuna, the sex ratio of females fluctuated between 0.25 and 0.87, with a notable predominance of females in the 200 cm class (Table 2). However, it is important to approach this trend with caution due to the low number of samples in the larger size classes. Nevertheless, we believe that the analysis presented provides a plausible estimate for the study period.

Table 2. Proportion of females relative to the total number of fish captured by 10 cm size class for swordfish (SWO) and bigeye tuna (BET).

| | SWO | | BET | |
|---|---|---|---|---|
| Length class (cm) | Total.Freq | Prop.Females | Total.Freq | Prop.Females |
| [50,60] | 1 | 1.0000000 | 20 | 0.2500000 |
| (60,70] | 47 | 0.1489362 | 78 | 0.2820513 |
| (70,80] | 227 | 0.2158590 | 60 | 0.3500000 |
| (80,90] | 470 | 0.3680851 | 88 | 0.3409091 |
| (90,100] | 1154 | 0.3171577 | 259 | 0.3359073 |
| (100,110] | 1894 | 0.3030623 | 776 | 0.3182990 |
| (110,120] | 4134 | 0.2404451 | 1372 | 0.3717201 |
| (120,130] | 6760 | 0.2828402 | 1791 | 0.3277499 |
| (130,140] | 14009 | 0.2934542 | 2431 | 0.4236940 |
| (140,150] | 15251 | 0.3256180 | 2037 | 0.4275896 |
| (150,160] | 11091 | 0.3911279 | 1022 | 0.4726027 |
| (160,170] | 10129 | 0.4548327 | 566 | 0.4540636 |
| (170,180] | 6949 | 0.5058282 | 424 | 0.4363208 |
| (180,190] | 4206 | 0.6552544 | 104 | 0.5480769 |
| (190,200] | 2467 | 0.8094852 | 35 | 0.5428571 |
| (200,210] | 2242 | 0.7957181 | 8 | 0.8750000 |
| (210,220] | 1330 | 0.8496241 | - | - |
| (220,230] | 946 | 0.8900634 | - | - |
| (230,240] | 798 | 0.8596491 | - | - |
| (240,250] | 504 | 0.8630952 | - | - |
| (250,260] | 206 | 0.9174757 | - | - |
| (260,270] | 102 | 0.8725490 | - | - |
| (270,280] | 79 | 0.9240506 | - | - |
| (280,290] | 57 | 0.7894737 | - | - |
| (290,300] | 14 | 0.9285714 | - | - |

*Model fitting and selection*

Swordfish

The model fitted using a GLM revealed that both latitude and sex are highly significant variables ($p < 0.001$), suggesting a strong relationship between these variables and LJFL (Table 3). The interactions between latitude and sex, as well as between latitude and year, were also significant, indicating that the influence of latitude on LJFL varies according to sex and year. The model explained a considerable amount of variation in the data, with a residual deviance of 55,042,408 compared to the null deviance of 70,716,426, reflecting the adequacy of the fit. The inclusion of interactions between temporal and spatial variables highlights the complexity in LJFL variation across different temporal

and geographical scales.

Table 3. Results of the Generalized Linear Model (GLM) for swordfish length, considering the variables flag, sex, year, month, and squared longitude ($lon^2$). The table presents the degrees of freedom (Df), deviance explained by each factor, residual degrees of freedom (Resid. Df), residual deviance (Resid. Dev), and the F-value for each factor.

| | Df | Deviance | Resid. Df | Resid. Dev | Pr (>F) |
|---|---|---|---|---|---|
| NULL | | | 83646 | 70716426 | |
| flag | 6 | 1322623 | 83640 | 69393803 | 0 |
| lat2 | 1 | 359987.6 | 83639 | 69033815 | 1.64E-121 |
| SEX | 1 | 6614812 | 83638 | 62419004 | 0 |
| year | 4 | 1903773 | 83634 | 60515231 | 0 |
| month | 11 | 2874327 | 83623 | 57640903 | 0 |
| lon2 | 1 | 402801.9 | 83622 | 57238101 | 1.00E-135 |
| lat2:SEX | 1 | 31593.37 | 83621 | 57206508 | 3.81E-12 |
| lat2:year | 4 | 236161.3 | 83617 | 56970347 | 9.65E-77 |
| lat2:month | 11 | 651742.1 | 83606 | 56318605 | 2.54E-206 |
| lat2:lon2 | 1 | 69058.51 | 83605 | 56249546 | 9.94E-25 |
| SEX:year | 4 | 503655.5 | 83601 | 55745891 | 4.50E-165 |
| SEX:month | 11 | 605928.3 | 83590 | 55139962 | 2.80E-191 |
| SEX:lon2 | 1 | 9519.652 | 83589 | 55130443 | 0.000138 |
| year:lon2 | 4 | 88034.3 | 83585 | 55042408 | 4.52E-28 |

The residuals versus fitted values plot (Figure 4a) indicates that the residuals are reasonably randomly distributed around zero, suggesting that the model does not exhibit major specification issues. The Normal Q-Q plot (Figure 4b) suggests that although most residuals follow an approximately normal distribution, there are slight deviations in the tails, especially in the lower quantiles, which may indicate the presence of outliers. The Scale-Location plot reveals slight heteroscedasticity (Figure 4c), with the smoothed line showing variation in the spread of the residuals along the predicted values, suggesting that the error variance is not completely constant. The Residuals vs Leverage plot (Figure 4d) highlights a few influential points, as indicated by Cook's distances, suggesting that these points may be exerting a significant impact on the model fit and require further investigation.

Despite these minor deviations, the diagnostics suggest that the model is adequate for the proposed analysis, capturing the main data trends in a robust manner. The slight heteroscedasticity and the influential points do not compromise the model's ability to provide valuable insights into the length variation of the species studied.

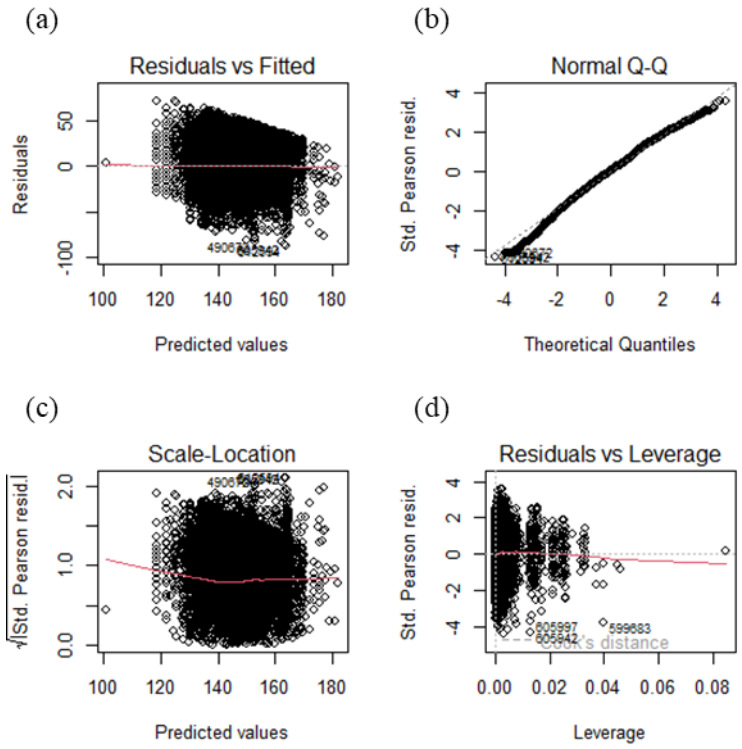


*Figure 4. Diagnostic plots of the fitted model for the analysis of swordfish (Xiphias gladius) length caught by the Brazilian pelagic longline fleet between 2005 and 2011 (residuals versus fitted values plot (a), normal Q-Q plot (b), scale-location plot (c), residuals vs leverage plot (d)).*

Bigeye tuna

All variables showed significant effects on length (Table 4). Flag (Deviance = 175,413.9; F = 80.91) and lon² (Deviance = 68,440.99; F = 189.40) indicate important spatial variations, while sex (Deviance = 20,885.88; F = 57.80), year (Deviance = 83,155.61; F = 57.53), and month (Deviance = 159,396.4; F = 40.10) reveal temporal differences and variations between males and females. These results suggest that spatial, temporal, and biological factors significantly influence bigeye tuna length. The analysis confirms that there is significant variation in length across time and space, which may be crucial for species management and sustainable fishing practices.

Table 4. Results of the Generalized Linear Model (GLM) for bigeye tuna length, considering the variables flag, sex, year, month, and squared longitude (lon²). The table presents the degrees of freedom (Df), deviance explained by each factor, residual degrees of freedom (Resid. Df), residual deviance (Resid. Dev), and the F-value for each factor.

| | Df | Deviance | Resid. Df | Resid. Dev | F | Pr (>F) |
|---|---|---|---|---|---|---|

| | | | | | | |
|---|---|---|---|---|---|---|
| NULL | | | 9400 | 3895686 | | |
| flag | 6 | 175413.9 | 9394 | 3720272 | 80.90639 | 4.52E-99 |
| SEX | 1 | 20885.88 | 9393 | 3699387 | 57.79932 | 3.18E-14 |
| year | 4 | 83155.61 | 9389 | 3616231 | 57.53096 | 4.86E-48 |
| month | 11 | 159396.4 | 9378 | 3456834 | 40.10106 | 1.40E-85 |
| lon2 | 1 | 68440.99 | 9377 | 3388394 | 189.4028 | 1.11E-42 |

The residuals versus fitted values plot (Figure 5a) and the scale-location plot (Figure 5c) indicate that the residuals are well distributed, without major systematic deviations, suggesting that the model captured the variability of the data well. The normal Q-Q plot (Figure 5b) also shows that the residuals follow an approximately normal distribution, reinforcing the adequacy of the model. However, the residuals versus leverage plot (Figure 5d) identified some points with high Cook's distances, indicating the presence of influential observations that may be impacting the model fit. Although these points warrant further investigation, the overall performance of the diagnostics suggests that the model is suitable for the study's purposes.

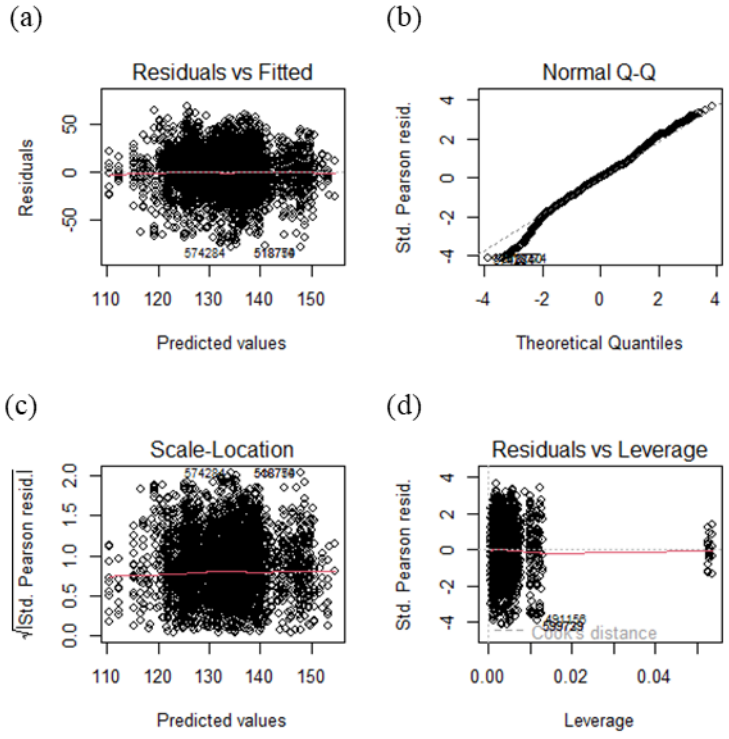


Figure 5. Diagnostic plots of the fitted model for the analysis of bigeye tuna (Thunnus obesus) length, caught by the Brazilian pelagic longline fleet between 2005 and 2011 (residuals versus fitted values plot (a), normal Q-Q plot (b), scale-location plot (c), residuals vs leverage plot (d)).

A higher presence of intermediate and large-sized individuals of swordfish is noted in regions closer to the Brazilian coast, while northern areas show a greater proportion of smaller individuals (Figure 6a). For bigeye tuna (Figure 6b), a similar trend is observed, with a higher presence of large and intermediate fish in coastal and northern areas, while a notably smaller proportion of small-sized fish is found in the southern regions.

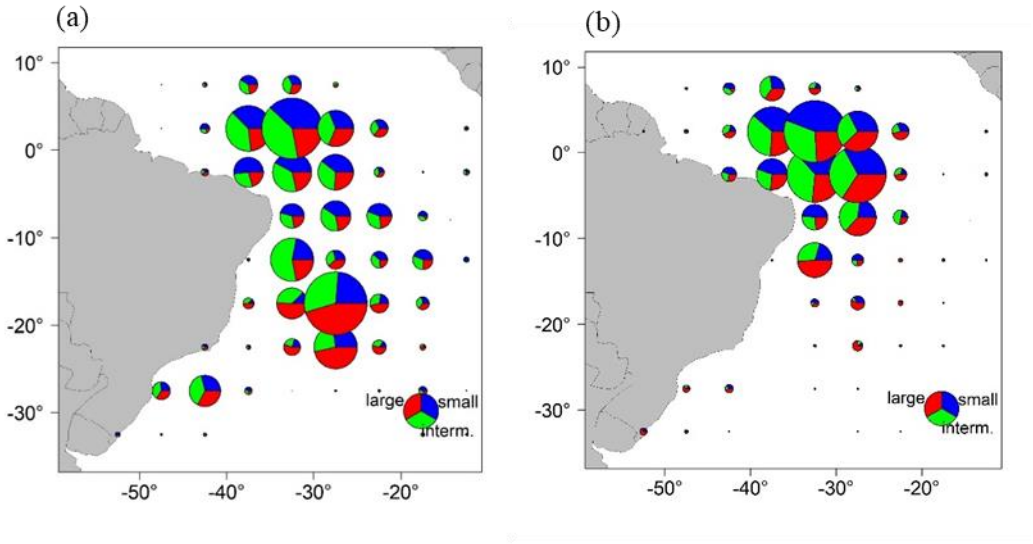


Figure 6. Spatial distribution of length categories of swordfish (a) and bigeye tuna (b) captured by the Brazilian pelagic longline fleet between 2005 and 2011. The slices in blue, green, and red represent the proportions of small, intermediate, and large individuals, respectively, in each 5° x 5° latitude and longitude cell. The size of the pie charts reflects the total number of individuals captured.

*Sex ratios analysis*

The overall female proportion was 0.415 for swordfish and 0.450 for bigeye tuna, with a 95% confidence interval (CI) of 0.397–0.415 and 0.426–0.475, respectively. The hypothesis that the proportions of females and males are equal was rejected ($p < 2.2 \times 10^{-16}$) for both species. There is evidence that the proportion of males is greater than that of females. In general, for both species analyzed, the numbers of males were higher than those of females in the equatorial and tropical regions, north of 20° S (Figure 7). However, the number of female swordfish was greater in samples of fish captured in the south (Figure 7a).

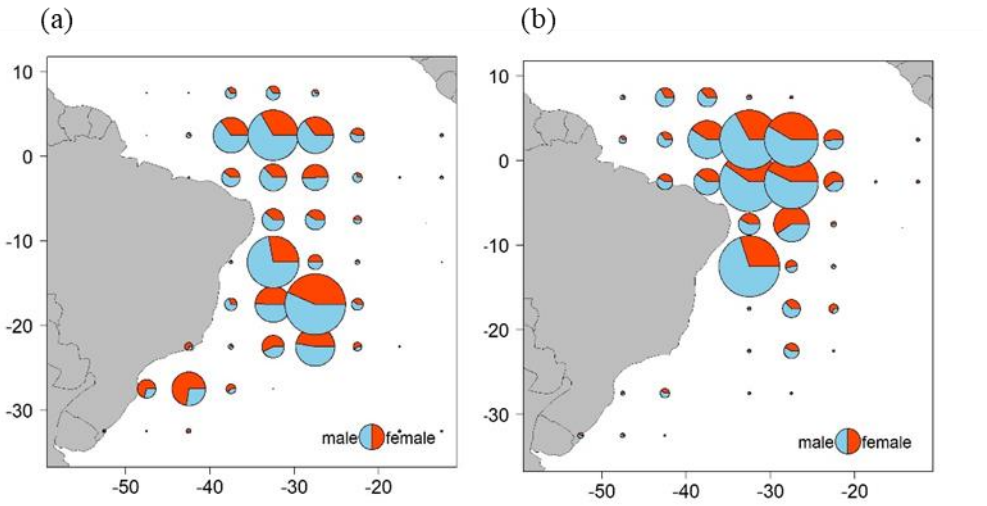


Figure 7. Spatial distribution of female and male swordfish (a) and bigeye tuna (b) sampled by the Brazilian pelagic longline fleet between 2005 and 2011.

Swordfish

The variability in the female proportion for swordfish was relatively high, but there was no clear temporal trend over the years, with estimates ranging between 0.3 and 0.5 (Figure 8a). The lowest proportion was found in 2008, while the highest was in 2010. The sample sizes for 2005, 2009, and 2011 were low, whereas the sample in 2007 was large (> 40,000 individuals). The variability in the female proportion over the months was high, but no seasonal pattern was observed. The proportion fluctuated around 0.4 throughout the months (Figure 8b). The exception was July, when the proportion exceeded 0.6. Sample sizes were high in April and July and relatively low in March, June, and October. Regarding the origin of the vessels, the proportions of females were below 0.5 for all flags, except for the vessels of Portuguese origin, which showed values above 0.8 (Figure 8c), despite the low number of measured fish. In general, the sample sizes were below 11,000 individuals, but the chartered vessels from Spain were the exception, with numbers exceeding 64,000 fish.

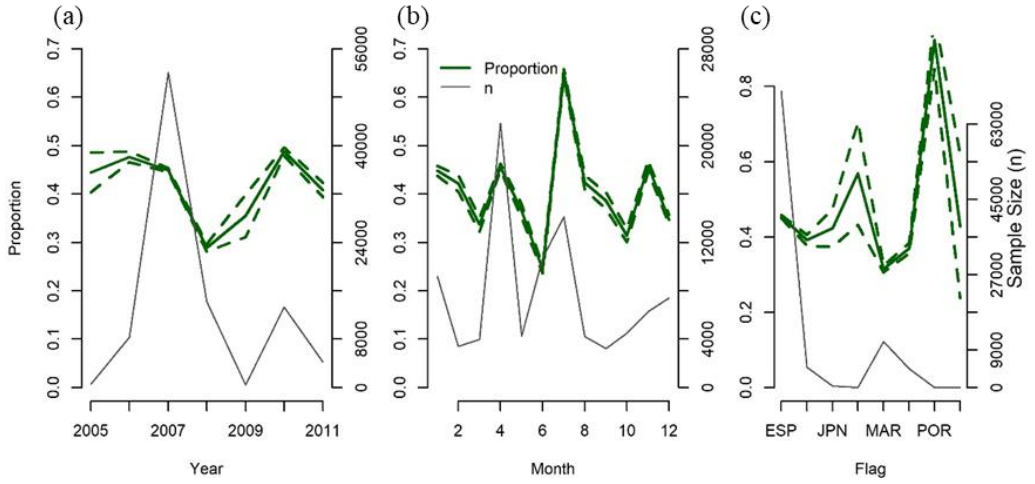


Figure 8. Sample size (n) and female proportion of swordfish sampled by the Brazilian pelagic longline fleet between 2005 and 2011, calculated by year (a), month (b), and flag (c). The proportion is calculated based on catches from chartered vessels from Honduras (HND), Morocco (MAR), Panama (PAN), Spain (ESP), Portugal (POR), Saint Kitts and Nevis (KNA), Japan (JPN), and the Republic of Vanuatu (VUT). The dashed lines represent the 2.5% and 97.5% quantiles of a binomial distribution.

Bigeye tuna

The variability in the female proportion values for bigeye tuna was quite similar to that observed for swordfish (Figure 9a). Overall, the measures fluctuated between 0.3 and 0.6, with the lowest value reported in 2008 and the highest in 2009. The sample size was relatively low (< 8,000 individuals) compared to the results obtained for swordfish. In the monthly analysis, no seasonal pattern was detected, with values remaining around 0.4 throughout the months (Figure 9b), except in January (0.54), November (0.5), and June (0.3). In terms of sample size, it remained stable for all months (< 4,000 individuals). All the flags analyzed maintained female proportion values for bigeye tuna close to 0.4, with the number of specimens measured being below 8,000 fish (Figure 9c).

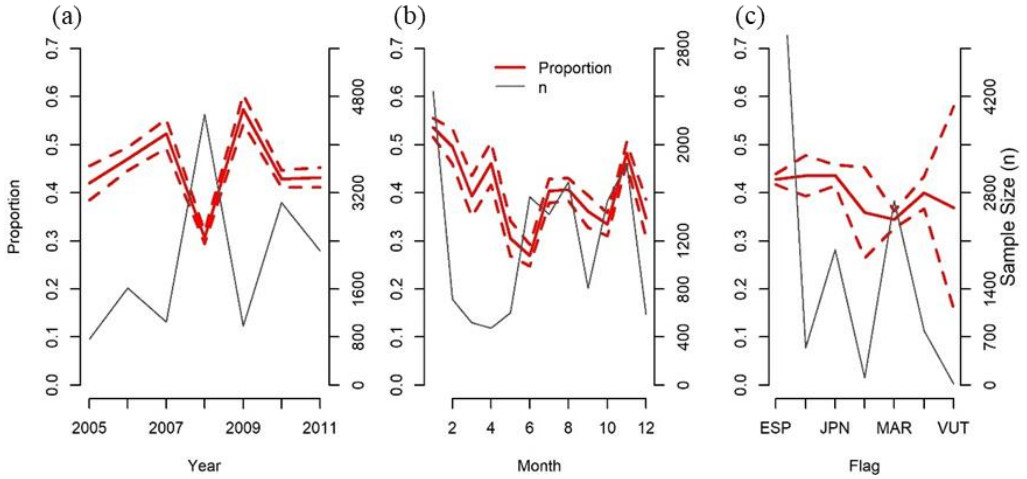


Figure 9. Sample size (n) and female proportion of bigeye tuna sampled by the Brazilian pelagic longline fleet between 2005 and 2011, calculated by year (a), month (b), and flag (c). The proportion is calculated based on catches from chartered vessels from Honduras (HND), Morocco (MAR), Panama (PAN), Spain (ESP), Saint Kitts and Nevis (KNA), Japan (JPN), and the Republic of Vanuatu (VUT). The dashed lines represent the 2.5% and 97.5% quantiles of a binomial distribution.

*Model Fitting and Selection*

Swordfish

The model was fitted only for the data from 2006–2008 and 2010 due to the small sample size in other years. Additionally, there was no convergence when all interactions were considered. The model converged only if year and flag were not included in the interactions. Thus, the largest fitted model was:

$$(ns, nf) \sim year + (\text{LJFL} + month + lat^2 + lon^2)^2$$

The results of the backward elimination approach based on AIC indicate that all main effects and interactions should be retained in the model mentioned above. The deviance analysis is presented in Table 5. The initial deviance was 53.335, while the final deviance, after including the variables and their interactions, was reduced to 37.079, representing a decrease of 30.45%. This reduction indicates that the inclusion of the variables "year," "month," "latitude," "longitude," and their interactions significantly contributed to improving the model fit to the data.

Table 5. Deviance analysis of the adjusted binomial model for the sex ratio data of swordfish sampled by the Brazilian pelagic longline fleet between 2005 and 2011.

| | Df | Deviance | Resid. Df | Resid. Dev | F |
|---|---|---|---|---|---|

| | | | | | |
|---|---|---|---|---|---|
| NULL | | | 7581 | 53335 | |
| year | 4 | 1480.5 | 7577 | 51855 | 2.4e-319 |
| LJFL | 1 | 8772.6 | 7576 | 43082 | 0 |
| month | 11 | 3379.6 | 7565 | 39702 | 0 |
| lat2 | 1 | 359.8 | 7564 | 39343 | 3.09E-80 |
| lon2 | 1 | 226.5 | 7563 | 39116 | 3.48E-51 |
| LJFL:month | 11 | 798.1 | 7552 | 38318 | 4.86E-164 |
| LJFL:lat2 | 1 | 16.9 | 7551 | 38301 | 3.89E-05 |
| LJFL:lon2 | 1 | 37.0 | 7550 | 38264 | 1.18E-09 |
| month:lat2 | 11 | 798.4 | 7539 | 37466 | 4.27E-164 |
| month:lon2 | 11 | 187.8 | 7528 | 37278 | 2.51E-34 |
| lat2:lon2 | 1 | 198.5 | 7527 | 37079 | 4.52E-45 |

The expected residuals were close to zero across all types of predictions (from low to high) (Figure 10a). The data were assumed to follow a binomial distribution; therefore, violations of normality in the tails of the plot (Figure 10b) are not a major concern for the fit. However, it is important to remember that inference for binomial generalized linear models is based on the assumption that the distribution of residuals asymptotically follows a normal distribution. Thus, violations of normality imply a deterioration of the power of $\chi^2$ tests (sum of squares of standard normal distributions). The distribution of residuals is approximately homoscedastic, at least when high proportions of females were predicted (Figure 10c). Additionally, there are many influential data points with high leverage and Cook's distance values (Figure 10d).

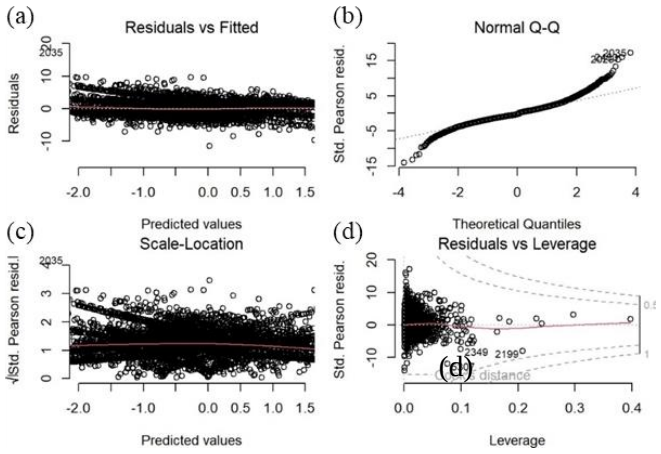


Figure 10. Standard residual diagnostic plots of the model fit for swordfish sampled by the Brazilian pelagic longline fleet between 2005 and 2011.

Bigeye tuna

The model was fitted for the years 2005, 2006, 2008, and 2011, as the data for the other years were insufficient. Furthermore, convergence was achieved when the

explanatory variables year and flag were included in the interactions. Thus, the largest fitted model was:

$$(ns, nf) \sim year + \text{FL} + (lat2 + lon2 + month)\text{^}2 + flag - lat2 : lon2$$

The inclusion of the variables "year," "FL," "latitude," "longitude," "month," "flag," and the interactions between "latitude" and "month" substantially contributed to the model's fit (Table 6). The variable "year" had a remarkable impact, with a highly significant p-value (Pr > Chi = 2.19E-36), followed by other variables like "longitude" and "month," which also showed statistical significance (Pr > Chi < 0.05).

Table 6. Deviance analysis of the binomial model fitted for sex ratio data of bigeye tuna sampled by the Brazilian pelagic longline fleet between 2005 and 2011.

| | GL | Deviance | GL Resid. | Dev. Resid. | Pr (>Chi) |
|---|---|---|---|---|---|
| NULL | | | 2827 | 5810.778688 | |
| year | 3 | 168.9119836 | 2824 | 5641.866705 | 2.19E-36 |
| FL | 1 | 45.12403252 | 2823 | 5596.742672 | 1.85E-11 |
| lat2 | 1 | 3.078287116 | 2822 | 5593.664385 | 0.079344047 |
| lon2 | 1 | 29.22322225 | 2821 | 5564.441163 | 6.45E-08 |
| month | 11 | 123.3897983 | 2810 | 5441.051365 | 3.77E-21 |
| flag | 6 | 43.66663789 | 2804 | 5397.384727 | 8.61E-08 |
| lat2:month | 11 | 61.5732851 | 2793 | 5335.811442 | 4.72E-09 |
| lon2:month | 11 | 21.22161046 | 2782 | 5314.589831 | 0.031146458 |

The standard residual diagnostic plots are shown in Figure 11. The model was slightly biased, with the residual expectations being close to, but slightly above, zero for low predictions (Figure 11a). The quantile plot indicates that the residual distribution approaches normality (Figure 11b). In summary, the residuals are approximately homoscedastic, although there is a not-too-pronounced trend of increasing variance for lower predictions (Figure 11c). High residual values are associated with high leverage, and some influential points were detected in the residuals (Figure 11d). Overall, the model is considered sufficient for the purposes of this study, although it should be revisited in the future.

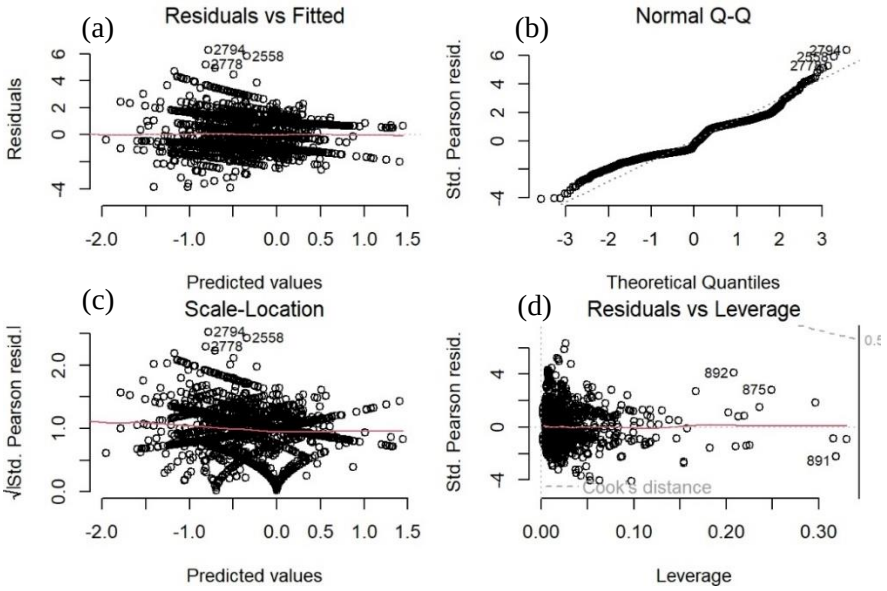


Figure 11. Standard residual diagnostic plots for the model fit of bigeye tuna sampled by the Brazilian pelagic longline fleet between 2005 and 2011 (residuals vc fitted plot (a), normal Q-Q plot (b), scale-location plot (c), residuals vc leverage plot (d)).

Effect of explanatory variables by year

The proportion of female swordfish exceeded 0.5 in the southwest (south of 20° S and west of 25° W) in all years, while males dominated in catches across most other parts of the South Atlantic in 2007, 2008, 2010, and 2011, particularly in the northwest sector (Figure 12a). On the other hand, bigeye tuna females did not exhibit specific regions with a high sex ratio (values above 0.5) (Figure 12b). However, in 2006, moderate female proportions were observed in tropical regions near the boundaries of 5–25° S and 20° W (Figure 12b). High male proportions were identified in 2008 in oceanic areas to the north and the far south of Brazil.

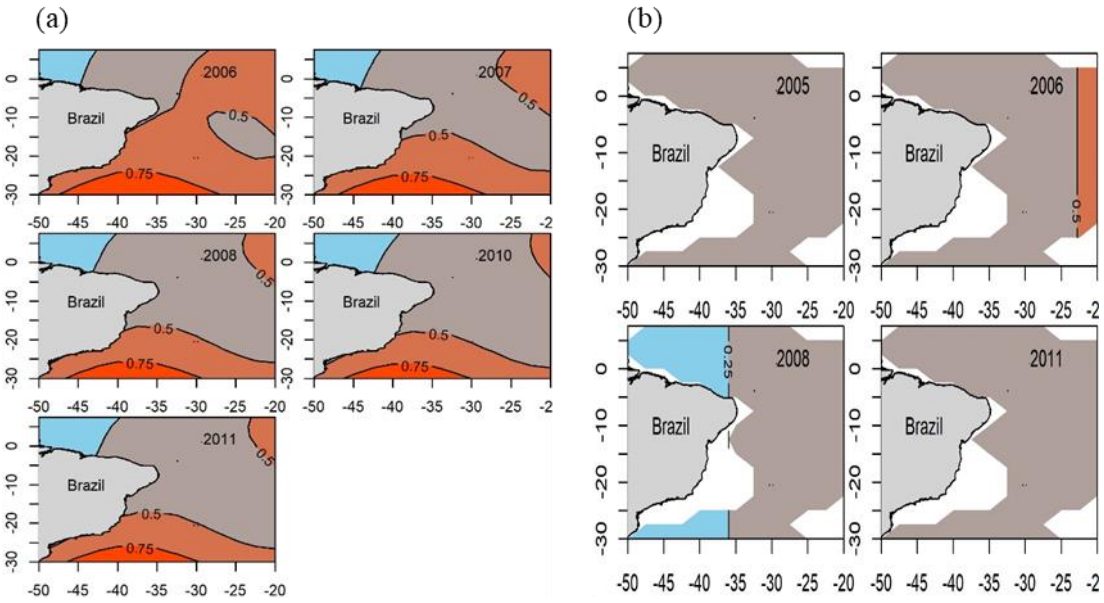


Figure 12. Marginal effect of year, latitude, and longitude on the proportion of female swordfish (a) and bigeye tuna (b) sampled by the Brazilian pelagic longline fleet between 2005 and 2011. The fading from red to blue indicates the transition from female dominance to male dominance. The contour lines represent the proportion of females.

Effect of explanatory variables by month

The proportion of females was clearly high in the southern (or southwestern) sector from December to April and from August to October (Figure 13). In the other four months, the proportion of males exceeded that of females. The proportion of males was higher in the northwestern sector in eleven months, except in June, when males were more abundant around the longitude of 30° W at all latitudes from 5° N to 30° S.

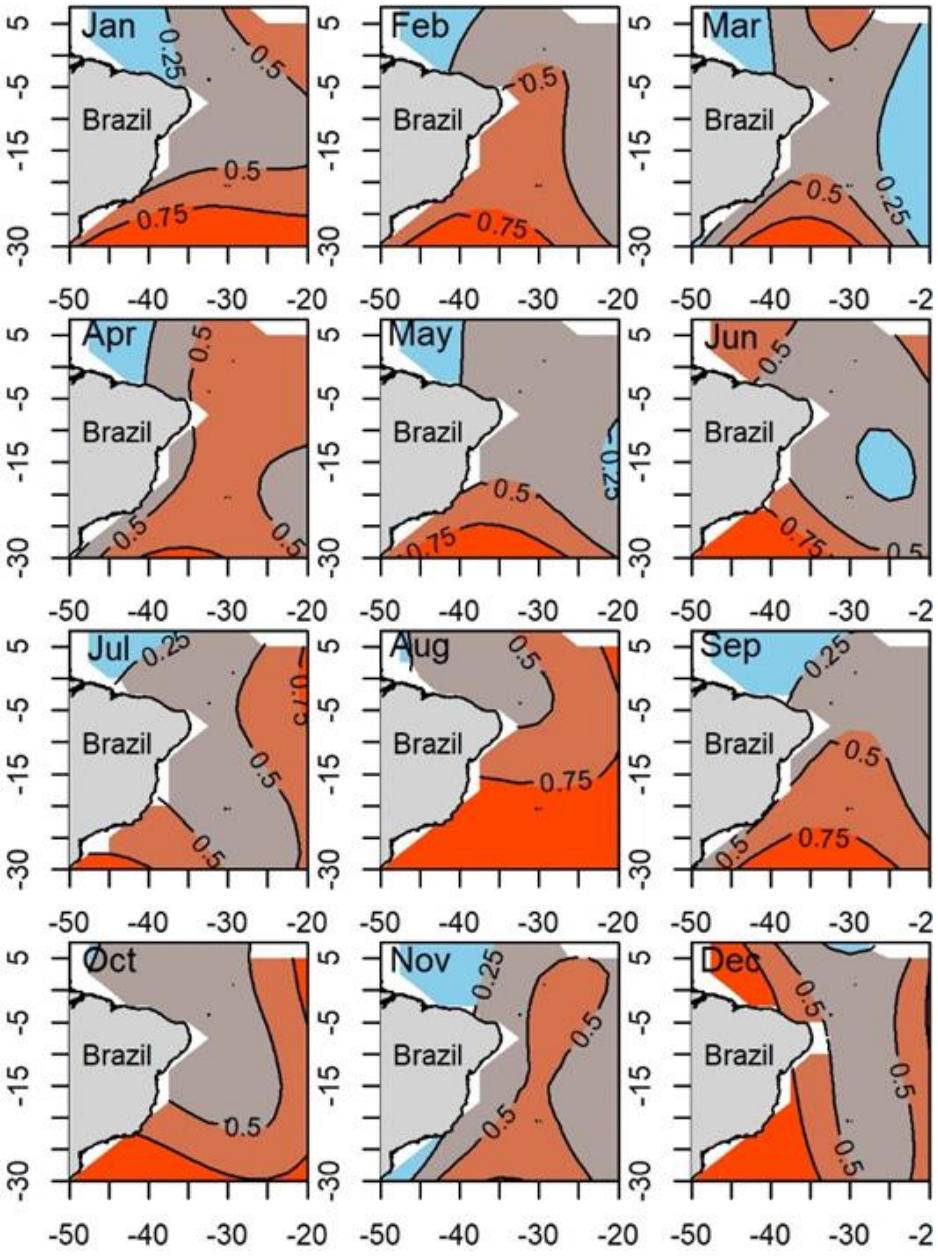


Figure 13. Marginal effect of month, latitude, and longitude on the proportion of female swordfish sampled by the Brazilian pelagic longline fleet between 2005 and 2011. The fade from red to blue indicates the transition from female dominance to male dominance. The contour lines represent the proportion of females.

The monthly catches of female bigeye tuna showed a homogeneous distribution throughout almost the entire intertropical zone, with proportion values below 0.5 (Figure 14). However, there are values exceeding 0.5 located near the meridians of 20° W and 25° W in February, July, November, and December. Additionally, the proportions of males were extremely high (>0.75) in the northwest and southern sectors for three months (July, October, and December) and in areas near the longitudes of 25° W in May and June.

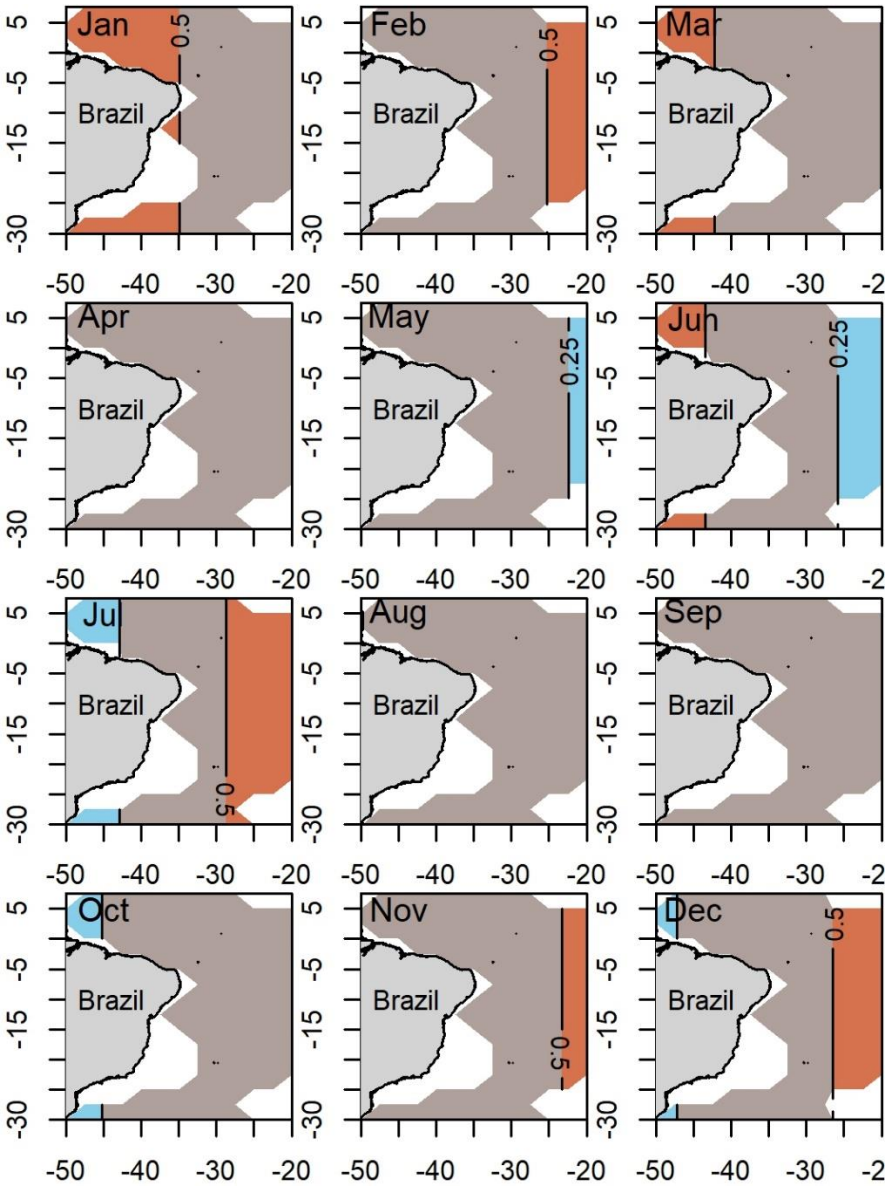


Figure 14. Marginal effect of month, latitude, and longitude on the proportion of female bigeye tuna sampled by the Brazilian pelagic longline fleet between 2005 and 2011. The transition from red to blue indicates the shift from female dominance to male dominance. The contour lines represent the proportion of females.

Effect of Explanatory Variables by Flag

The predominance of female swordfish in the southwestern sector and males particularly in the northwestern sector appears for all flags (Figure 15a). However, in the central part of the analyzed area, the proportion of females was higher in the catches from Spain and Honduras, while the proportion of males was higher in the catches from Morocco and Panama. Regarding the bigeye tuna, the main flag responsible for capturing

females was Honduras, while the others showed the same pattern, with catches of males exceeding those of females across the entire analyzed area (Figure 15b).

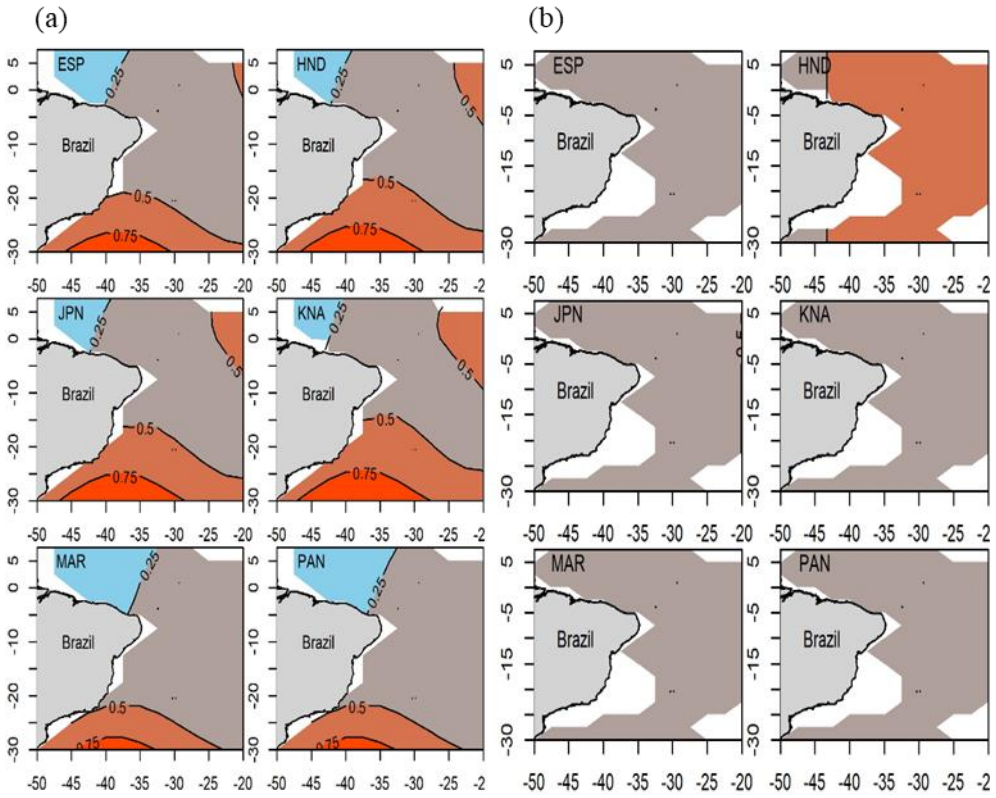


Figure 15. Marginal effect of flag, latitude, and longitude on the proportion of female swordfish (a) and bigeye tuna (b) sampled by the Brazilian pelagic longline fleet between 2005 and 2011. The gradient from red to blue indicates the transition from female dominance to male dominance. The contour lines represent the proportion of females.

## 4. DISCUSSION

The present study revealed notable insights into the spatial patterns of sexual segregation of swordfish and bigeye tuna in the southwestern Atlantic Ocean. The analyses uncovered distinct patterns in gender proportions, with significant implications for the reproductive ecology of these species. Notably, the catch data with sex records for swordfish significantly exceeded those for bigeye tuna, a phenomenon attributed in part to the prevalence of recorded catches from chartered vessels from Spain. Overall, throughout the development of the pelagic longline fishery in Brazil, a high number of different vessels and substantial variations in the flags of the charters were involved (Mourato, 2011; Rodrigues et al., 2020). Furthermore, the prominent presence of Spanish vessels from the late 1990s to 2012 played a crucial role in shaping pelagic fishing with

longlines in Brazilian waters (Hazin & Travassos, 2007) and was essential for the capture of swordfish throughout the South Atlantic.

*Length analysis*

Swordfish

The variation in sexual proportion by size class observed in this study reflects the different growth parameters between the sexes, with females of swordfish growing more rapidly and reaching larger sizes than males (Taylor and Murphy, 1992; Tserpes, 1995; Sun et al., 2002). This pattern was evidenced by the longitudinal distributions, where females predominated in size classes exceeding 180 cm. This behavior can be explained by the reproductive strategy of males, who mature earlier and allocate energy towards reproduction, limiting growth (DeMartini et al., 2000). The overall proportion of females was 41.5%, with a variation ranging from 14% to 92%, highlighting the male predominance in smaller size classes. This differential pattern of sexual growth in swordfish has been reported in the Atlantic (Ehrhardt et al., 1995), Pacific (Sun et al., 2002), and Indian (Vanpouille et al., 2001) oceans. The spatial and temporal variability in sexual proportion and body length may be associated with different behaviors during spawning, feeding, or migrative behaviors (de la Serna et al., 1992; Tserpes et al., 2001; Mejuto, 2018; Abid et al., 2019).

Bigeye tuna

In the case of the bigeye tuna, the results indicate an intrinsic biological stability, with a median length consistently around 148 cm throughout the analyzed years. The proportion of females in the 200 cm class varied from 25% to 87%, highlighting a predominance of females at larger sizes. Male catches were more frequent, except in 2006, when the proportion of females increased in specific tropical regions. In the case of bigeye tuna, previous studies have reported differential growth patterns between sexes in various fishing areas (Kume, 1969a); however, some investigations found no significant differences between males and females, suggesting regional or methodological variations in growth analysis (Alves et al., 2002; Sun et al., 2001).

Unlike the swordfish, this stability in length distribution over the years suggests a differentiated environmental response, reinforcing the need for species-specific approaches. These observed differences in the ecology and adaptive responses of the two

species are fundamental for sustainable management. These data are crucial for understanding population dynamics and guiding conservation and management policies tailored to each species.

*Sex ratios analysis*

Swordfish

The spatial analysis of the proportions of female and male swordfish revealed a pattern of sexual segregation in different regions of the southwestern Atlantic. For instance, females were more abundant in the south, while males predominated in the north. This observation suggests that the distribution of swordfish populations in the region is linked to sexual factors, such as habitat preference or distinct migratory behaviors between the sexes. Additionally, the stability of female and male proportions over the years indicates a relative temporal consistency in these patterns.

The preference of females for the southern region of the southwestern Atlantic Ocean, characterized by cooler temperatures compared to equatorial waters, may be attributed to the biological characteristics of the species. Previous studies indicate that females generally grow larger and are more tolerant of lower temperatures (Palko et al., 1981; Taylor & Murphy, 1992; Tserpes, 1995; Sun et al., 2002). This preference for different temperature ranges may result in spatial segregation, with females migrating to cooler areas, such as the south, while males tend to remain in warmer regions, like the equatorial areas. However, it is important to note that mature females eventually return to spawning areas in warmer waters, where males are more abundant (Palko et al., 1981; Mejuto, 2018).

The high presence of male swordfish in equatorial waters is also related to the overlap with spawning and reproduction areas identified in the literature for the species in the South Atlantic. These spawning areas are generally located between 15°–35° S and 20°–40° W (Mejuto & García, 1997; Mejuto, 1998; Mejuto, 2018; Nóbrega et al., 2023), which coincides with the studied region. The observed proportion of males captured in spawning regions, particularly between 10° W and latitudes 5° N and 5° S, was substantially higher than in non-reproductive areas. This pattern has been documented in other oceans, indicating a consistent trend across different geographic regions (Taylor & Murphy, 1992; Mejuto et al., 1998; DeMartini et al., 2000; Tserpes et al., 2001; Tserpes

et al., 2008; Poisson & Fauvel, 2009). Therefore, in warmer waters, female swordfish may have a lower catchability or may be found at greater depths, making them less accessible to surface longline fishing gear (Mejuto et al., 1998).

In general, swordfish reproductive aggregations in the western South Atlantic occur between spring and summer, predominantly in areas located to the west, characterized by high primary production and greater resource availability (Mejuto & García-Cortés, 2014; Mejuto, 2018; Nóbrega et al., 2023). These reproductive aggregations to the west are influenced by the prevailing environmental conditions in the eastern region, such as decreased resources and sea surface temperature (SST), along with the latitudinal oscillation of the South Equatorial Current (SEC), which seems to drive reproductive migration westward (Rey, 1988; Wu et al., 2019).

SST plays a crucial role in the onset of maturation and reproduction of swordfish, influencing larval survival and the species' reproductive success (Rey, 1988), with generally more favorable conditions above 22 °C (Palko et al., 1981; Arocha, 2007; Mejuto & García-Cortés, 2014). Similar reproductive patterns related to SST have also been observed in the Caribbean and Antilles seas (Arocha, 2007), the Indian Ocean (Poisson & Fauvel, 2009), the Atlantic Ocean (Mejuto & García-Cortés, 2014), and the Levant Basin (Tserpes et al., 2008).

Bigeye tuna

The bigeye tuna exhibited a remarkable pattern of male predominance in the catch across almost the entire study area, except in 2006, when significantly higher proportions of females were recorded in tropical regions near the geographic boundaries of 5–25° S and 20° W.

The predominance of males in certain oceanic fishing areas can be explained by several theories. Schaefer et al. (2005) suggested the possibility of a higher proportion of males in aggregations of reproductively active females, with recruitment occurring both north and south, influenced by the bifurcation of the South Equatorial Current (Brill et al., 2005; Nóbrega et al., 2023). This theory aligns with the observed behavior of bigeye tuna, as regions near the analyzed geographic boundaries tend to be influenced by these currents, which may direct the migratory and reproductive patterns of the species.

Additionally, like other tuna species, bigeye tuna shares the characteristic of spawning in tropical and subtropical regions, with significant overlap between spawning and feeding areas, and prolonged spawning periods lasting several months to nearly the entire year (Llopiz & Hobday, 2015; Reglero et al., 2014; Schaefer, 2001). These characteristics may influence recruitment patterns and the spatial distribution of tuna populations, including bigeye tuna, leading to variations in sex ratios across different regions.

Additionally, similar patterns of sex ratios for bigeye tuna have been observed in various fleets and fishing areas. For instance, studies conducted by Taiwanese longliners in the western Pacific Ocean (Su et al., 2013) and data from Japanese longline fisheries in the North Pacific Ocean (Kume, 1969a) and the Equatorial and Southern Pacific Ocean (Kume, 1969b) indicated a higher proportion of males with increasing individual size for the species, suggesting a possible slower growth rate or higher natural mortality for females compared to males.

## 5. CONCLUSION

The dynamics of swordfish and bigeye tuna catches highlight the influence of ecological and behavioral factors, as well as specific fishing practices in the study area. Therefore, it is crucial to understand the interactions between species in mixed fisheries and consider tailored management strategies to ensure the sustainability of these populations in the South Atlantic. The study results underscore distinct spatial distribution patterns by sex, with a higher proportion of female swordfish in the southern sector and males predominating in the western equatorial sector, while bigeye tuna exhibited a predominance of male catches, except in 2006, when there was a high proportion of females in specific tropical regions. The observation of sexual segregation in certain sectors of the region emphasizes the importance of considering such dynamics in sustainable fishery management. These findings highlight the urgency for continuous monitoring and improvement of conservation strategies, given the scarcity of data and the vulnerability of the species. Identifying limitations, such as low sample sizes in certain years, underscores the importance of future research to enhance the understanding of sexual segregation and its impact on the population dynamics of these species. This information is essential for guiding effective management and conservation measures for fishery resources in the South Atlantic.

## 6. REFERENCES

Abid, N., Laglaoui, A., Arakrak, A., & Bakkali, M. (2019). The reproductive biology of swordfish (*Xiphias gladius*) in the Strait of Gibraltar. Journal of the Marine Biological Association of the United Kingdom, 99(3), 649-659. https://doi.org/10.1017/S0025315418000346.

Akaike , H. 1974. Um novo olhar sobre o modelo de identificação estatística. Transações IEEE em Controle Automático, 19: 716-723,1974.

Alglave, B., Rivot, E., Etienne, M. P., Woillez, M., Thorson, J. T., & Vermard, Y. (2022). Combining scientific survey and commercial catch data to map fish distribution. *ICES Journal of Marine Science*, *79*(4), 1133-1149.

Alves, A., de Barros, P., & Pinho, M. R. (2002). Age and growth studies of bigeye tuna *Thunnus obesus* from Madeira using vertebrae. *Fisheries Research*, *54*(3), 389-393.

Arocha, F. (2007). Swordfish reproduction in the Atlantic Ocean: and overview. Gulf Caribb. Res., 19 (2), 21-36, 10.18785/gcr.1902.05.

Baylis, AMM, Orben, RA, Costa, DP, Arnould, JPY e Staniland, IJ (2016). Sexual segregation in habitat use is smaller than expected in a highly dimorphic marine predator, the southern sea lion. Marine Ecology Progress Series, 554, 201-211. https://doi.org/10.3354/meps11759

Beal, M., Catry, P., Regalla, A., Barbosa, C., Pires, A. J., Mestre, J., ... & Patrício, A. R. (2022). Satellite tracking reveals sex-specific migration distance in green turtles (Chelonia mydas). Biology Letters, 18(9), 20220325. https://doi.org/10.1098/rsbl.2022.0325

Brill, R. W., Bigelow, K. A., Musyl, M. K., Fritsches, K. A., & Warrant, E. J. (2005). Bigeye tuna (*Thunnus obesus*) behavior and physiology and their relevance to stock assessments and fishery biology. *Col. Vol. Sci. Pap. ICCAT*, *57*(2), 142-161.

Casini, M., Hjelm, J., Molinero, J. C., Lövgren, J., Cardinale, M., Bartolino, V., ... & Kornilovs, G. (2009). Trophic cascades promote threshold-like shifts in pelagic marine ecosystems. Proceedings of the National Academy of Sciences, 106(1), 197-202. 10.1073/pnas.0806649105

Collette, B.B., Boustany, A., Fox, W., Graves, J., Juan Jorda, M. & Restrepo, V. 2021. *Thunnus obesus*. The IUCN Red List of Threatened Species 2021: e.T21859A46912402. https://dx.doi.org/10.2305/IUCN.UK.2021-2.RLTS.T21859A46912402.en. Accessed on 17 January 2024.

Collette, B.B., Di Natale, A., Fox, W., Graves, J., Juan Jorda, M., Pohlot, B., Restrepo, V. & Schratwieser, J. 2022. *Xiphias gladius*. The IUCN Red List of Threatened Species 2022: e.T23148A46625751. https://dx.doi.org/10.2305/IUCN.UK.2022-1.RLTS.T23148A46625751.en. Accessed on 17 January 2024.

De la Serna, J. M., Alot, E., & Mejuto, J. (1992). Analysis preliminar del sex ratio por clase de talla del pez espada (*Xiphias gladius*) en el area atlantica proxima al estrecho de Gibraltar. Collect. Vol. Sci. Pap. ICCAT, 39(2), 514-521.

DeMartini, E. E., Uchiyama, J. H., & Williams, H. A. (2000). Sexual maturity, sex ratio, and size composition of swordfish, *Xiphias gladius*, caught by the Hawaii-based pelagic longline fishery. Fishery Bulletin, 98(3), 489-489.

Ehrhardt, N. M., Robbins, R. J., & Arocha, F. (1995). Age validation and growth of swordfish, *Xiphias gladius*, in the northwest Atlantic. Collective Volume Of Scientific Papers-International Commission For The Conservation Of Atlantic Tunas, 45, 358-367.

Erauskin-Extramiana, M., Arrizabalaga, H., Hobday, A. J., Cabré, A., Ibaibarriaga, L., Arregui, I., ... & Chust, G. (2019). Large-scale distribution of tuna species in a warming ocean. Global change biology, 25(6), 2043-2060. https://doi.org/10.1111/gcb.14630

Estes, J. A., Terborgh, J., Brashares, J. S., Power, M. E., Berger, J., Bond, W. J., ... & Wardle, D. A. (2011). Trophic downgrading of planet Earth. science, 333(6040), 301-306. 10.1126/science.1205106

FAO. The state of world fisheries and aquaculture 2022: Sustainability in action. 224p.

Fujinami, Y., Kurashima, A., Shiozaki, K., Hiraoka, Y., Semba, Y., Ohshimo, S., ... & Kai, M. (2022). New insights into spatial segregation by sex and life-history stage in blue sharks Prionace glauca in the northwestern Pacific. Marine Ecology Progress Series, 696, 69-84. https://doi.org/10.1016/j.gecco.2020.e01211

Hawkins, ER, Pogson-Manning, L., Jaehnichen, C., & Meager, JJ (2020). Social dynamics and sexual segregation of Australian humpback dolphins (Sousa sahulensis) in Moreton Bay, Queensland. Marine Mammal Science , 36 (2), 500-521. https://doi.org/10.1111/mms.12657

Hazin, F. H. V., & Travassos, P. E. (2007). A pesca oceânica no Brasil no Século 21. Revista Brasileira de Engenharia de Pesca, 2(1), 60-75. https://doi.org/10.18817/repesca.v2i1.34

Hollander, M. e Wolfe, D. Métodos Estatísticos Não Paramétricos. Nova York: John Wiley & Sons. Páginas 15-22, 1973.

ICCAT. (2017). Report of the 2017 ICCAT- Atlantic swordfish data preparatory session. Collect. Vol. Sci. Pap. ICCAT, 74(3): 841-967.

ICCAT. (2022). Report of the 2022 ICCAT- Atlantic swordfish data preparatory session. Collect. Vol. Sci. Pap. ICCAT, 79(2), 001-133.

ICCAT. (2023). Report for the Biennial Period, 2022-2023, Part I (2022). SCRS PLENARY SESSIONS 1 – 9.4 , Madrid, Spain.

ICCAT. (2024).Report for Biennial Period, 2022-2023 - PART II (2024). SCRS PLENARY SESSIONS 1-545, Madrid, Spain .

Kume, S. (1969a). Ecological studies on bigeye tuna – V. A critical review on distribution, size composition and stock structure of bigeye tuna in the north Pacific Ocean (north of 16°N). *Far Seas Fisheries Research Laboratory Bulletin* **1,** 57–75.

Kume, S. (1969b). Ecological studies on bigeye tuna – VI. A review on distribution and size composition of bigeye tuna in the equatorial and south Pacific Ocean. *Far Seas Fisheries Research Laboratory Bulletin* **1,** 77–98.

Leung, E. S., Chilvers, B. L., Nakagawa, S., Moore, A. B., & Robertson, B. C. (2012). Sexual segregation in juvenile New Zealand sea lion foraging ranges: implications for intraspecific competition, population dynamics and conservation. https://doi.org/10.1371/journal.pone.0045389

Lira, M. G., de Nóbrega, M. F., Oliveira, J. E. L (2017). Caracterização da pescaria industrialde espinhel-de-superfície no Rio Grande do Norte. Boletim do Instituto de Pesca, 43(3), 446-458. Doi: 10.20950/1678-2305.2017v43n3p446

Llopiz JK, Hobday AJ (2015) A global comparative analysis of the feeding dynamics and environmental conditions of larval tunas, mackerels, and billfishes. Deep Sea Res II 113:113–124. https://doi.org/10.1016/j.dsr2.2014.05.014

Lombal, AJ, O'dwyer, JE, Friesen, V., Woehler, EJ e Burridge, CP (2020 Identifying mechanisms of genetic differentiation among populations in vagile species: historical factors dominate genetic differentiation in seabirds. Biological Reviews , 95 (3), 625-651. https://doi.org/10.1111/brv.12580

Mejuto, J. (2018). A Review Of Sex-Ratio Patterns In The Atlantic Swordfish (*Xiphias gladius*): Background, Progress, Updates And Limitations. Collect. Vol. Sci. Pap. ICCAT, 75(4), 719-742.

Mejuto, J., De la Serna, J. M., & Garcia, B. (1998). SCRS/97/32 (Rev.) Some considerations on the spatial and temporal variability in the sex-ratio at size of the swordfish (*Xiphias gladius* L.). Collective Volume of Scientific Papers-International Commission For The Conservation Of Atlantic Tunas, 48, 205-215.

Mejuto, J., García-Cortés, B., & Ramos-Cartelle, A. (2008). Reproductive activity of swordfish (*Xiphias gladius*) in the Pacific Ocean on the basis of different macroscopic indicators. 4th Regular Session of the Scientific Committee of the WCPFC. BI-2008/WP 06: 1-23.

Mejuto-García, J., & García-Cortés, B. (2014). Reproductive activity of swordfish *Xiphias gladius*, in the Atlantic Ocean inferred on the basis of macroscopic indicators. Revista de biología marina y oceanografía, 49, 427-447. http://dx.doi.org/10.4067/S0718-19572014000300003

Mourato, B. L.; Arfelli, C. A.; Amorim, A. F.; Hazin, H. G.; Carvalho, F. C.; Hazin, F. H. V. Spatio-temporal distribution and target species in a longline fishery off the southeastern coast of Brazil. Brazilian Journal of Oceanography, v.59, p. 185-194, 2011.

Mourato, B., Sant'ana, R., Gustavo Cardoso, L., & Travassos, P. (2022). Catch rates of swordfish from Brazilian longline Fisheries in the South Atlantic (1994-2020). Collect. Vol. Sci. Pap. ICCAT, 79(2), 335-346

Mucientes, G. R., Queiroz, N., Sousa, L. L., Tarroso, P., & Sims, D. W. (2009). Sexual segregation of pelagic sharks and the potential threat from fisheries. Biology letters, 5(2), 156-159. https://doi.org/10.1098/rsbl.2008.0761

Nóbrega, M. F., Oliveira, M. A., Lira, M. G., de Souza Rocha, S., & Oliveira, J. E. L. (2023). Sustainability of tunas and swordfish exploitation in the equatorial tropical Atlantic Ocean. Marine Policy, 155, 105755.https://doi.org/10.1016/j.marpol.2023.105755

Orgeret, F., Reisinger, R. R., Carpenter-Kling, T., Keys, D. Z., Corbeau, A., Bost, C. A., ... & Pistorius, P. A. (2021). Spatial segregation in a sexually dimorphic central place forager: Competitive exclusion or niche divergence?. Journal of Animal Ecology, 90(10), 2404-2420

Palko, B. J., Beardsley, G. L., & Richards, W. J. (1981). Synopsis of the biology of the swordfish, *Xiphias gladius* Linnaeus (No. 127). US Department of Commerce, National Oceanic and Atmospheric Administration, National Marine Fisheries Service.

Pinto, C., Travers-Trolet, M., Macdonald, J. I., Rivot, E., & Vermard, Y. (2019). Combining multiple data sets to unravel the spatiotemporal dynamics of a data-limited fish stock. Canadian Journal of Fisheries and Aquatic Sciences, 76(8), 1338-1349. https://doi.org/10.1139/cjfas-2018-0149

Poisson, F., & Fauvel, C. (2009). Reproductive dynamics of swordfish (*Xiphias gladius*) in the southwestern Indian Ocean (Reunion Island). Part 1: oocyte development, sexual maturity and spawning. Aquatic Living Resources, 22(1), 45-58. 10.1051/alr/2009007

R Core Team (2024). R: A language and environment for statistical computing. R Foundation for Statistical Computing, Vienna, Austria. URL https://www.R-project.org/.

Reglero P, Tittensor DP, Alvarez-Berastegiu D, Aparicio-Gonzalez A, Worm B (2014) Worldwide distributions of tuna larvae: revisiting hypotheses on environmental requirements for spawning habitats. Mar Ecol Prog Ser 501:207–224.doi: doi: 10.3354/meps10666.

Rey, J. C. (1988). Comentarios sobre las areas de reproduccion del pez espada (*Xiphias gladius*) en el Atlantico y Mediterraneo. Col. Vol. Sci. Pap. ICCAT, 27, 180-192.

Rodrigues, S. L., Carneiro, V. G. O., de Freitas, A. J. R., & de Andrade, H. A. Spatiotemporal Variability Of Target-Species In Tuna And Tuna-Like Fishing In Brazil. Boletim do Instituto de Pesca, v.46, n.2, e587 , 2020)

Ruckstuhl, K. E., & Neuhaus, P. (2002). Sexual segregation in ungulates: a comparative test of three hypotheses. Biological Reviews, 77(1), 77-96.

Schaefer KM (2001) Reproductive biology of tunas. In: Block BA, Stevens DE (eds) Tuna: physiology, ecology and evolution. Fish physiology, vol 19. Academic Press, New York, pp 225–270. https://doi.org/10.1016/S1546-5098(01)19007-2.

Schaefer, K. M., Fuller, D. W. & Miyabe, N. (2005). Reproductive biology of bigeye tuna (*Thunnus obesus*) in the eastern and central Pacific Ocean. Inter-American TropicalTuna Commission Bulletin23,1 – 31.

Sun, C. L., Wang, S. P., & Yeh, S. Z. (2002). Age and growth of the swordfish (*Xiphias gladius* L.) in the waters around Taiwan determined from anal-fin rays. Fishery Bulletin, 100(4), pp. 822-835. http://hdl.handle.net/1834/31104

Sun, C. L., Yeh, S. Z., Chang, Y. J., Chang, H. Y., & Chu, S. L. (2013). Reproductive biology of female bigeye tuna *Thunnus obesus* in the western Pacific Ocean. *Journal of fish biology*, *83*(2), 250-271. https://doi.org/10.1111/jfb.12161.

Taylor, R. G., & Murphy, M. D. (1992). Reproductive biology of the swordfish *Xiphias gladius* in the Straits of Florida and adjacent waters. Fishery Bulletin, 90(4), 809-816.

Tserpes, G. (1995). Determination of age and growth of swordfish, *Xiphias gladius* L., 1758. Fishery Bulletin, 93, 594-602.

Tserpes, G., Peristeraki, P., & Somarakis, S. (2001). On the reproduction of swordfish (*Xiphias gladius* L.) in the eastern Mediterranean. Col. Vol. Sci. Pap. ICCAT, 52(2), 740-744.

Tserpes, G., Peristeraki, P., & Valavanis, V. D. (2008). Distribution of swordfish in the eastern Mediterranean, in relation to environmental factors and the species biology. Hydrobiologia, 612, 241-250. 10.1007/s10750-008-9499-5

Van Dam, R. P., Diez, C. E., Balazs, G. H., Colón, L. A. C., McMillan, W. O., & Schroeder, B. (2008). Sex-specific migration patterns of hawksbill turtles breeding at Mona Island, Puerto Rico. Endangered Species Research, 4(1-2), 85-94. https://doi.org/10.3354/esr00044

Vandeperre, F., Aires-da-Silva, A., Fontes, J., Santos, M., Serrão Santos, R., & Afonso, P. (2014). Movements of Blue Sharks (*Prionace glauca*) across Their Life History. PLoS One , 9 (8), e103538. https://doi.org/10.1371/journal.pone.0103538

Vanpouille, K., Poisson, F., Taquet, M., Ogor, A., & Troadec, H. (2001). Étude de la croissance de l'espadon (*Xiphias gladius*). Etude des caractéristiques biologiques de l'espadon (*Xiphias gladius*) dans le sud-ouest de l'Océan Indien, 205, 139-169.

Wearmouth, V. J., & Sims, D. W. (2008). Sexual segregation in marine fish, reptiles, birds and mammals: behaviour patterns, mechanisms and conservation implications. Advances in marine biology, 54, 107-170. https://doi.org/10.1016/S0065-2881(08)00002-3

Wu, C. R., Lin, Y. F., & Qiu, B. (2019). Impact of the Atlantic multidecadal oscillation on the Pacific North Equatorial Current bifurcation. *Scientific reports*, *9*(1), 2162.

## 4. CONSIDERAÇÕES FINAIS

Os resultados desse estudo ressaltam a importância de uma abordagem multidimensional para a avaliação e gestão de espécies marinhas altamente migratórias. A pesquisa integrou análises espaciais detalhadas, considerando fatores sexuais e temporais, para fornecer uma visão mais robusta das dinâmicas populacionais e ecológicas do espadarte e da albacora-bandolim. Os desafios na coleta de dados refinados e na implementação de estratégias de gestão eficazes foram destacados como áreas críticas que necessitam de atenção contínua.

No primeiro artigo, o desenvolvimento de um protocolo de análise em três etapas permitiu uma avaliação mais precisa da abundância relativa do espadarte, eliminando os efeitos dos fatores relacionados à capturabilidade. A análise mostrou uma tendência geral de declínio da abundância do espadarte entre 2010 e 2017, com picos de dependência espacial em certos anos. Esses resultados destacam a importância de considerar múltiplas abordagens na avaliação da abundância de espécies marinhas, pois o método proposto detectou tendências de declínio antes das padronizações convencionais. Conclui-se que é essencial aprimorar a coleta de dados e implementar estratégias de gestão que possam responder aos sinais de esgotamento iminente dos estoques, evitando consequências ecológicas e socioeconômicas severas.

No segundo artigo, a análise da distribuição espacial diferenciada por sexo do espadarte e da albacora-bandolim revelou padrões de segregação sexual importantes para a gestão das pescarias. As fêmeas de espadarte predominam no setor sul do Atlântico Sul, enquanto os machos são mais comuns no setor equatorial oeste. Em contraste, a albacora-bandolim apresentou uma predominância de machos em quase toda a área de estudo, exceto em 2006, quando as fêmeas foram capturadas em maior proporção em regiões tropicais. Estas descobertas ressaltam a complexidade das interações ecológicas e a necessidade de estratégias de gestão adaptadas às especificidades de cada espécie. Conclui-se que é urgente um monitoramento contínuo e aprimorado, bem como a realização de pesquisas adicionais para compreender melhor a segregação sexual e suas implicações na dinâmica populacional.

As percepções obtidas são fundamentais para orientar políticas de manejo e conservação que garantam a sustentabilidade das populações de espadarte e albacora-bandolim no Atlântico Sudoeste, assegurando que as futuras gerações possam continuar a depender desses valiosos recursos pesqueiros. É recomendado que futuros estudos

explorem a integração de dados ambientais mais refinados, detalhes mais precisos dos equipamentos e estratégias de pesca utilizadas, e a continuidade do desenvolvimento de metodologias que considerem a estrutura espacial das populações. Tais avanços são cruciais para o uso sustentável dos recursos aquáticos e a conservação a longo prazo das espécies estudadas.

## 5. REFERÊNCIAS

ABID, N.; LAGLAOUI, A.; ARAKRAK, A.; BAKKALI, M. The reproductive biology of swordfish (Xiphias gladius) in the Strait of Gibraltar. Journal of the Marine Biological Association of the United Kingdom, v. 99, n. 3, p. 649-659, 2019. https://doi.org/10.1017/S0025315418000346.

ALIÇLI, T. Z., ORAY, I. K., KARAKULAK, F. S., & KAHRAMAN, A. E. Age, sex ratio, length-weight relationships and reproductive biology of Mediterranean swordfish, Xiphias gladius L., 1758, in the eastern Mediterranean. *African Journal of Biotechnology*, *11*(15), 3673-3680, 2012.

AMORIM, S.; SANTOS, M. N.; COELHO, R., & FERNANDEZ-CARVALHO, J. Effects of 17/0 circle hooks and bait on fish catches in a southern Atlantic swordfish longline fishery. **Aquatic Conservation: Marine and Freshwater Ecosystems**, v. 25, n. 4, p. 518-533, 2015. https://doi.org/10.1002/aqc.2443.

ARMITAGE, D. R.; PLUMMER, R.; BERKES, F.; ARTHUR, R. I.; CHARLES, A. T.; DAVIDSON-HUNT, I. J., ... & WOLLENBERG, E. K. Adaptive co-management for social–ecological complexity. *Frontiers in Ecology and the Environment*, *7*(2), 95-102, 2009. https://doi.org/10.1890/070089.

AROCHA, F. Swordfish reproduction in the Atlantic Ocean: an overview. Gulf and Caribbean Research, v. 19, n. 2, p. 21-36, 2007. https://doi.org/10.18785/gcr.1902.05.

ÁVILA-DA-SILVA, A. O.; VAZ-DOS-SANTOS, A. M. Análise das capturas de atuns e afins pelos métodos de vara e isca viva e corrico realizadas pelo N/Pq Malacostraca de 1980 a 1991. Boletim do Instituto de Pesca, v. 26, n. 2, p. 211-221, 2000.

BERGER, A. M.; NIELSEN, J.; O'SULLIVAN, S.; MCGILL, R.; ZUIDEMA, P.; PINNEGAR, J.; KEMP, A. Space oddity: the mission for spatial integration. Canadian Journal of Fisheries and Aquatic Sciences, v. 74, n. 11, p. 1698-1716, 2017.

BORNATOWSKI, H.; ANGELINI, R.; COLL, M.; BARRETO, R. R.; AMORIM, A. F. Ecological role and historical trends of large pelagic predators in a subtropical marine ecosystem of the South Atlantic. Reviews in Fish Biology and Fisheries, v. 28, n. 1, p. 241-259, 2018.

BRILL, R. W.; BIGELOW, K. A.; MUSYL, M. K.; FRITSCHES, K. A.; WARRANT, E. J. Bigeye tuna (Thunnus obesus) behavior and physiology and their relevance to stock

assessments and fishery biology. Col. Vol. Sci. Pap. ICCAT, v. 57, n. 2, p. 142-161, 2005.

CADRIN, S. X. Defining spatial structure for fishery stock assessment. Fisheries Research, v. 221, p. 105397, 2020.

CADRIN, S. X.; MAUNDER, M. N.; PUNT, A. E. Spatial Structure: Theory, estimation and application in stock assessment models. Fisheries Research, v. 229, p. 105608, 2020.

CAMPBELL, R. A. A new spatial framework incorporating uncertain stock and fleet dynamics for estimating fish abundance. Fish and Fisheries, v. 17, p. 56–77, 2016.

CAMPELLO, T. H. P.; COMASSETTO, L. E.; GOMES HAZIN, H.; PACHECO DOS SANTOS, J. C.; KERSTETTER, D., & VIEIRA HAZIN, F. H. Comparative analysis of three bait types in deep-set pelagic longline gear in the Equatorial Atlantic Ocean. **Boletim do Instituto de Pesca**, v. 48, n. Special Edition], 2022. Doi: 10.20950/1678-2305/bip.2022.48.e678.

CAYRÉ, P.; AMON KOTHIAS, J. B.; DIOUF, T.; STRETTA, J. M. Biologia do atum. In: FONTENEAU, A.; MARCILLE, J. (Eds.). Recursos, pesca e biologia dos atuns tropicais do Atlântico Centro-Oriental. Roma: FAO Fisheries Document Paper no 292, FAO, 1993. p. 147-244.

COLLETTE, B. B. Scombridae. Atunes, bacoretas, bonitos, caballas, estorninos, melva, etc. In: FISCHER, W.; KRUPP, F.; SCHNEIDER, W.; SOMMER, C.; CARPENTER, K. E.; NIEM, V. (Eds.). Guia FAO para Identificação de Espécies para Fins de Pesca. Pacífico Centro-Oriental. 3 Vols. FAO, Rome, 1995. p. 1521-1543. Disponível em: http://www.fao.org/docrep/010/v6250s/v6250s00.htm. Acesso em: 6 maio 2024.

COLLETTE, B. B. Scombridae. Tunas (also, albacore, bonitos, mackerels, seerfishes, and wahoo). In: CARPENTER, K. E.; NIEM, V. (Eds.). FAO species identification guide for fishery purposes. The living marine resources of the Western Central Pacific. Vol. 6. Bony fishes part 4 (Labridae to Latimeriidae), estuarine crocodiles. FAO, Rome, 2001. p. 3721-3756. Disponível em: http://www.fao.org/docrep/009/x2401e/x2401e00.htm. Acesso em: 6 maio 2024.

COLLETTE, B.B. AND C.E. NAUEN. FAO Species Catalogue. Vol. 2. Scombrids of the world. An annotated and illustrated catalogue of tunas, mackerels, bonitos and related species known to date. Rome: FAO. FAO Fish. Synop. 125(2):1983. p. 137.

COLUCHI, R.; GIFFONI, B.B.; SALES, G.; et al. Caracterização das pescarias com espinhel pelágico que interagem com tartarugas marinhas no Brasil. In: Livro de Resumos, II Jornada de Conservação e Pesquisa de Tartarugas Marinhas no Atlântico Sul Ocidental, NEMA, Rio Grande, pp. 80–83, 2005.

CULLIS-SUZUKI, S.; PAULY, D. Failing the high seas: a global evaluation of regional fisheries management organizations. **Marine Policy**, v. 34, n. 5, p. 1036-1042, 2010. https://doi.org/10.1016/j.marpol.2010.03.002.

ERAUSKIN-EXTRAMIANA, M.; ARRIZABALAGA, H.; HOBDAY, A. J.; CABRÉ, A.; IBAIBARRIAGA, L.; ARREGUI, I.; MURUA, H.; CHUST, G. Large-scale

distribution of tuna species in a warming ocean. Global Change Biology, v. 25, n. 6, p. 2043-2060, 2019. https://doi.org/10.1111/gcb.14630.

FAO. The State of World Fisheries and Aquaculture 2022: Towards Blue Transformation. Rome: FAO, 2022. https://doi.org/10.4060/cc0461en.

GARCÍA, Jaime Mejuto. **Aspectos biológicos y pesqueros del pez espada (Xiphias gladius Linnaeus, 1758) del Océano Atlántico, con especial referencia a las áreas de actividad de la flota española**. 2007. Tese de Doutorado. Universidade de Santiago de Compostela.

GEBREMEDHIN, S., BRUNEEL, S., GETAHUN, A., ANTENEH, W., & GOETHALS, P. Scientific methods to understand fish population dynamics and support sustainable fisheries management. *Water*, *13*(4), 574, 2021. **https://doi.org/10.3390/w13040574**.

GILMAN, E.; CHALOUPKA, M.; BACH, P.; FENNELL, H.; HALL, M.; MUSYL, M., ... & SONG, L. Effect of pelagic longline bait type on species selectivity: a global synthesis of evidence. **Reviews in Fish Biology and Fisheries**, v. 30, n. 3, p. 535-551, 2020. Doi:10.1007/s11160-020-09612-0.

GUOPING, Z., XIAOJIE, D., LIMING, S., & LIUXIONG, X. Size at sexual maturity of bigeye tuna Thunnus obesus (Perciformes: Scombridae) in the tropical waters: a comparative analysis. *Turkish Journal of Fisheries and Aquatic Sciences*, *11*(1), 2011.
HAAS, B.; MCGEE, J., FLEMING, A.; & HAWARD, M. Factors influencing the performance of regional fisheries management organizations. *Marine Policy*, *113*, 103787, 2020.https://doi.org/10.1016/j.marpol.2019.103787.

HANAMOTO, E. Efeito do ambiente oceanográfico na distribuição do atum patudo. Boletim da Sociedade Japonesa de Oceanografia Pesqueira, v. 51, p. 203-216, 1987.

HATZONIKOLAKIS, Y., TSIARAS, K., TSERPES, G., SOMARAKIS, S., JOHN, M. A. S., PERISTERAKI, P., ... & TRIANTAFYLLOU, G. Investigating growth and reproduction of the Mediterranean swordfish Xiphias gladius through a full life cycle bioenergetics model. *Marine Ecology Progress Series*, *680*, 51-77, 2021.

HAZIN, F.H.V.; HAZIN, H.G. & TRAVASSOS, P.E.P. Influence of the Type of Longline on the Catch Rate and Size Composition of Swordfish, Xiphias gladius (Lineus, 1758), in the Southwestern Equatorial Atlantic Ocean. Collective Volume of Scientific Papers, ICCAT, 54 (5): 1555-1559, 2002.

HAZIN, F.H.V.; ZAGAGLIA,J.R.; BROADHURST, M.K; TRAVASSOS, P.E.P. & BEZERRA, T.R.Q. Review of a Small-scale Pelagic Longline Fishery off Northeastern Brazil. Marine Fisheries Review. 60 (3), 1998.

HAZIN, H. G. 2006. Influência das variáveis oceanográficas na dinâmica populacional e pesca do espadarte, Xiphias gladius Linnaeus 1758, capturados pela frota brasileira (Tese de Doutorado). Universidade do Algarve, Faro, 202 pp.

HURTADO-FERRO, F.; PUNT, A. E.; HILL, K. T. Use of multiple selectivity patterns

as a proxy for spatial structure. Fisheries Research, v. 158, p. 102-115, 2014.

IBAMA. 1985 Relatório da III Reunião Anual do Grupo Permanente de Estudos sobre Atuns e afins. SUDEPE/PDP Ser. Doc. Téc. 33:71-128.

ICCAT. Report for biennial period, 2022-23 - PART II (2023). Col. Vol. Sci. Pap. ICCAT, v. 2, n. 2, p. 1-545, 2024.

ICCAT. Report of the 2022 ICCAT-Atlantic swordfish data preparatory session. Col. Vol. Sci. Pap. ICCAT, v. 79, n. 2, p. 1-133, 2022.

JENSEN, O. P.; BRANCH, T. A.; HILBORN, R. Marine fisheries as ecological experiments. Theoretical Ecology, v. 5, n. 1, p. 3-22, 2012.

LEE, R. E. K. D. Report to the Government of Brazil on tuna fisheries development: Northeastern coast of Brazil. FAO, Expanded Technical Assistance Program, Report no. 739, 47 p., 1957.

MAFRA, E. O., FIEDLER, F., & SCHRAMM, M. Influência da variabilidade meteo-oceanográfica no oceano Atlântico sudoeste sobre a pesca tubarão-azul, Prionace glauca (Linnaeus, 1758). *Metodologias e Aprendizado*, *2*, 72-75, 2019.

MAUNDER, M. N.; PUNT, A. E. Standardizing catch and effort data: a review of recent approaches. Fisheries Research, v. 70, n. 2, p. 141-159, 2004.

MEJUTO-GARCÍA, J.; GARCÍA-CORTÉS, B. Reproductive activity of swordfish Xiphias gladius in the Atlantic Ocean inferred on the basis of macroscopic indicators. Revista de Biología Marina y Oceanografía, v. 49, p. 427-447, 2014. http://dx.doi.org/10.4067/S0718-19572014000300003.

MENESES DE LIMA, J. H.; KOTAS, J. E.; LIN, C. F. A historical review of the Brazilian longline fishery and catch of swordfish. Collective Volume of Scientific Papers ICCAT, v. 51, n. 4, p. 1329-1357, 2000.

MIYAKE, M. Manual de operações para estatísticas e amostragem de túnidos e espécies afins no Oceano Atlântico. 3ª ed. Comissão Internacional para a Conservação do Atum Atlântico, Madrid, Espanha, 1990.

MONTEALEGRE-QUIJANO, S.; Bem, R.; Dolci, D.; & Dumont, L. F. Pesca e recursos pesqueiros. R. Calazans, Org.,"Estudos oceanográficos: do instrumental ao prático", Editora Textos, Pelotas, p. 296-337, 2011.

MOONEY-SEUS, M.L. AND ROSENBERG, A.L. Best Practices for High Seas Fisheries Management: Lessons Learned. London, UK, Chatham House, 8pp. (EEDP BP 07/03), 2007. DOI: http://dx.doi.org/10.25607/OBP-95.

MORFIN, M.; FROMENTIN, J. N.; JADAUD, A.; BEZ, N. Spatio-Temporal Patterns of Key Exploited Marine Species in the Northwestern Mediterranean Sea. PLoS One, v. 7, n. 5, p. e0152466, 2012.

MOURATO, B. L. Padronização da captura por unidade de esforço de espadarte, Xiphias gladius L., 1758 e de tubarão azul, Prionace glauca (L., 1758) capturados pela frota atuneira brasileira no oceano Atlântico. 2007. 156 p. Dissertação (Mestrado em Aquicultura) – Instituto de Pesca, São Paulo, 2007.

MOURATO, B. L.; ARFELLI, C. A.; AMORIM, A. F.; HAZIN, H. G.; CARVALHO, F. C.; HAZIN, F. H. V. Spatio-temporal distribution and target species in a longline fishery off the southeastern coast of Brazil. Brazilian Journal of Oceanography, v.59, p. 185-194, 2011.

NAKAMURA, I. FAO species catalogue. Vol. 5. Billfishes of the world. An annotated and illustrated catalogue of marlins, sailfishes, spearfishes and swordfishes known to date. FAO Fish. Synop. 125(5):65p. Rome: FAO, 1985. Disponível em: http://www.fao.org/docrep/009/ac480e/ac480e00.htm. Acesso em: 6 maio 2006.

PALK, B. J.; BEARDSLEY, G. L.; RICHARDS, W. J. Synopsis of the biology of the swordfish, Xiphias gladius Linnaeus (No. 127). US Department of Commerce, National Oceanic and Atmospheric Administration, National Marine Fisheries Service, 1981.

POISSON, F., ARNAUD-HAOND, S., DEMARCQ, H., MÉTRAL, L., BRISSET, B., CORNELLA, D., & WENDLING, B. French Bluefin Tuna Longline Fishery Bycatch Programme. In: Oceanography Challenges to Future Earth. Springer, Cham. p. 401-405, 2019.

PUNT, A. E. Spatial stock assessment methods: A viewpoint on current issues and assumptions. Fisheries Research, v. 213, p. 132-143, 2019.

RAZA, H., LIU, Q., HANIF, M. T., & HAN, Y. Stock evaluation of the data-limited fisheries: a case study of five major commercially important fishes from the western Indian ocean, Pakistan. *Pakistan Journal of Zoology*, *55*(3), 1099-1108, 2023. https://dx.doi.org/10.17582/journal.pjz/20211108201136

REUCHLIN-HUGENHOLTZ, E.; SHACKELL, N. L.; HUTCHINGS, J.A,. The potential for spatial distribution indices to signal thresholds in marine fish biomass. PLoS One, v. 10, n. 3, p. e0120500, 2015.

REY, J. C. Comentarios sobre las areas de reproduccion del pez espada (Xiphias gladius) en el Atlantico y Mediterraneo. Col. Vol. Sci. Pap. ICCAT, 27, 180-192, 1998.

RUFINO, M. M.; BEZ, N.; BRIND'AMOUR, A. Integrating spatial indicators in the surveillance of exploited marine ecosystems. PloS one, v. 13, n. 11, p. e0207538, 2018.

RUFINO, M. M.; BEZ, N.; BRIND'AMOUR, A. Influence of data pre-processing on the behavior of spatial indicators. Ecological indicators, v. 99, p. 108-117, 2019.

SARAUX, C.; FROMENTIN, J. M.; BIGOT, J. L.; BOURDEIX, J. H.; MORFIN, M.; ROOS, D.; BEVEREN, E. V.; BEZ, N. Spatial Structure and Distribution of Small Pelagic Fish in the Northwestern Mediterranean Sea. PloS one, v. 9, n. 11, p. e111211, 2014.

SCHAEFER, K. M.; FULLER, D. W.; MIYABE, N. Reproductive biology of bigeye tuna (Thunnus obesus) in the eastern and central Pacific Ocean. Inter-American Tropical Tuna Commission Bulletin, 23, 1-31, 2005.

STILLWELL, C.E.; KOHLER, N.E. Food and feeding ecology of the swordfish Xiphias gladius in the Western North Atlantic with estimates of daily ration. Mar. Ecol. Vol 22:239-247, 1985.

SUDEPE. Relatório da III Reunião do Grupo Permanente de Estudos sobre de Atuns e Afins. Santos (SP), 08 a 10 de Junho de 1983.

SUN, C. L., YEH, S. Z., CHANG, Y. J., CHANG, H. Y., & CHU, S. L. Reproductive biology of female bigeye tuna Thunnus obesus in the western Pacific Ocean. *Journal of fish biology*, *83*(2), 250-271, 2013.

SUN, C. L.; WANG, S. P.; YEH, S. Z. Age and growth of the swordfish (Xiphias gladius L.) in the waters around Taiwan determined from anal-fin rays. Fishery Bulletin, 100(4), pp. 822-835, 2002. Disponível em: http://hdl.handle.net/1834/31104. Acesso em: 6 maio 2006.

SUN, C.L.; HUANG, C.L.; YEH, S.Z. Idade e crescimento do atum patudo, Thunnus obesus, no Oceano Pacífico ocidental. Fishery Bulletin, 99: 502-509, 2001.

TAYLOR, R. G.; MURPHY, M. D. Reproductive biology of the swordfish Xiphias gladius in the Straits of Florida and adjacent waters. Fishery Bulletin, 90(4), 809-816, 1992.

THORSON, J.T.; RINDORF, A.; GAO, J.; HANSELMAN, D. H.; WINKER, H. Density-dependent changes in effective area occupied for sea-bottom-associated marine fishes. Proceedings of the Royal Society B: Biological Sciences, v. 283, n. 1840, p. 20161853, 2016.

TIBBO, S.N.; DAY, L. R.; DOUCET, W. F. The swordfish (Xiphias gladius L.) its life-history and economic importance in the Northwest Atlantic. J. Fish. Res. Bd. Can., 130, 47 p, 1961.

TSERPES, G.; PERISTERAKI, P.; VALAVANIS, V. D. Distribution of swordfish in the eastern Mediterranean, in relation to environmental factors and the species biology. Hydrobiologia, 612, 241-250, 2008. 10.1007/s10750-008-9499-5.

WANG, S. P.; MAUNDER, M. N.; NISHIDA, T.; CHEN, Y. R. Influence of model misspecification, temporal changes, and data-weighting in stock assessment models: Application to swordfish (Xiphias gladius) in the Indian Ocean. Fisheries Research, v.166, p.119–128, 2015.

WATSON, J.W. & KERSTETTER, D.W. Pelagic longline fishing gear: a brief history and review of research efforts to improve selectivity. *Marine Technology Society Journal*, **40**(3), 6–11, 2006. https://doi.org/10.4031/002533206787353259.

XU, L.; CHEN, X.; GUAN, W.; TIAN, S.; CHEN, Y. The impact of spatial

autocorrelation on CPUE standardization between two different fisheries. Journal of Oceanology and Limnology, v. 36, n. 3, p. 973-980, 2018.

ZHU, G., DAI, X., XU, L., & ZHOU, Y. Reproductive biology of Bigeye Tuna, Thunnus obesus,(Scombridae) in the eastern and central tropical Pacific Ocean. *Environmental biology of fishes*, *88*, 253-260, 2010.

## ANEXOS

## Appendix: Complementary Material

A total of 22,910 trip observations were available for the period from 2005 to 2017. Both catches and fishing effort were clearly affected by the seasonality of the flags analyzed throughout the time series (Figure 1). These operations were concentrated during the period from 2005 to 2007, contributing to an increase in both fishing effort and swordfish catches. Overall, three distinct phases were observed in the development of this activity. The first phase (2005-2007) was characterized by the presence of a large number of chartered and national vessels, with the highest catch values (>30,000 specimens) and fishing effort recorded (average of 3.9 million hooks). The second phase, which lasted from 2008 to 2012, was marked by a decrease in both catch (<25,000 specimens) and the number of chartered boats, and consequently in the fishing effort employed (average of 1.5 million hooks). Finally, the last period (2013-2017) was marked by the dominance of national vessels and a reduction in swordfish catches (<20,000 specimens).

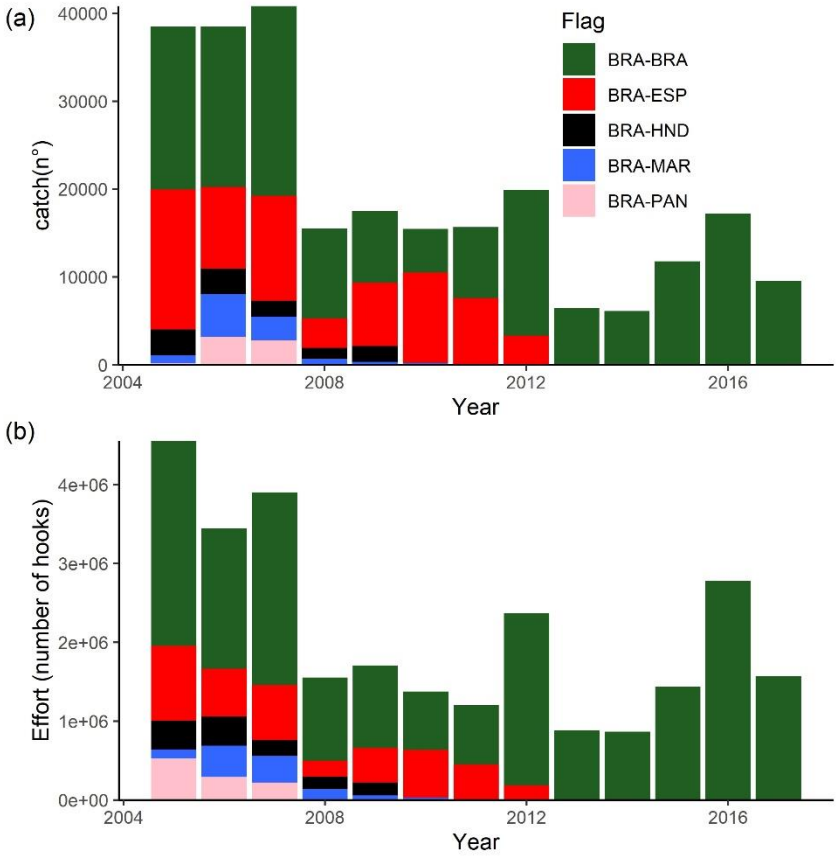


Figure 1. Number of swordfish specimens captured (A) and fishing effort in number of hooks (B) for national vessels (BRA-BRA) and vessels leased from Spain (BRA-ESP), Honduras (BRA-HND), Morocco (BRA-MAR), and Panama (PAN), as recorded in the National Database of Tunas and Related Species (BNDA).

The reduction and absence of chartered vessels also affected the distribution area of fishing effort (Figure 2). The present study found that until 2007, the analyzed area encompassed nearly the entire tropical-oceanic region. However, from 2008 onwards, there was a gradual reduction in spatial coverage, particularly near latitudes 5° to 10° S.

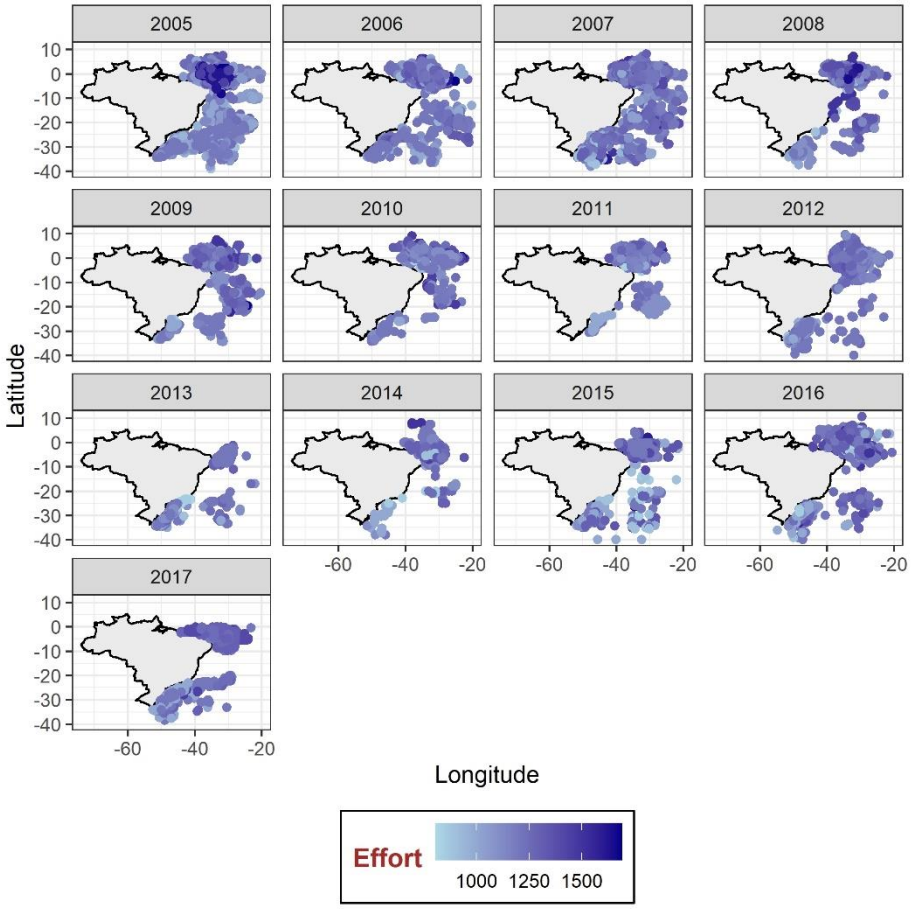


Figure 2. Annual distribution of fishing effort, measured in the number of hooks, for the Brazilian pelagic longline fleet, as recorded in the National Database of Tunas and Related Species (BNDA).

The data were analyzed up to 2017, as the coverage of hooks per basket (HPB) after this period was drastically reduced, not reaching 50% of the total recorded fishing sets (Table 1). HPB was used as an indicator variable for fleet targeting.

Table 1. Record and coverage of fishing sets documented with the specification of hooks per basket (HPB) in the swordfish catch data registered in the National Database of Tunas and Related Species (BNDA).

| Year | HPB | HPB (%) |
|---|---|---|
| 2005 | 3778 | 100 |
| 2006 | 2872 | 100 |
| 2007 | 3224 | 100 |
| 2008 | 1259 | 100 |
| 2009 | 1395 | 100 |

| | | |
|---|---|---|
| 2010 | 1106 | 100 |
| 2011 | 1018 | 100 |
| 2012 | 2004 | 100 |
| 2013 | 756 | 100 |
| 2014 | 723 | 100 |
| 2015 | 1209 | 100 |
| 2016 | 2289 | 100 |
| 2017 | 1277 | 100 |
| 2018 | 3142 | 40,00637 |
| 2019 | 1740 | 0 |
| 2020 | 1485 | 8,148148 |

*Generalized Linear Models (GLMs):*

To investigate the relationship between the independent variables and the response variable, which is the catch in the number of Swordfish (SWO) specimens, component and residual plots were generated (Figure 3). These plots were constructed for the independent variables Flag, Month, HPB (hooks per basket), Lat (latitude), and Lon (longitude). The results indicate that all variables exhibit a linear relationship with the response variable SWO.

The component and residual plot for Flag demonstrated that different vessel flags of origin have a consistent linear relationship with swordfish abundance, suggesting that the nationality of the vessels may influence the catches. The plot for Month revealed a linear seasonal variation, with different months showing consistent patterns in relation to swordfish abundance. For the numerical variables HPB (hooks per basket), Lat (latitude), and Lon (longitude), the component and residual plots also indicated linear relationships, showing that increases in these variables are associated with linear changes in swordfish abundance. These results support the use of a generalized linear model (GLM) to model swordfish abundance with these explanatory variables, justifying the appropriateness of the linear fits in the catch data.

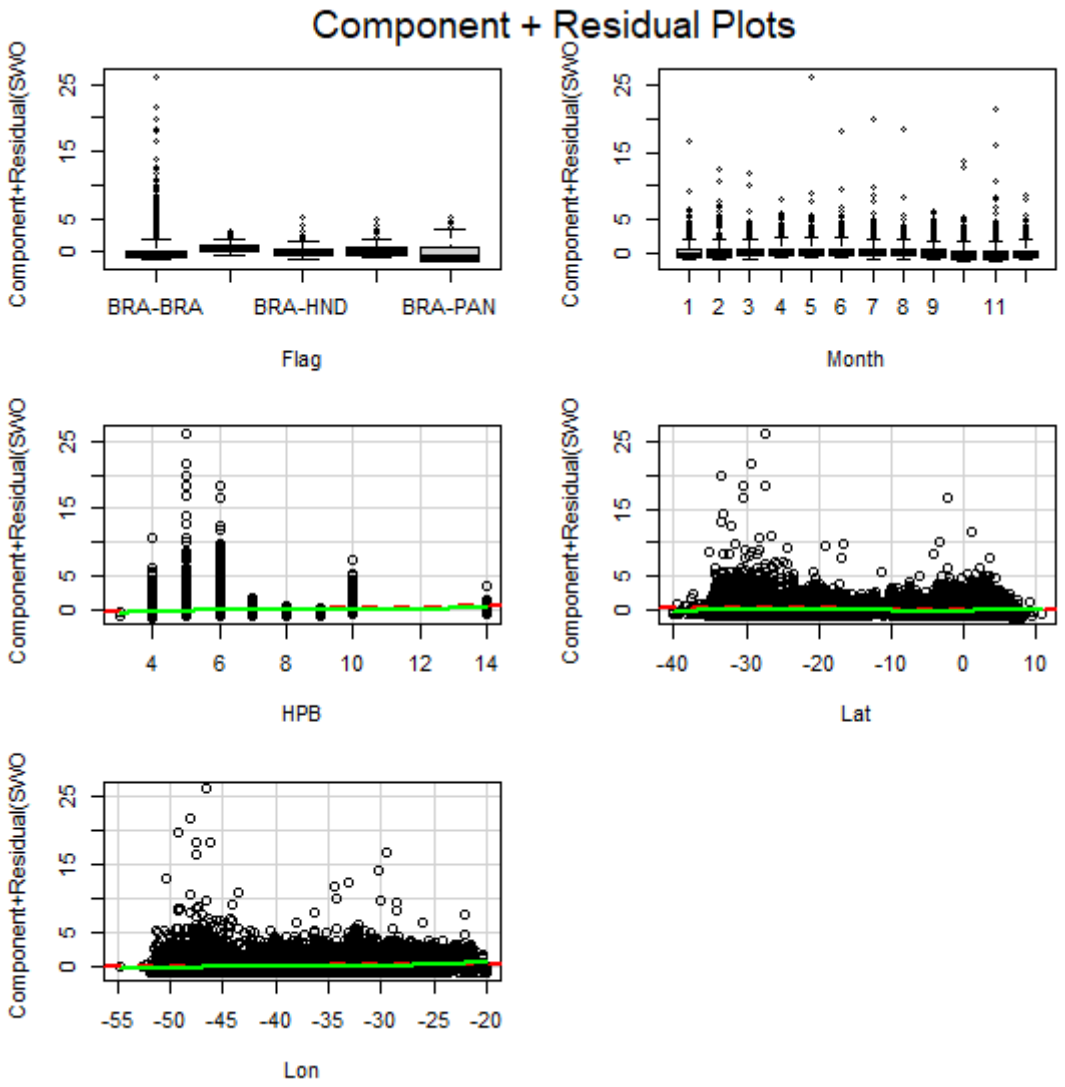


Figure 3: Component and Residual Plots of Independent Variables in Relation to Swordfish Abundance (SWO). Each panel represents an independent variable: Flag (origin flag of the vessels), Month (month of capture), HPB (hooks per basket), Lat (latitude), and Lon (longitude). The red dashed line represents the estimated relationship between the independent variable and the response variable, while the green line indicates the reference line (zero residual).

***Poisson model***

Initially, the catch per unit effort (CPUE) for swordfish (SWO) was standardized using a Poisson model. The results indicate that all variables and interactions in the Poisson model have significant effects on swordfish catches (p-value < 0.001) (Tabela2). Fishing flags, months, hooks per basket (HPB), and geographical coordinates (latitude and longitude), as well as their interactions, play critical roles in determining catch rates. The leased flags from Spain and Panama show very strong positive effects (estimate: 0.34580, p-value: <2.2e-16), while Morocco and Honduras exhibited negative effects (-1.024947

and -0.4534244, p-value < 2.2e-16). Significant effects were observed for most months compared to January, indicating seasonal variation in swordfish abundance. For instance, March (estimate: 0.76925472, p-value: <2e-16) and June (estimate: -1.7084877, p-value: <2.2e-16). HPB showed a significant positive effect (0.34580, p-value: <2.2e-16), suggesting an increase in the response variable with more hooks per basket. Regarding the geographical variables, latitude and longitude have small but significant negative effects (-0.0224231 and -0.0031879, p-value < 2.2e-16).

Table 2. Analysis of estimated coefficients from the Poisson model adjusted for swordfish (SWO) catch. The figure presents parameter estimates, standard errors, test statistics, and p-values for each term included in the model.

| term | estimate | std.error | statistic | p.value |
|---|---|---|---|---|
| (Intercept) | 1.317676456 | 0.002445222 | 538.8779726 | <2.2e-16 |
| FlagBRA-ESP | 1.309174601 | 0.001169088 | 1119.825573 | <2.2e-16 |
| FlagBRA-HND | -0.453424418 | 0.002424525 | -187.0157728 | <2.2e-16 |
| FlagBRA-MAR | -1.024946954 | 0.00423166 | -242.2091918 | <2.2e-16 |
| FlagBRA-PAN | 5.311679195 | 0.006386811 | 831.6637997 | <2.2e-16 |
| Month2 | 0.466091404 | 0.002111342 | 220.7559997 | <2.2e-16 |
| Month3 | 0.76925472 | 0.002205318 | 348.8180159 | <2.2e-16 |
| Month4 | -0.426705184 | 0.002450776 | -174.1102578 | <2.2e-16 |
| Month5 | -1.254296511 | 0.0022669 | -553.3090426 | <2.2e-16 |
| Month6 | -1.708487705 | 0.002383323 | -716.8509943 | <2.2e-16 |
| Month7 | -1.351118348 | 0.002447035 | -552.1450812 | <2.2e-16 |
| Month8 | -0.829416407 | 0.002731295 | -303.6714578 | <2.2e-16 |
| Month9 | -1.235632039 | 0.002667808 | -463.1638623 | <2.2e-16 |
| Month10 | -1.201656608 | 0.002378995 | -505.1110033 | <2.2e-16 |
| Month11 | -0.671259613 | 0.00291645 | -230.1632782 | <2.2e-16 |
| Month12 | 0.151421294 | 0.002265185 | 66.84719528 | <2.2e-16 |
| HPB | 0.267027988 | 0.000382131 | 698.7861337 | <2.2e-16 |
| Lat | -0.02242305 | 5.5731E-05 | -402.3440352 | <2.2e-16 |
| Lon | -0.003187859 | 7.51385E-05 | -42.42642122 | <2.2e-16 |
| FlagBRA-ESP:Month2 | -0.062339681 | 0.000651623 | -95.66833697 | <2.2e-16 |
| FlagBRA-HND:Month2 | 0.190394722 | 0.001885114 | 100.999072 | <2.2e-16 |
| FlagBRA-MAR:Month2 | 0.24973831 | 0.001573881 | 158.6767058 | <2.2e-16 |
| FlagBRA-PAN:Month2 | -0.147932703 | 0.002603785 | -56.81448736 | <2.2e-16 |
| FlagBRA-ESP:Month3 | 0.012270114 | 0.000674547 | 18.19015833 | 6.17615E-74 |
| FlagBRA-HND:Month3 | 0.155901181 | 0.001697033 | 91.86689738 | <2.2e-16 |
| FlagBRA-MAR:Month3 | -0.268881462 | 0.00174458 | -154.123907 | <2.2e-16 |
| FlagBRA-PAN:Month3 | 0.467372888 | 0.002138846 | 218.5163837 | <2.2e-16 |
| FlagBRA-ESP:Month4 | 0.285505783 | 0.000681542 | 418.911544 | <2.2e-16 |
| FlagBRA-HND:Month4 | 0.181794524 | 0.00169976 | 106.95304 | <2.2e-16 |
| FlagBRA-MAR:Month4 | -0.000830913 | 0.001531821 | -0.542434931 | 0.587518921 |
| FlagBRA-PAN:Month4 | 0.659271401 | 0.002107677 | 312.7952659 | <2.2e-16 |

| | | | | |
|---|---|---|---|---|
| FlagBRA-ESP:Month5 | 0.216149082 | 0.000681572 | 317.1331758 | <2.2e-16 |
| FlagBRA-HND:Month5 | 0.081826585 | 0.001678104 | 48.76133986 | <2.2e-16 |
| FlagBRA-MAR:Month5 | -0.247218075 | 0.001552487 | -159.2400203 | <2.2e-16 |
| FlagBRA-PAN:Month5 | 0.267342474 | 0.002217975 | 120.5344832 | <2.2e-16 |
| FlagBRA-ESP:Month6 | 0.053126801 | 0.00070236 | 75.64038362 | <2.2e-16 |
| FlagBRA-HND:Month6 | -0.036808953 | 0.001821275 | -20.2105412 | <2.2e-16 |
| FlagBRA-MAR:Month6 | -0.426764926 | 0.001632847 | -261.362402 | <2.2e-16 |
| FlagBRA-PAN:Month6 | 0.661582988 | 0.002371665 | 278.9529605 | <2.2e-16 |
| FlagBRA-ESP:Month7 | 0.198310652 | 0.000756013 | 262.3110166 | <2.2e-16 |
| FlagBRA-HND:Month7 | -0.091947412 | 0.001846636 | -49.79185335 | <2.2e-16 |
| FlagBRA-MAR:Month7 | 0.336502366 | 0.001690314 | 199.076828 | <2.2e-16 |
| FlagBRA-PAN:Month7 | 1.056921932 | 0.002479585 | 426.2495686 | <2.2e-16 |
| FlagBRA-ESP:Month8 | 0.241563911 | 0.000765722 | 315.4719567 | <2.2e-16 |
| FlagBRA-HND:Month8 | 0.350986903 | 0.001744783 | 201.1635956 | <2.2e-16 |
| FlagBRA-MAR:Month8 | 0.252817841 | 0.001641505 | 154.0158508 | <2.2e-16 |
| FlagBRA-PAN:Month8 | 1.496528735 | 0.002521034 | 593.6169799 | <2.2e-16 |
| FlagBRA-ESP:Month9 | 0.40999487 | 0.000811312 | 505.348118 | <2.2e-16 |
| FlagBRA-HND:Month9 | 0.364823688 | 0.001759648 | 207.3276738 | <2.2e-16 |
| FlagBRA-MAR:Month9 | 0.580418312 | 0.001662069 | 349.2142747 | <2.2e-16 |
| FlagBRA-PAN:Month9 | 0.230437384 | 0.002673599 | 86.18994874 | <2.2e-16 |
| FlagBRA-ESP:Month10 | 0.384482346 | 0.000909155 | 422.9007463 | <2.2e-16 |
| FlagBRA-HND:Month10 | 0.46043897 | 0.001832228 | 251.3000189 | <2.2e-16 |
| FlagBRA-MAR:Month10 | 0.286242891 | 0.001820371 | 157.2442686 | <2.2e-16 |
| FlagBRA-PAN:Month10 | 1.555639434 | 0.002396465 | 649.1391636 | <2.2e-16 |
| FlagBRA-ESP:Month11 | 0.09622876 | 0.00095633 | 100.6229366 | <2.2e-16 |
| FlagBRA-HND:Month11 | 0.736596567 | 0.001933614 | 380.9429784 | <2.2e-16 |
| FlagBRA-MAR:Month11 | 0.141673158 | 0.001830532 | 77.39450781 | <2.2e-16 |
| FlagBRA-PAN:Month11 | 1.220443275 | 0.002527233 | 482.9168408 | <2.2e-16 |
| FlagBRA-ESP:Month12 | 0.120774112 | 0.000820087 | 147.2698255 | <2.2e-16 |
| FlagBRA-HND:Month12 | 0.440640691 | 0.001897718 | 232.1950244 | <2.2e-16 |
| FlagBRA-MAR:Month12 | 0.406499789 | 0.001583813 | 256.6590044 | <2.2e-16 |
| FlagBRA-PAN:Month12 | 1.606433974 | 0.002657389 | 604.5158359 | <2.2e-16 |
| FlagBRA-ESP:Lat | 0.002032522 | 1.66457E-05 | 122.1048122 | <2.2e-16 |
| FlagBRA-HND:Lat | 0.019834872 | 3.18084E-05 | 623.5728839 | <2.2e-16 |
| FlagBRA-MAR:Lat | 0.047404398 | 0.000142375 | 332.9543679 | <2.2e-16 |
| FlagBRA-PAN:Lat | 0.213998985 | 0.000247808 | 863.5665369 | <2.2e-16 |
| FlagBRA-ESP:Lon | 0.024376954 | 3.53301E-05 | 689.9766911 | <2.2e-16 |
| FlagBRA-HND:Lon | -0.01650634 | 6.71721E-05 | -245.7321289 | <2.2e-16 |
| FlagBRA-MAR:Lon | -0.039524372 | 0.000121085 | -326.4191352 | <2.2e-16 |
| FlagBRA-PAN:Lon | 0.1861791 | 0.000180762 | 1029.96881 | <2.2e-16 |
| Month2:HPB | -0.088633655 | 0.000298873 | -296.5597865 | <2.2e-16 |
| Month3:HPB | -0.109867912 | 0.000307929 | -356.7964123 | <2.2e-16 |
| Month4:HPB | -0.131459622 | 0.000318405 | -412.8696577 | <2.2e-16 |
| Month5:HPB | -0.087319156 | 0.0002838 | -307.6779836 | <2.2e-16 |
| Month6:HPB | -0.043343538 | 0.000294651 | -147.1010544 | <2.2e-16 |
| Month7:HPB | -0.15199473 | 0.000293845 | -517.2611065 | <2.2e-16 |
| Month8:HPB | -0.122847246 | 0.000272743 | -450.4142594 | <2.2e-16 |

| | | | | |
|---|---|---|---|---|
| Month9:HPB | -0.038057503 | 0.00031468 | -120.9404969 | <2.2e-16 |
| Month10:HPB | -0.081172272 | 0.000309451 | -262.3107851 | <2.2e-16 |
| Month11:HPB | -0.08494707 | 0.000407493 | -208.4624477 | <2.2e-16 |
| Month12:HPB | -0.030961632 | 0.000311356 | -99.44133649 | <2.2e-16 |
| Month2:Lat | -0.000804787 | 2.5111E-05 | -32.04918752 | <2.2e-16 |
| Month3:Lat | 0.009771676 | 2.53681E-05 | 385.1947838 | <2.2e-16 |
| Month4:Lat | 0.019228423 | 2.71462E-05 | 708.328798 | <2.2e-16 |
| Month5:Lat | 0.023780744 | 2.59202E-05 | 917.458203 | <2.2e-16 |
| Month6:Lat | 0.028578394 | 2.65174E-05 | 1077.72078 | <2.2e-16 |
| Month7:Lat | 0.019594763 | 3.12254E-05 | 627.5267149 | <2.2e-16 |
| Month8:Lat | 0.003761726 | 3.829E-05 | 98.24311338 | <2.2e-16 |
| Month9:Lat | 0.007003822 | 4.00153E-05 | 175.0287071 | <2.2e-16 |
| Month10:Lat | 0.002823132 | 3.60714E-05 | 78.26501041 | <2.2e-16 |
| Month11:Lat | 0.01137574 | 3.56404E-05 | 319.1811156 | <2.2e-16 |
| Month12:Lat | 0.00398369 | 3.12515E-05 | 127.4720162 | <2.2e-16 |
| Month2:Lon | -0.002153125 | 5.21035E-05 | -41.3239589 | <2.2e-16 |
| Month3:Lon | -0.002220566 | 5.36657E-05 | -41.37776988 | <2.2e-16 |
| Month4:Lon | -0.044498056 | 5.48534E-05 | -811.2174172 | <2.2e-16 |
| Month5:Lon | -0.0612348 | 5.29024E-05 | -1157.505575 | <2.2e-16 |
| Month6:Lon | -0.069412953 | 5.4612E-05 | -1271.020899 | <2.2e-16 |
| Month7:Lon | -0.069879758 | 6.13833E-05 | -1138.416265 | <2.2e-16 |
| Month8:Lon | -0.045811168 | 7.11591E-05 | -643.7846892 | <2.2e-16 |
| Month9:Lon | -0.042853409 | 6.95943E-05 | -615.7607708 | <2.2e-16 |
| Month10:Lon | -0.04054748 | 6.14231E-05 | -660.1344252 | <2.2e-16 |
| Month11:Lon | -0.029246596 | 6.43327E-05 | -454.6144607 | <2.2e-16 |
| Month12:Lon | 0.003418803 | 5.78387E-05 | 59.10929802 | <2.2e-16 |
| HPB:Lat | -0.003227715 | 7.42024E-06 | -434.9881988 | <2.2e-16 |
| HPB:Lon | 0.004838007 | 1.11717E-05 | 433.060744 | <2.2e-16 |
| Lat:Lon | -0.000619019 | 1.06074E-06 | -583.5708617 | <2.2e-16 |

The ANOVA table presented below summarizes the analysis of the effects of explanatory variables and their interactions on the response variable SWO in a Poisson model (Table 3). The results indicate that all main variables and their interactions are statistically significant in explaining the variability in swordfish catch (p-value < 2.2e-16). This underscores the complexity and importance of considering multiple factors and their interactions when modeling swordfish abundance in the South Atlantic Ocean.

Table 3: Analysis of Variance (ANOVA) for the Poisson Model

| | Df | Deviance | Resid. Df | Resid. Dev | Pr(>Chi) |
|---|---|---|---|---|---|
| NULL | | | 22909 | 232118944.5 | |
| Flag | 4 | 30864988.7 | 22905 | 201253955.8 | < 2.2e-16 |
| Month | 11 | 3775565.28 | 22894 | 197478390.5 | < 2.2e-16 |
| HPB | 1 | 808116.198 | 22893 | 196670274.3 | < 2.2e-16 |
| Lat | 1 | 764349.392 | 22892 | 195905925 | < 2.2e-16 |

| | | | | | |
|---|---|---|---|---|---|
| Lon | 1 | 606524.986 | 22891 | 195299400 | < 2.2e-16 |
| Flag:Month | 44 | 3783236.19 | 22847 | 191516163.8 | < 2.2e-16 |
| Flag:Lat | 4 | 1122724.22 | 22843 | 190393439.6 | < 2.2e-16 |
| Flag:Lon | 4 | 1175802.34 | 22839 | 189217637.2 | < 2.2e-16 |
| Month:HPB | 11 | 469837.362 | 22828 | 188747799.9 | < 2.2e-16 |
| Month:Lat | 11 | 2650560.02 | 22817 | 186097239.8 | < 2.2e-16 |
| Month:Lon | 11 | 6062556.64 | 22806 | 180034683.2 | < 2.2e-16 |
| HPB:Lat | 1 | 6314.76197 | 22805 | 180028368.4 | < 2.2e-16 |
| HPB:Lon | 1 | 239692.366 | 22804 | 179788676.1 | < 2.2e-16 |
| Lat:Lon | 1 | 296097.479 | 22803 | 179492578.6 | < 2.2e-16 |

Residual analysis was conducted using the DHARMa (Diagnostics for Hierarchical Regression Models) package in R. The results from the residual tests, specifically testOutliers, testDispersion, and testQuantiles, indicated significant anomalies in the data. This suggests the presence of outliers, excessive dispersion (6.5432, p-value < 2.2e-16), and deviation from expected quantiles(Figure x). Furthermore, the application of a zero-inflation test confirmed the presence of an excess of zeros in the data (48.519, p-value < 2.2e-16).

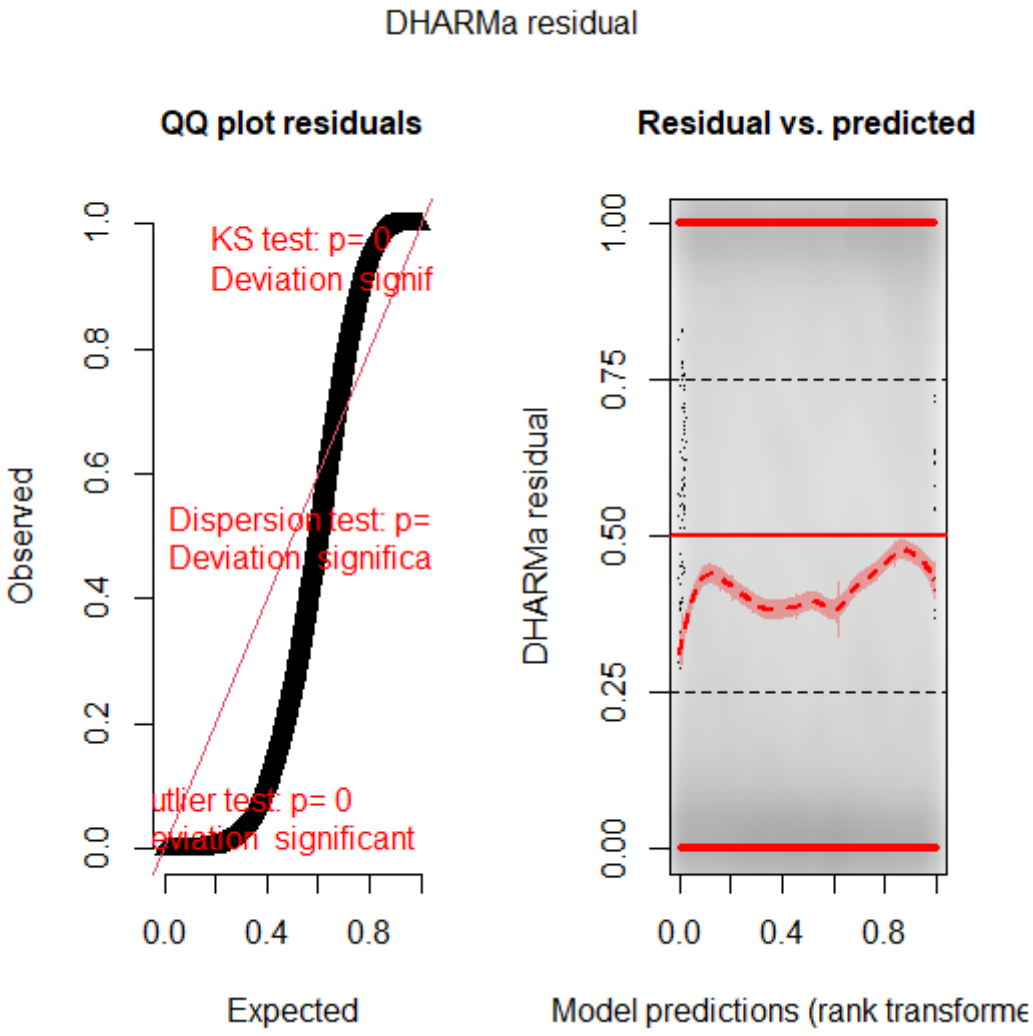


Figure 4: Diagnostics for Hierarchical Regression Models for the Poisson Model

***Binomial Negativo model (BN)***

A Negative Binomial (NB) model was fitted to the SWO catch data, as the Poisson model did not adequately fit the data, exhibiting overdispersion and an excess of zeros. In summary, the NB model presented results similar to those of the Poisson model (Tables 4 and 5).

Table 4. Analysis of estimated coefficients from the Binomial Negativo model adjusted for swordfish (SWO) catch. The figure presents parameter estimates, standard errors, test statistics, and p-values for each term included in the model.

| term | estimate | std.error | statistic | p.value |
|---|---|---|---|---|
| (Intercept) | 0.610054046 | 0.007802113 | 78.19087694 | <2.2e-16 |

| | | | | |
|---|---|---|---|---|
| FlagBRA-ESP | 1.449750436 | 0.004227176 | 342.9595594 | <2.2e-16 |
| FlagBRA-HND | -0.508342305 | 0.006726984 | -75.56764411 | <2.2e-16 |
| FlagBRA-MAR | -1.322036711 | 0.013015987 | -101.5702227 | <2.2e-16 |
| FlagBRA-PAN | 9.13754009 | 0.017315714 | 527.7021864 | <2.2e-16 |
| Month2 | 0.619330609 | 0.006465686 | 95.78730257 | <2.2e-16 |
| Month3 | 0.979808528 | 0.006641392 | 147.5306008 | <2.2e-16 |
| Month4 | -0.000715556 | 0.007594534 | -0.094219881 | 0.924934492 |
| Month5 | -1.049784944 | 0.007125601 | -147.325815 | <2.2e-16 |
| Month6 | -1.6570177 | 0.007534042 | -219.9374074 | <2.2e-16 |
| Month7 | -0.965413912 | 0.007396144 | -130.5293573 | <2.2e-16 |
| Month8 | -0.556359787 | 0.008154923 | -68.22379668 | <2.2e-16 |
| Month9 | -1.259004104 | 0.008091078 | -155.6040086 | <2.2e-16 |
| Month10 | -0.862621045 | 0.006930878 | -124.4605816 | <2.2e-16 |
| Month11 | -0.387604538 | 0.007929897 | -48.87888379 | <2.2e-16 |
| Month12 | 0.252091074 | 0.006677884 | 37.75014257 | <2.2e-16 |
| HPB | 0.345802338 | 0.001288525 | 268.370609 | <2.2e-16 |
| Lat | -0.026415925 | 0.00016776 | -157.4625102 | <2.2e-16 |
| Lon | -0.020358848 | 0.000233461 | -87.20454542 | <2.2e-16 |
| FlagBRA-ESP:Month2 | -0.065891937 | 0.002268242 | -29.0497827 | 1.5486E-185 |
| FlagBRA-HND:Month2 | 0.222711677 | 0.005152985 | 43.21993797 | <2.2e-16 |
| FlagBRA-MAR:Month2 | 0.333383864 | 0.004707615 | 70.81800403 | <2.2e-16 |
| FlagBRA-PAN:Month2 | -0.337668109 | 0.004772273 | -70.75624866 | <2.2e-16 |
| FlagBRA-ESP:Month3 | 0.037656641 | 0.002354334 | 15.99460646 | 1.39336E-57 |
| FlagBRA-HND:Month3 | 0.176669475 | 0.004529285 | 39.00604133 | <2.2e-16 |
| FlagBRA-MAR:Month3 | -0.244194867 | 0.00505189 | -48.3373315 | <2.2e-16 |
| FlagBRA-PAN:Month3 | 0.3228726 | 0.004232081 | 76.29168729 | <2.2e-16 |
| FlagBRA-ESP:Month4 | 0.282775289 | 0.00238688 | 118.4706971 | <2.2e-16 |
| FlagBRA-HND:Month4 | 0.241399603 | 0.004688716 | 51.4852266 | <2.2e-16 |
| FlagBRA-MAR:Month4 | 0.067910171 | 0.004744478 | 14.31351689 | 1.80167E-46 |
| FlagBRA-PAN:Month4 | 0.786686493 | 0.004280483 | 183.7845161 | <2.2e-16 |
| FlagBRA-ESP:Month5 | 0.221125008 | 0.002335669 | 94.67308271 | <2.2e-16 |
| FlagBRA-HND:Month5 | 0.096993612 | 0.00458187 | 21.16900206 | 1.8442E-99 |
| FlagBRA-MAR:Month5 | -0.207389187 | 0.004579656 | -45.28487958 | <2.2e-16 |
| FlagBRA-PAN:Month5 | 0.286216694 | 0.00447197 | 64.0023765 | <2.2e-17 |
| FlagBRA-ESP:Month6 | 0.065757901 | 0.002360607 | 27.85634899 | 9.0234E-171 |
| FlagBRA-HND:Month6 | -0.04299078 | 0.00502394 | -8.557184183 | 1.15658E-17 |
| FlagBRA-MAR:Month6 | -0.439490282 | 0.004688182 | -93.74427821 | <2.2e-16 |
| FlagBRA-PAN:Month6 | 1.205822782 | 0.005435534 | 221.8407319 | <2.2e-17 |
| FlagBRA-ESP:Month7 | 0.187597802 | 0.002568305 | 73.04342955 | <2.2e-18 |
| FlagBRA-HND:Month7 | -0.039440748 | 0.004867563 | -8.102770779 | 5.37214E-16 |

| | | | | |
|---|---|---|---|---|
| FlagBRA-MAR:Month7 | 0.405108507 | 0.005155009 | 78.58541118 | <2.2e-16 |
| FlagBRA-PAN:Month7 | 1.691203917 | 0.005952463 | 284.1183252 | <2.2e-16 |
| FlagBRA-ESP:Month8 | 0.260443134 | 0.002629555 | 99.04458175 | <2.2e-16 |
| FlagBRA-HND:Month8 | 0.387346922 | 0.004861076 | 79.68337711 | <2.2e-16 |
| FlagBRA-MAR:Month8 | 0.398660098 | 0.004786185 | 83.29392185 | <2.2e-16 |
| FlagBRA-PAN:Month8 | 2.105180038 | 0.006398481 | 329.0124798 | <2.2e-16 |
| FlagBRA-ESP:Month9 | 0.388048061 | 0.002854842 | 135.9262969 | <2.2e-16 |
| FlagBRA-HND:Month9 | 0.411273323 | 0.004783975 | 85.96894767 | <2.2e-16 |
| FlagBRA-MAR:Month9 | 0.751843282 | 0.004960586 | 151.5634012 | <2.2e-16 |
| FlagBRA-PAN:Month9 | 0.291502438 | 0.006133315 | 47.52771486 | <2.2e-16 |
| FlagBRA-ESP:Month10 | 0.378772403 | 0.003020169 | 125.414319 | <2.2e-16 |
| FlagBRA-HND:Month10 | 0.478824645 | 0.004967836 | 96.38496123 | <2.2e-16 |
| FlagBRA-MAR:Month10 | 0.417322214 | 0.005070278 | 82.30756037 | <2.2e-16 |
| FlagBRA-PAN:Month10 | 1.6059837 | 0.005679763 | 282.7554039 | <2.2e-16 |
| FlagBRA-ESP:Month11 | 0.114171799 | 0.003020913 | 37.79380472 | <2.2e-16 |
| FlagBRA-HND:Month11 | 0.73463862 | 0.005470732 | 134.2852411 | <2.2e-16 |
| FlagBRA-MAR:Month11 | 0.240353345 | 0.005075496 | 47.35564093 | <2.2e-16 |
| FlagBRA-PAN:Month11 | 1.135209456 | 0.005819197 | 195.080093 | <2.2e-16 |
| FlagBRA-ESP:Month12 | 0.093294351 | 0.002886211 | 32.32416367 | 3.2016E-229 |
| FlagBRA-HND:Month12 | 0.482845077 | 0.005075557 | 95.1314459 | <2.2e-16 |
| FlagBRA-MAR:Month12 | 0.409602258 | 0.004626961 | 88.52511933 | <2.2e-17 |
| FlagBRA-PAN:Month12 | 1.700881233 | 0.006885712 | 247.016041 | <2.2e-18 |
| FlagBRA-ESP:Lat | 0.001700859 | 5.86752E-05 | 28.98768805 | 9.4062E-185 |
| FlagBRA-HND:Lat | 0.019407389 | 9.41697E-05 | 206.0895467 | <2.2e-16 |
| FlagBRA-MAR:Lat | 0.052124143 | 0.000447413 | 116.5011937 | <2.2e-17 |
| FlagBRA-PAN:Lat | 0.198560615 | 0.00063857 | 310.9455849 | <2.2e-18 |
| FlagBRA-ESP:Lon | 0.028833523 | 0.000126178 | 228.5148274 | <2.2e-19 |
| FlagBRA-HND:Lon | -0.01712838 | 0.000192673 | -88.89888848 | <2.2e-20 |
| FlagBRA-MAR:Lon | -0.046688656 | 0.000375779 | -124.2448217 | <2.2e-21 |
| FlagBRA-PAN:Lon | 0.306242662 | 0.000501489 | 610.6665967 | <2.2e-22 |
| Month2:HPB | -0.10044678 | 0.000941415 | -106.6976641 | <2.2e-23 |
| Month3:HPB | -0.139576633 | 0.000944023 | -147.8530228 | <2.2e-24 |
| Month4:HPB | -0.176099906 | 0.000995777 | -176.8467056 | <2.2e-25 |
| Month5:HPB | -0.117045386 | 0.000904024 | -129.4715251 | <2.2e-26 |
| Month6:HPB | -0.052413844 | 0.000963533 | -54.39754868 | <2.2e-27 |
| Month7:HPB | -0.192235079 | 0.000902168 | -213.081342 | <2.2e-28 |
| Month8:HPB | -0.166317172 | 0.000882905 | -188.3749185 | <2.2e-29 |
| Month9:HPB | -0.033396989 | 0.001010233 | -33.05869326 | 1.1668E-239 |
| Month10:HPB | -0.113023943 | 0.000943835 | -119.7497378 | <2.2e-16 |
| Month11:HPB | -0.129667922 | 0.001141212 | -113.623029 | <2.2e-17 |

| | | | | |
|---|---|---|---|---|
| Month12:HPB | -0.056630288 | 0.000948633 | -59.69670382 | <2.2e-18 |
| Month2:Lat | -0.00327495 | 7.51114E-05 | -43.60121499 | <2.2e-19 |
| Month3:Lat | 0.005954925 | 7.73897E-05 | 76.94729699 | <2.2e-20 |
| Month4:Lat | 0.015841641 | 8.5316E-05 | 185.6820389 | <2.2e-21 |
| Month5:Lat | 0.022223037 | 8.08252E-05 | 274.9518622 | <2.2e-22 |
| Month6:Lat | 0.027302402 | 8.2171E-05 | 332.2632443 | <2.2e-23 |
| Month7:Lat | 0.017370956 | 9.7197E-05 | 178.719053 | <2.2e-24 |
| Month8:Lat | 0.003114144 | 0.000113585 | 27.41685102 | 1.727E-165 |
| Month9:Lat | 0.009690556 | 0.000118709 | 81.6326723 | <2.2e-16 |
| Month10:Lat | 0.000370739 | 0.00010071 | 3.68125923 | 0.000232085 |
| Month11:Lat | 0.008881942 | 9.69793E-05 | 91.5859326 | <2.2e-16 |
| Month12:Lat | 0.004472578 | 8.92075E-05 | 50.13677749 | <2.2e-16 |
| Month2:Lon | 0.001542014 | 0.000152203 | 10.13131907 | 4.012E-24 |
| Month3:Lon | 0.00070277 | 0.000157997 | 4.447983231 | 8.66803E-06 |
| Month4:Lon | -0.037902776 | 0.000171118 | -221.5006778 | <2.2e-16 |
| Month5:Lon | -0.058637208 | 0.000163235 | -359.2190422 | <2.2e-16 |
| Month6:Lon | -0.068063109 | 0.000166423 | -408.9777574 | <2.2e-16 |
| Month7:Lon | -0.064241202 | 0.000186206 | -345.0006573 | <2.2e-16 |
| Month8:Lon | -0.043920286 | 0.000210297 | -208.8492856 | <2.2e-16 |
| Month9:Lon | -0.043919097 | 0.000205041 | -214.1969132 | <2.2e-16 |
| Month10:Lon | -0.034869853 | 0.000173264 | -201.2524533 | <2.2e-16 |
| Month11:Lon | -0.026453185 | 0.000175184 | -151.0019246 | <2.2e-16 |
| Month12:Lon | 0.002431266 | 0.000161761 | 15.03002595 | 4.66823E-51 |
| HPB:Lat | -0.004074181 | 2.35123E-05 | -173.2788173 | <2.2e-16 |
| HPB:Lon | 0.006311934 | 3.70899E-05 | 170.1791876 | <2.2e-16 |
| Lat:Lon | -0.00088765 | 3.07966E-06 | -288.2301652 | <2.2e-16 |

Table 5. Analysis of Variance (ANOVA) for the Binomial Negativo Model

| | Df | Deviance | Resid. Df | Resid. Dev | Pr(>Chi) |
|---|---|---|---|---|---|
| NULL | | | 22909 | 38718450 | < 2.2e-16 |
| Flag | 4 | 3290848 | 22905 | 35427602 | < 2.2e-16 |
| Month | 11 | 543076.1 | 22894 | 34884525 | < 2.2e-16 |
| Lat | 1 | 121824.8 | 22893 | 34762701 | < 2.2e-16 |
| HPB | 1 | 85802.04 | 22892 | 34676899 | < 2.2e-16 |
| Lon | 1 | 79859.02 | 22891 | 34597040 | < 2.2e-16 |
| Flag:Month | 44 | 597080.5 | 22847 | 33999959 | < 2.2e-16 |
| Flag:Lat | 4 | 148483.1 | 22843 | 33851476 | < 2.2e-16 |
| Flag:Lon | 4 | 360993 | 22839 | 33490483 | < 2.2e-16 |
| Month:Lat | 11 | 333218.4 | 22828 | 33157265 | < 2.2e-16 |
| Month:HPB | 11 | 66749.21 | 22817 | 33090515 | < 2.2e-16 |
| Month:Lon | 11 | 709708.8 | 22806 | 32380807 | < 2.2e-16 |

| | | | | | |
|---|---|---|---|---|---|
| HPB:Lat | 1 | 950.6607 | 22805 | 32379856 | < 2.2e-16 |
| Lat:Lon | 1 | 80752.89 | 22804 | 32299103 | < 2.2e-16 |
| HPB:Lon | 1 | 32470.85 | 22803 | 32266632 | < 2.2e-16 |

The results of the negative binomial model residual analyses demonstrated a reduction in data dispersion (0.06, p-value < 0.001) compared to the Poisson model. However, there remains an excess of zeros and a pattern in the residuals (Figure 5).

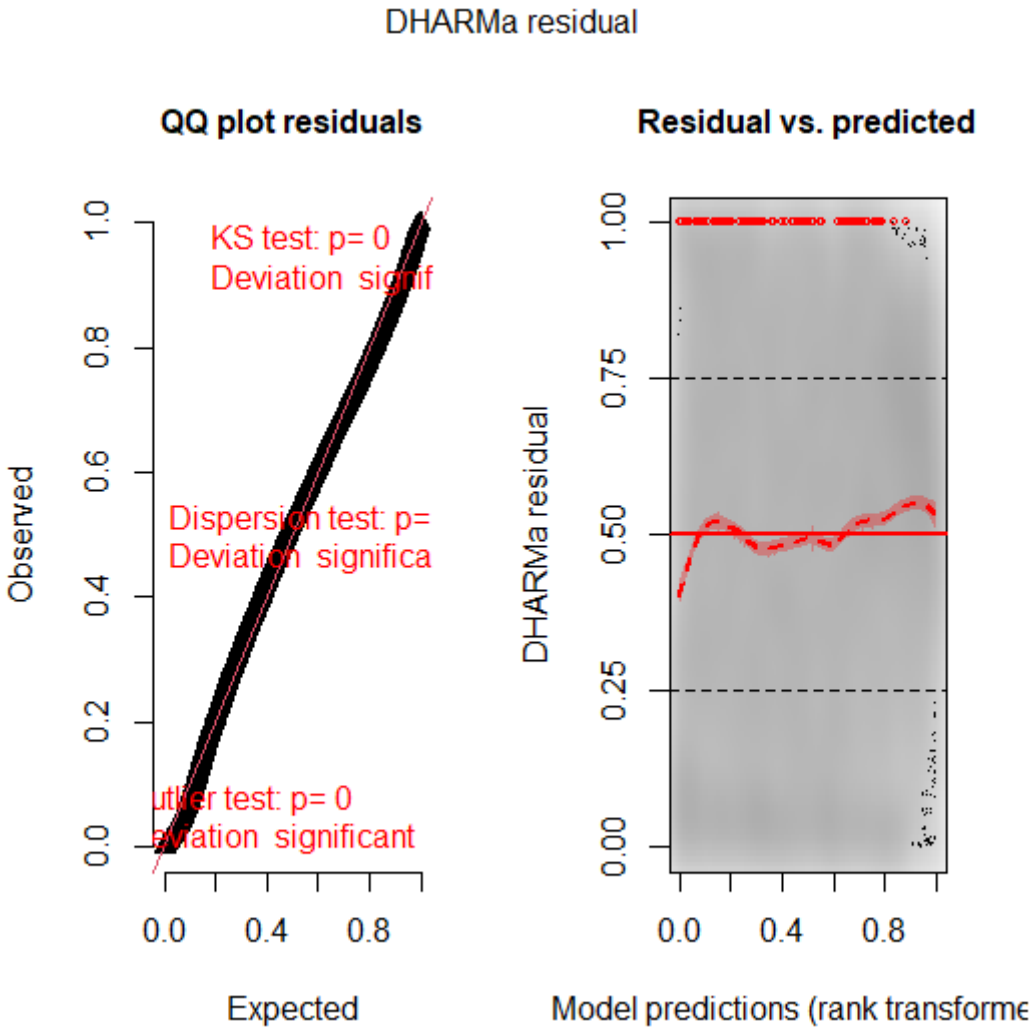


Figure 5: Diagnostics for Hierarchical Regression Models for the Negative Binomial Model.

In light of these results, it became evident that standard GLM models (P and BN) were not adequate to capture the complexity of the data. Therefore, a model that considers the excess of zeros was chosen, opting for a zero-inflated model, which is more appropriate

for data with a large number of zeros. This adjustment aims to provide a better fit and interpretation of swordfish catch data, taking into account the zero-inflation structure present in the data (Tables 6, 7, and 8).

Table 6. Analysis of estimated coefficients from the Zero-Inflated Poisson (ZIP) model adjusted for swordfish (SWO) catch. The figure presents parameter estimates, standard errors, test statistics, and p-values for each term included in the model.

| Term | Estimate | Std. Error | z value | Pr(>\|z\|) |
|---|---|---|---|---|
| (Intercept) | -6.084667773 | 0.087962989 | -69.17304436 | 0 |
| FlagBRA-ESP | 1.570008206 | 0.054355897 | 28.88386144 | 1.9042E-183 |
| FlagBRA-HND | 0.232783286 | 0.12015242 | 1.937399892 | 0.05269648 |
| FlagBRA-MAR | -1.655960709 | 0.195923415 | -8.452081683 | 2.86154E-17 |
| FlagBRA-PAN | 0.538990704 | 0.351251863 | 1.534484971 | 0.124910388 |
| Month2 | 0.751198276 | 0.070288255 | 10.68739396 | 1.16601E-26 |
| Month3 | 1.064211741 | 0.074242876 | 14.33419343 | 1.33792E-46 |
| Month4 | -0.1718276 | 0.083507671 | -2.057626534 | 0.039625998 |
| Month5 | -0.736030009 | 0.077104281 | -9.545903223 | 1.34927E-21 |
| Month6 | -1.087093223 | 0.08226445 | -13.2146173 | 7.22529E-40 |
| Month7 | -0.913627398 | 0.083209687 | -10.97982016 | 4.77874E-28 |
| Month8 | -0.838627083 | 0.096354761 | -8.70353552 | 3.21702E-18 |
| Month9 | -0.680335141 | 0.092930455 | -7.32090617 | 2.46302E-13 |
| Month10 | -0.787343131 | 0.082140592 | -9.585311167 | 9.21794E-22 |
| Month11 | -0.66922215 | 0.104630183 | -6.396071645 | 1.59425E-10 |
| Month12 | 0.336127434 | 0.077274446 | 4.349787692 | 1.36269E-05 |
| HPB | 0.31263131 | 0.01489968 | 20.98241726 | 9.49426E-98 |
| Lat | -0.000760442 | 0.001536009 | -0.495076472 | 0.620546141 |
| Lon | -0.015015821 | 0.00259752 | -5.780830871 | 7.43326E-09 |
| FlagBRA-ESP:Month2 | -0.069333929 | 0.022455263 | -3.087647117 | 0.002017479 |
| FlagBRA-HND:Month2 | 0.150691339 | 0.065308046 | 2.307393176 | 0.021032911 |
| FlagBRA-MAR:Month2 | 0.148466965 | 0.058058819 | 2.557181961 | 0.0105524 |
| FlagBRA-PAN:Month2 | 0.004699736 | 0.123745583 | 0.037979016 | 0.969704413 |
| FlagBRA-ESP:Month3 | -0.002970248 | 0.02323337 | -0.127844026 | 0.898272409 |
| FlagBRA-HND:Month3 | 0.103974571 | 0.059038046 | 1.761145188 | 0.078213832 |
| FlagBRA-MAR:Month3 | -0.295948187 | 0.062178346 | -4.759666442 | 1.93913E-06 |
| FlagBRA-PAN:Month3 | 0.524226829 | 0.094929645 | 5.522266802 | 3.34654E-08 |
| FlagBRA-ESP:Month4 | 0.258832137 | 0.023577567 | 10.97789829 | 4.88148E-28 |
| FlagBRA-HND:Month4 | 0.191831325 | 0.059442529 | 3.227173029 | 0.001250198 |
| FlagBRA-MAR:Month4 | -0.035498636 | 0.055689814 | -0.63743499 | 0.523841543 |
| FlagBRA-PAN:Month4 | 0.585999614 | 0.095035353 | 6.166122315 | 6.9985E-10 |
| FlagBRA-ESP:Month5 | 0.175484972 | 0.02354936 | 7.451793713 | 9.20796E-14 |
| FlagBRA-HND:Month5 | 0.037202353 | 0.058533402 | 0.63557475 | 0.525053631 |
| FlagBRA-MAR:Month5 | -0.255403205 | 0.055835826 | -4.574181529 | 4.78085E-06 |
| FlagBRA-PAN:Month5 | 0.330097899 | 0.098787191 | 3.341505073 | 0.000833255 |
| FlagBRA-ESP:Month6 | -0.035181752 | 0.024389918 | -1.442471093 | 0.149169521 |
| FlagBRA-HND:Month6 | -0.126456546 | 0.063591788 | -1.988567239 | 0.04674899 |
| FlagBRA-MAR:Month6 | -0.457145337 | 0.059019171 | -7.745709179 | 9.50498E-15 |

| | | | | |
|---|---|---|---|---|
| FlagBRA-PAN:Month6 | 0.247497779 | 0.102615041 | 2.411905465 | 0.015869396 |
| FlagBRA-ESP:Month7 | 0.16267311 | 0.026006215 | 6.255162905 | 3.97101E-10 |
| FlagBRA-HND:Month7 | -0.123664137 | 0.06410112 | -1.929204006 | 0.053705541 |
| FlagBRA-MAR:Month7 | 0.243796646 | 0.06087462 | 4.004898029 | 6.20442E-05 |
| FlagBRA-PAN:Month7 | 0.730963325 | 0.105689815 | 6.916118893 | 4.64185E-12 |
| FlagBRA-ESP:Month8 | 0.22583624 | 0.026319582 | 8.580540525 | 9.44284E-18 |
| FlagBRA-HND:Month8 | 0.305177151 | 0.060514038 | 5.043080231 | 4.58097E-07 |
| FlagBRA-MAR:Month8 | 0.26635539 | 0.058645327 | 4.541800717 | 5.57758E-06 |
| FlagBRA-PAN:Month8 | 1.048506683 | 0.109222116 | 9.599765342 | 8.01266E-22 |
| FlagBRA-ESP:Month9 | 0.355186161 | 0.02796851 | 12.69950266 | 5.95067E-37 |
| FlagBRA-HND:Month9 | 0.266128907 | 0.061160857 | 4.351294576 | 1.35336E-05 |
| FlagBRA-MAR:Month9 | 0.522227796 | 0.060237607 | 8.669464483 | 4.34157E-18 |
| FlagBRA-PAN:Month9 | 0.110639317 | 0.108638911 | 1.018413352 | 0.30848156 |
| FlagBRA-ESP:Month10 | 0.357454797 | 0.031021469 | 11.52281968 | 1.01243E-30 |
| FlagBRA-HND:Month10 | 0.371839981 | 0.063995401 | 5.810417236 | 6.23173E-09 |
| FlagBRA-MAR:Month10 | 0.307313248 | 0.06502046 | 4.726408379 | 2.28526E-06 |
| FlagBRA-PAN:Month10 | 1.105647383 | 0.098975423 | 11.17092862 | 5.65862E-29 |
| FlagBRA-ESP:Month11 | 0.123301623 | 0.032692119 | 3.771600872 | 0.000162204 |
| FlagBRA-HND:Month11 | 0.609508545 | 0.067647318 | 9.010091785 | 2.05884E-19 |
| FlagBRA-MAR:Month11 | 0.025618677 | 0.065646573 | 0.39025156 | 0.696350538 |
| FlagBRA-PAN:Month11 | 1.142792541 | 0.10759812 | 10.62093411 | 2.38166E-26 |
| FlagBRA-ESP:Month12 | 0.187557468 | 0.028288055 | 6.630270903 | 3.35071E-11 |
| FlagBRA-HND:Month12 | 0.313871518 | 0.066248449 | 4.73779419 | 2.16057E-06 |
| FlagBRA-MAR:Month12 | 0.321668851 | 0.056812167 | 5.661971168 | 1.49644E-08 |
| FlagBRA-PAN:Month12 | 1.347157511 | 0.110511282 | 12.19022612 | 3.50448E-34 |
| FlagBRA-ESP:HPB | -0.083623097 | 0.007392238 | -11.31228422 | 1.1408E-29 |
| FlagBRA-HND:HPB | -0.113892064 | 0.017578802 | -6.478943387 | 9.23671E-11 |
| FlagBRA-MAR:HPB | 0.032381104 | 0.019718713 | 1.642150967 | 0.100558722 |
| FlagBRA-PAN:HPB | 0.433841275 | 0.032238097 | 13.45740958 | 2.7851E-41 |
| FlagBRA-ESP:Lat | 0.000942726 | 0.000556773 | 1.693196824 | 0.090418009 |
| FlagBRA-HND:Lat | 0.02497865 | 0.001308897 | 19.08373768 | 3.44704E-81 |
| FlagBRA-MAR:Lat | 0.039828184 | 0.005181889 | 7.686035846 | 1.51764E-14 |
| FlagBRA-PAN:Lat | 0.120450994 | 0.009392248 | 12.82451174 | 1.19537E-37 |
| FlagBRA-ESP:Lon | 0.019682038 | 0.001164194 | 16.90615145 | 4.05329E-64 |
| FlagBRA-HND:Lon | -0.013704504 | 0.002421219 | -5.660166212 | 1.51226E-08 |
| FlagBRA-MAR:Lon | -0.051507324 | 0.00428876 | -12.0098419 | 3.15448E-33 |
| FlagBRA-PAN:Lon | 0.10189744 | 0.007450955 | 13.67575498 | 1.41729E-42 |
| Month2:HPB | -0.100977246 | 0.009823509 | -10.27914223 | 8.75029E-25 |
| Month3:HPB | -0.120582704 | 0.010208284 | -11.81223995 | 3.3745E-32 |
| Month4:HPB | -0.105535519 | 0.010722416 | -9.842512651 | 7.38432E-23 |
| Month5:HPB | -0.094274915 | 0.009498295 | -9.925456653 | 3.22623E-23 |
| Month6:HPB | -0.059277191 | 0.009934334 | -5.966901274 | 2.41802E-09 |
| Month7:HPB | -0.131837155 | 0.009888387 | -13.33252401 | 1.49744E-40 |
| Month8:HPB | -0.117934748 | 0.009355181 | -12.60635625 | 1.94793E-36 |
| Month9:HPB | -0.065356279 | 0.010679218 | -6.119949945 | 9.36048E-10 |
| Month10:HPB | -0.11453202 | 0.010541953 | -10.86440248 | 1.70335E-27 |

| | | | | |
|---|---|---|---|---|
| Month11:HPB | -0.063627776 | 0.014493404 | -4.390119693 | 1.13288E-05 |
| Month12:HPB | -0.052554583 | 0.010537032 | -4.987607929 | 6.11315E-07 |
| Month2:Lat | 0.000681725 | 0.000872684 | 0.781181656 | 0.434695661 |
| Month3:Lat | 0.012035519 | 0.000880119 | 13.67487953 | 1.43445E-42 |
| Month4:Lat | 0.023283379 | 0.000919753 | 25.3148175 | 2.1941E-141 |
| Month5:Lat | 0.027598988 | 0.000867701 | 31.80701526 | 5.1775E-222 |
| Month6:Lat | 0.031614164 | 0.000897979 | 35.20591715 | 1.6233E-271 |
| Month7:Lat | 0.024215917 | 0.001066209 | 22.71217265 | 3.3963E-114 |
| Month8:Lat | 0.014840781 | 0.001344506 | 11.03809069 | 2.50295E-28 |
| Month9:Lat | 0.012623185 | 0.001393546 | 9.058321384 | 1.32473E-19 |
| Month10:Lat | 0.008022291 | 0.001264205 | 6.345721344 | 2.21386E-10 |
| Month11:Lat | 0.017074687 | 0.00125893 | 13.56286174 | 6.64905E-42 |
| Month12:Lat | 0.002696106 | 0.001102514 | 2.445416707 | 0.014468486 |
| Month2:Lon | 0.00446917 | 0.001764112 | 2.533382482 | 0.011296761 |
| Month3:Lon | 0.00544341 | 0.001820044 | 2.990812524 | 0.002782363 |
| Month4:Lon | -0.032809611 | 0.001860142 | -17.63823268 | 1.25319E-69 |
| Month5:Lon | -0.047031184 | 0.001795226 | -26.19791355 | 2.8069E-151 |
| Month6:Lon | -0.054607652 | 0.001875345 | -29.11871623 | 2.0806E-186 |
| Month7:Lon | -0.054296042 | 0.002095188 | -25.91463778 | 4.5553E-148 |
| Month8:Lon | -0.046330505 | 0.002507671 | -18.47550973 | 3.25142E-76 |
| Month9:Lon | -0.030979563 | 0.002440317 | -12.69489411 | 6.31153E-37 |
| Month10:Lon | -0.034047013 | 0.002143099 | -15.88681283 | 7.82039E-57 |
| Month11:Lon | -0.027853021 | 0.002235452 | -12.45967939 | 1.23868E-35 |
| Month12:Lon | 0.005681472 | 0.001992899 | 2.850857849 | 0.004360146 |
| HPB:Lat | -0.004147195 | 0.000275385 | -15.05964912 | 2.98366E-51 |
| HPB:Lon | 0.006342586 | 0.000411763 | 15.40348488 | 1.55081E-53 |

Table 7. Analysis of estimated coefficients from the Zero-Inflated Negative Binomial (ZINB) model adjusted for swordfish (SWO) catch. The figure presents parameter estimates, standard errors, test statistics, and p-values for each term included in the model.

| Term | Estimate | Std. Error | z value | Pr(>\|z\|) |
|---|---|---|---|---|
| (Intercept) | -6.216243617 | 0.248037402 | -25.06171878 | 1.301E-138 |
| FlagBRA-ESP | 1.612853299 | 0.165424206 | 9.749802247 | 1.84828E-22 |
| FlagBRA-HND | 0.11168632 | 0.300125956 | 0.372131492 | 0.70979495 |
| FlagBRA-MAR | -1.840155829 | 0.547544406 | -3.360742636 | 0.000777332 |
| FlagBRA-PAN | 1.029907207 | 0.928016446 | 1.109794133 | 0.267087748 |
| Month2 | 0.75844057 | 0.199383318 | 3.803931932 | 0.000142417 |
| Month3 | 0.990726446 | 0.203815606 | 4.860895913 | 1.16856E-06 |
| Month4 | 0.175985314 | 0.237269642 | 0.741710199 | 0.458262939 |
| Month5 | -0.736172303 | 0.221782608 | -3.319341895 | 0.000902299 |
| Month6 | -1.140741834 | 0.245549238 | -4.645674505 | 3.38967E-06 |
| Month7 | -0.909091169 | 0.225617202 | -4.029352205 | 5.59308E-05 |
| Month8 | -0.877652609 | 0.264917535 | -3.312927577 | 0.000923249 |
| Month9 | -0.928512652 | 0.2563876 | -3.62151934 | 0.000292878 |

| | | | | |
|---|---|---|---|---|
| Month10 | -0.981905323 | 0.218311746 | -4.497720993 | 6.86858E-06 |
| Month11 | -0.086739792 | 0.255140036 | -0.339969347 | 0.733879612 |
| Month12 | 0.162993918 | 0.219546033 | 0.742413407 | 0.457836899 |
| HPB | 0.346469308 | 0.043777851 | 7.914260329 | 2.48727E-15 |
| Lat | 0.002779762 | 0.004186885 | 0.663921199 | 0.506740747 |
| Lon | -0.016512678 | 0.006991999 | -2.361653504 | 0.018193638 |
| FlagBRA-ESP:Month2 | -0.049952571 | 0.06554758 | -0.762081088 | 0.446011609 |
| FlagBRA-HND:Month2 | 0.177436673 | 0.153644051 | 1.154855477 | 0.248149614 |
| FlagBRA-MAR:Month2 | 0.160986828 | 0.150687612 | 1.068348123 | 0.285363509 |
| FlagBRA-PAN:Month2 | -0.046034205 | 0.20362285 | -0.226075832 | 0.821142441 |
| FlagBRA-ESP:Month3 | 0.012674147 | 0.068583903 | 0.184797695 | 0.853387716 |
| FlagBRA-HND:Month3 | 0.045728545 | 0.13507009 | 0.338554193 | 0.734945596 |
| FlagBRA-MAR:Month3 | -0.324622321 | 0.155372054 | -2.089322451 | 0.036678707 |
| FlagBRA-PAN:Month3 | 0.521077848 | 0.18184544 | 2.865498563 | 0.004163532 |
| FlagBRA-ESP:Month4 | 0.168327415 | 0.070940169 | 2.372808189 | 0.017653429 |
| FlagBRA-HND:Month4 | 0.222551737 | 0.140184124 | 1.587567342 | 0.112384208 |
| FlagBRA-MAR:Month4 | -0.116558022 | 0.149290907 | -0.78074428 | 0.434952911 |
| FlagBRA-PAN:Month4 | 0.638980137 | 0.180722082 | 3.535705936 | 0.000406687 |
| FlagBRA-ESP:Month5 | 0.181153552 | 0.068667202 | 2.638137945 | 0.008336266 |
| FlagBRA-HND:Month5 | 0.053573823 | 0.138629825 | 0.386452359 | 0.699161679 |
| FlagBRA-MAR:Month5 | -0.285460734 | 0.146138149 | -1.953362183 | 0.050776694 |
| FlagBRA-PAN:Month5 | 0.353790676 | 0.192118229 | 1.841525805 | 0.065544543 |
| FlagBRA-ESP:Month6 | -0.011265417 | 0.070453716 | -0.159898127 | 0.872961324 |
| FlagBRA-HND:Month6 | -0.204463383 | 0.151253159 | -1.351795781 | 0.176440654 |
| FlagBRA-MAR:Month6 | -0.549113152 | 0.150562466 | -3.647078624 | 0.000265239 |
| FlagBRA-PAN:Month6 | 0.418655904 | 0.20486856 | 2.043534181 | 0.040999587 |
| FlagBRA-ESP:Month7 | 0.178600799 | 0.075028143 | 2.380450747 | 0.017291472 |
| FlagBRA-HND:Month7 | -0.140740138 | 0.146112052 | -0.963234285 | 0.335429963 |
| FlagBRA-MAR:Month7 | 0.262924233 | 0.161792404 | 1.625071552 | 0.104147314 |
| FlagBRA-PAN:Month7 | 0.86750669 | 0.212936516 | 4.07401561 | 4.62094E-05 |
| FlagBRA-ESP:Month8 | 0.240071211 | 0.076071393 | 3.155867144 | 0.001600217 |
| FlagBRA-HND:Month8 | 0.28315127 | 0.144450076 | 1.960201603 | 0.049972231 |
| FlagBRA-MAR:Month8 | 0.334255278 | 0.154204461 | 2.167610953 | 0.0301883 |
| FlagBRA-PAN:Month8 | 1.209826131 | 0.237077518 | 5.103082489 | 3.34165E-07 |
| FlagBRA-ESP:Month9 | 0.33495651 | 0.083664951 | 4.003546362 | 6.24E-05 |
| FlagBRA-HND:Month9 | 0.236488432 | 0.143049772 | 1.653189854 | 0.098292231 |
| FlagBRA-MAR:Month9 | 0.577961414 | 0.162509297 | 3.556482141 | 0.000375854 |
| FlagBRA-PAN:Month9 | 0.149707964 | 0.217708937 | 0.687651898 | 0.491672018 |
| FlagBRA-ESP:Month10 | 0.387632606 | 0.08660808 | 4.475709505 | 7.6158E-06 |
| FlagBRA-HND:Month10 | 0.319572332 | 0.149473253 | 2.13799008 | 0.032517548 |
| FlagBRA-MAR:Month10 | 0.310152281 | 0.162868083 | 1.904315899 | 0.056869055 |
| FlagBRA-PAN:Month10 | 1.261669105 | 0.203647554 | 6.195356046 | 5.81534E-10 |
| FlagBRA-ESP:Month11 | 0.144853939 | 0.088509609 | 1.636589981 | 0.101716171 |
| FlagBRA-HND:Month11 | 0.679386729 | 0.163698617 | 4.150228875 | 3.32143E-05 |

| | | | | |
|---|---|---|---|---|
| FlagBRA-MAR:Month11 | 0.065826746 | 0.1601489 | 0.411034645 | 0.681047131 |
| FlagBRA-PAN:Month11 | 1.177359906 | 0.224529117 | 5.243684747 | 1.57401E-07 |
| FlagBRA-ESP:Month12 | 0.154209725 | 0.085266866 | 1.808553916 | 0.070520333 |
| FlagBRA-HND:Month12 | 0.297340096 | 0.152189799 | 1.953745244 | 0.050731353 |
| FlagBRA-MAR:Month12 | 0.248317039 | 0.14485192 | 1.714282 | 0.086476947 |
| FlagBRA-PAN:Month12 | 1.39252873 | 0.237275229 | 5.868833145 | 4.38873E-09 |
| FlagBRA-ESP:HPB | -0.08565806 | 0.022494754 | -3.807912772 | 0.000140145 |
| FlagBRA-HND:HPB | -0.105916881 | 0.045946009 | -2.305246575 | 0.021152768 |
| FlagBRA-MAR:HPB | -0.002700636 | 0.059918411 | -0.045071895 | 0.964050003 |
| FlagBRA-PAN:HPB | 0.486441635 | 0.082714018 | 5.881005979 | 4.0778E-09 |
| FlagBRA-ESP:Lat | -0.00269959 | 0.001664732 | -1.621636669 | 0.104881166 |
| FlagBRA-HND:Lat | 0.025277433 | 0.003339155 | 7.570009805 | 3.73196E-14 |
| FlagBRA-MAR:Lat | 0.042383875 | 0.014169622 | 2.991178948 | 0.002779026 |
| FlagBRA-PAN:Lat | 0.10754366 | 0.022646794 | 4.748736541 | 2.04691E-06 |
| FlagBRA-ESP:Lon | 0.021149821 | 0.00344985 | 6.130649423 | 8.75211E-10 |
| FlagBRA-HND:Lon | -0.017366765 | 0.005839024 | -2.974258402 | 0.002936976 |
| FlagBRA-MAR:Lon | -0.063242183 | 0.011487827 | -5.505147778 | 3.68859E-08 |
| FlagBRA-PAN:Lon | 0.12570051 | 0.020474499 | 6.139369279 | 8.28498E-10 |
| Month2:HPB | -0.10096349 | 0.030358 | -3.325762272 | 0.000881771 |
| Month3:HPB | -0.140328436 | 0.030209398 | -4.645191435 | 3.39761E-06 |
| Month4:HPB | -0.124510101 | 0.032958564 | -3.777776869 | 0.000158235 |
| Month5:HPB | -0.084885119 | 0.029568782 | -2.870768224 | 0.004094756 |
| Month6:HPB | -0.063531665 | 0.032420662 | -1.959604217 | 0.050042068 |
| Month7:HPB | -0.149816649 | 0.029877376 | -5.014384464 | 5.32035E-07 |
| Month8:HPB | -0.120414627 | 0.030141588 | -3.994966269 | 6.47035E-05 |
| Month9:HPB | -0.046179475 | 0.033363819 | -1.38411837 | 0.166322213 |
| Month10:HPB | -0.122481982 | 0.030442365 | -4.023405588 | 5.73626E-05 |
| Month11:HPB | -0.14372426 | 0.03787261 | -3.79493945 | 0.000147679 |
| Month12:HPB | -0.030179635 | 0.033579219 | -0.898759274 | 0.368780897 |
| Month2:Lat | 0.001617121 | 0.00237169 | 0.681843192 | 0.49533811 |
| Month3:Lat | 0.009164189 | 0.002420728 | 3.785716173 | 0.000153267 |
| Month4:Lat | 0.02027389 | 0.002552371 | 7.943160677 | 1.97093E-15 |
| Month5:Lat | 0.029557182 | 0.002401655 | 12.30700372 | 8.30495E-35 |
| Month6:Lat | 0.033561578 | 0.002484169 | 13.51018563 | 1.36178E-41 |
| Month7:Lat | 0.0263521 | 0.002863451 | 9.202917489 | 3.4836E-20 |
| Month8:Lat | 0.015989696 | 0.003607183 | 4.43273707 | 9.30443E-06 |
| Month9:Lat | 0.016125805 | 0.003536717 | 4.559541034 | 5.12655E-06 |
| Month10:Lat | 0.011692977 | 0.003222372 | 3.628686652 | 0.000284867 |
| Month11:Lat | 0.015769566 | 0.003099867 | 5.087174095 | 3.63438E-07 |
| Month12:Lat | 0.003624607 | 0.002879113 | 1.258931616 | 0.208055033 |
| Month2:Lon | 0.003843363 | 0.004392863 | 0.87491064 | 0.381622529 |
| Month3:Lon | -2.07887E-05 | 0.00450867 | -0.004610828 | 0.996321105 |
| Month4:Lon | -0.026751561 | 0.004884795 | -5.476496347 | 4.3383E-08 |
| Month5:Lon | -0.047036294 | 0.004649643 | -10.11610797 | 4.68684E-24 |

| | | | | |
|---|---|---|---|---|
| Month6:Lon | -0.057986764 | 0.00490291 | -11.82700859 | 2.8305E-32 |
| Month7:Lon | -0.05823948 | 0.005338441 | -10.90945424 | 1.03878E-27 |
| Month8:Lon | -0.049626508 | 0.006577446 | -7.544951494 | 4.52456E-14 |
| Month9:Lon | -0.038119034 | 0.006059929 | -6.290343325 | 3.16765E-10 |
| Month10:Lon | -0.043231338 | 0.00528212 | -8.184466526 | 2.73513E-16 |
| Month11:Lon | -0.021785688 | 0.005104361 | -4.268054181 | 1.97185E-05 |
| Month12:Lon | 0.002693238 | 0.004773406 | 0.564217257 | 0.572606285 |
| HPB:Lat | -0.004743768 | 0.000757449 | -6.262822147 | 3.78072E-10 |
| HPB:Lon | 0.007361389 | 0.001187705 | 6.197995149 | 5.71869E-10 |
| Log(theta) | 0.721376104 | 0.014197165 | 50.81127677 | 0 |

Table 8. Analysis of estimated coefficients from the Hurdle with Negative Binomial (HNB) model adjusted for swordfish (SWO) catch. The figure presents parameter estimates, standard errors, test statistics, and p-values for each term included in the model.

| Term | Estimate | Std. Error | z value | Pr(>\|z\|) |
|---|---|---|---|---|
| (Intercept) | -6.216243617 | 0.248037402 | -25.06171878 | 1.301E-138 |
| FlagBRA-ESP | 1.612853299 | 0.165424206 | 9.749802247 | 1.84828E-22 |
| FlagBRA-HND | 0.11168632 | 0.300125956 | 0.372131492 | 0.70979495 |
| FlagBRA-MAR | -1.840155829 | 0.547544406 | -3.360742636 | 0.000777332 |
| FlagBRA-PAN | 1.029907207 | 0.928016446 | 1.109794133 | 0.267087748 |
| Month2 | 0.75844057 | 0.199383318 | 3.803931932 | 0.000142417 |
| Month3 | 0.990726446 | 0.203815606 | 4.860895913 | 1.16856E-06 |
| Month4 | 0.175985314 | 0.237269642 | 0.741710199 | 0.458262939 |
| Month5 | -0.736172303 | 0.221782608 | -3.319341895 | 0.000902299 |
| Month6 | -1.140741834 | 0.245549238 | -4.645674505 | 3.38967E-06 |
| Month7 | -0.909091169 | 0.225617202 | -4.029352205 | 5.59308E-05 |
| Month8 | -0.877652609 | 0.264917535 | -3.312927577 | 0.000923249 |
| Month9 | -0.928512652 | 0.2563876 | -3.62151934 | 0.000292878 |
| Month10 | -0.981905323 | 0.218311746 | -4.497720993 | 6.86858E-06 |
| Month11 | -0.086739792 | 0.255140036 | -0.339969347 | 0.733879612 |
| Month12 | 0.162993918 | 0.219546033 | 0.742413407 | 0.457836899 |
| HPB | 0.346469308 | 0.043777851 | 7.914260329 | 2.48727E-15 |
| Lat | 0.002779762 | 0.004186885 | 0.663921199 | 0.506740747 |
| Lon | -0.016512678 | 0.006991999 | -2.361653504 | 0.018193638 |
| FlagBRA-ESP:Month2 | -0.049952571 | 0.06554758 | -0.762081088 | 0.446011609 |
| FlagBRA-HND:Month2 | 0.177436673 | 0.153644051 | 1.154855477 | 0.248149614 |
| FlagBRA-MAR:Month2 | 0.160986828 | 0.150687612 | 1.068348123 | 0.285363509 |

| | | | | |
|---|---|---|---|---|
| FlagBRA-PAN:Month2 | -0.046034205 | 0.20362285 | -0.226075832 | 0.821142441 |
| FlagBRA-ESP:Month3 | 0.012674147 | 0.068583903 | 0.184797695 | 0.853387716 |
| FlagBRA-HND:Month3 | 0.045728545 | 0.13507009 | 0.338554193 | 0.734945596 |
| FlagBRA-MAR:Month3 | -0.324622321 | 0.155372054 | -2.089322451 | 0.036678707 |
| FlagBRA-PAN:Month3 | 0.521077848 | 0.18184544 | 2.865498563 | 0.004163532 |
| FlagBRA-ESP:Month4 | 0.168327415 | 0.070940169 | 2.372808189 | 0.017653429 |
| FlagBRA-HND:Month4 | 0.222551737 | 0.140184124 | 1.587567342 | 0.112384208 |
| FlagBRA-MAR:Month4 | -0.116558022 | 0.149290907 | -0.78074428 | 0.434952911 |
| FlagBRA-PAN:Month4 | 0.638980137 | 0.180722082 | 3.535705936 | 0.000406687 |
| FlagBRA-ESP:Month5 | 0.181153552 | 0.068667202 | 2.638137945 | 0.008336266 |
| FlagBRA-HND:Month5 | 0.053573823 | 0.138629825 | 0.386452359 | 0.699161679 |
| FlagBRA-MAR:Month5 | -0.285460734 | 0.146138149 | -1.953362183 | 0.050776694 |
| FlagBRA-PAN:Month5 | 0.353790676 | 0.192118229 | 1.841525805 | 0.065544543 |
| FlagBRA-ESP:Month6 | -0.011265417 | 0.070453716 | -0.159898127 | 0.872961324 |
| FlagBRA-HND:Month6 | -0.204463383 | 0.151253159 | -1.351795781 | 0.176440654 |
| FlagBRA-MAR:Month6 | -0.549113152 | 0.150562466 | -3.647078624 | 0.000265239 |
| FlagBRA-PAN:Month6 | 0.418655904 | 0.20486856 | 2.043534181 | 0.040999587 |
| FlagBRA-ESP:Month7 | 0.178600799 | 0.075028143 | 2.380450747 | 0.017291472 |
| FlagBRA-HND:Month7 | -0.140740138 | 0.146112052 | -0.963234285 | 0.335429963 |
| FlagBRA-MAR:Month7 | 0.262924233 | 0.161792404 | 1.625071552 | 0.104147314 |
| FlagBRA-PAN:Month7 | 0.86750669 | 0.212936516 | 4.07401561 | 4.62094E-05 |
| FlagBRA-ESP:Month8 | 0.240071211 | 0.076071393 | 3.155867144 | 0.001600217 |
| FlagBRA-HND:Month8 | 0.28315127 | 0.144450076 | 1.960201603 | 0.049972231 |
| FlagBRA-MAR:Month8 | 0.334255278 | 0.154204461 | 2.167610953 | 0.0301883 |
| FlagBRA-PAN:Month8 | 1.209826131 | 0.237077518 | 5.103082489 | 3.34165E-07 |
| FlagBRA-ESP:Month9 | 0.33495651 | 0.083664951 | 4.003546362 | 6.24E-05 |
| FlagBRA-HND:Month9 | 0.236488432 | 0.143049772 | 1.653189854 | 0.098292231 |
| FlagBRA-MAR:Month9 | 0.577961414 | 0.162509297 | 3.556482141 | 0.000375854 |
| FlagBRA-PAN:Month9 | 0.149707964 | 0.217708937 | 0.687651898 | 0.491672018 |
| FlagBRA-ESP:Month10 | 0.387632606 | 0.08660808 | 4.475709505 | 7.6158E-06 |
| FlagBRA-HND:Month10 | 0.319572332 | 0.149473253 | 2.13799008 | 0.032517548 |
| FlagBRA-MAR:Month10 | 0.310152281 | 0.162868083 | 1.904315899 | 0.056869055 |
| FlagBRA-PAN:Month10 | 1.261669105 | 0.203647554 | 6.195356046 | 5.81534E-10 |
| FlagBRA-ESP:Month11 | 0.144853939 | 0.088509609 | 1.636589981 | 0.101716171 |
| FlagBRA-HND:Month11 | 0.679386729 | 0.163698617 | 4.150228875 | 3.32143E-05 |
| FlagBRA-MAR:Month11 | 0.065826746 | 0.1601489 | 0.411034645 | 0.681047131 |

| | | | | |
|---|---|---|---|---|
| FlagBRA-PAN:Month11 | 1.177359906 | 0.224529117 | 5.243684747 | 1.57401E-07 |
| FlagBRA-ESP:Month12 | 0.154209725 | 0.085266866 | 1.808553916 | 0.070520333 |
| FlagBRA-HND:Month12 | 0.297340096 | 0.152189799 | 1.953745244 | 0.050731353 |
| FlagBRA-MAR:Month12 | 0.248317039 | 0.14485192 | 1.714282 | 0.086476947 |
| FlagBRA-PAN:Month12 | 1.39252873 | 0.237275229 | 5.868833145 | 4.38873E-09 |
| FlagBRA-ESP:HPB | -0.08565806 | 0.022494754 | -3.807912772 | 0.000140145 |
| FlagBRA-HND:HPB | -0.105916881 | 0.045946009 | -2.305246575 | 0.021152768 |
| FlagBRA-MAR:HPB | -0.002700636 | 0.059918411 | -0.045071895 | 0.964050003 |
| FlagBRA-PAN:HPB | 0.486441635 | 0.082714018 | 5.881005979 | 4.0778E-09 |
| FlagBRA-ESP:Lat | -0.00269959 | 0.001664732 | -1.621636669 | 0.104881166 |
| FlagBRA-HND:Lat | 0.025277433 | 0.003339155 | 7.570009805 | 3.73196E-14 |
| FlagBRA-MAR:Lat | 0.042383875 | 0.014169622 | 2.991178948 | 0.002779026 |
| FlagBRA-PAN:Lat | 0.10754366 | 0.022646794 | 4.748736541 | 2.04691E-06 |
| FlagBRA-ESP:Lon | 0.021149821 | 0.00344985 | 6.130649423 | 8.75211E-10 |
| FlagBRA-HND:Lon | -0.017366765 | 0.005839024 | -2.974258402 | 0.002936976 |
| FlagBRA-MAR:Lon | -0.063242183 | 0.011487827 | -5.505147778 | 3.68859E-08 |
| FlagBRA-PAN:Lon | 0.12570051 | 0.020474499 | 6.139369279 | 8.28498E-10 |
| Month2:HPB | -0.10096349 | 0.030358 | -3.325762272 | 0.000881771 |
| Month3:HPB | -0.140328436 | 0.030209398 | -4.645191435 | 3.39761E-06 |
| Month4:HPB | -0.124510101 | 0.032958564 | -3.777776869 | 0.000158235 |
| Month5:HPB | -0.084885119 | 0.029568782 | -2.870768224 | 0.004094756 |
| Month6:HPB | -0.063531665 | 0.032420662 | -1.959604217 | 0.050042068 |
| Month7:HPB | -0.149816649 | 0.029877376 | -5.014384464 | 5.32035E-07 |
| Month8:HPB | -0.120414627 | 0.030141588 | -3.994966269 | 6.47035E-05 |
| Month9:HPB | -0.046179475 | 0.033363819 | -1.38411837 | 0.166322213 |
| Month10:HPB | -0.122481982 | 0.030442365 | -4.023405588 | 5.73626E-05 |
| Month11:HPB | -0.14372426 | 0.03787261 | -3.79493945 | 0.000147679 |
| Month12:HPB | -0.030179635 | 0.033579219 | -0.898759274 | 0.368780897 |
| Month2:Lat | 0.001617121 | 0.00237169 | 0.681843192 | 0.49533811 |
| Month3:Lat | 0.009164189 | 0.002420728 | 3.785716173 | 0.000153267 |
| Month4:Lat | 0.02027389 | 0.002552371 | 7.943160677 | 1.97093E-15 |
| Month5:Lat | 0.029557182 | 0.002401655 | 12.30700372 | 8.30495E-35 |
| Month6:Lat | 0.033561578 | 0.002484169 | 13.51018563 | 1.36178E-41 |
| Month7:Lat | 0.0263521 | 0.002863451 | 9.202917489 | 3.4836E-20 |
| Month8:Lat | 0.015989696 | 0.003607183 | 4.43273707 | 9.30443E-06 |
| Month9:Lat | 0.016125805 | 0.003536717 | 4.559541034 | 5.12655E-06 |

| | | | | |
|---|---|---|---|---|
| Month10:Lat | 0.011692977 | 0.003222372 | 3.628686652 | 0.000284867 |
| Month11:Lat | 0.015769566 | 0.003099867 | 5.087174095 | 3.63438E-07 |
| Month12:Lat | 0.003624607 | 0.002879113 | 1.258931616 | 0.208055033 |
| Month2:Lon | 0.003843363 | 0.004392863 | 0.87491064 | 0.381622529 |
| Month3:Lon | -2.07887E-05 | 0.00450867 | -0.004610828 | 0.996321105 |
| Month4:Lon | -0.026751561 | 0.004884795 | -5.476496347 | 4.3383E-08 |
| Month5:Lon | -0.047036294 | 0.004649643 | -10.11610797 | 4.68684E-24 |
| Month6:Lon | -0.057986764 | 0.00490291 | -11.82700859 | 2.8305E-32 |
| Month7:Lon | -0.05823948 | 0.005338441 | -10.90945424 | 1.03878E-27 |
| Month8:Lon | -0.049626508 | 0.006577446 | -7.544951494 | 4.52456E-14 |
| Month9:Lon | -0.038119034 | 0.006059929 | -6.290343325 | 3.16765E-10 |
| Month10:Lon | -0.043231338 | 0.00528212 | -8.184466526 | 2.73513E-16 |
| Month11:Lon | -0.021785688 | 0.005104361 | -4.268054181 | 1.97185E-05 |
| Month12:Lon | 0.002693238 | 0.004773406 | 0.564217257 | 0.572606285 |
| HPB:Lat | -0.004743768 | 0.000757449 | -6.262822147 | 3.78072E-10 |
| HPB:Lon | 0.007361389 | 0.001187705 | 6.197995149 | 5.71869E-10 |
| Log(theta) | 0.721376104 | 0.014197165 | 50.81127677 | 0 |

***Comparison of Relative Abundance Index***

The table 9 presents a comparison between the official 2022 CPUE, the official 2017 CPUE, and the proposed indices for swordfish (Xiphias gladius) in the South Atlantic, covering the period from 1994 to 2020.

Table 9. Comparison of CPUE time series for swordfish (*Xiphias gladius*) in the South Atlantic. The official 2022 CPUE, the official 2017 CPUE, and the proposed indices for the period from 2005 to 2017 are presented.

| **Year** | **CPUE official 2022** | **CPUE official 2017** | **Índices proposto** |
|---|---|---|---|
| 1994 | 1.052 | | |
| 1995 | 1.436 | | |
| 1996 | 1.581 | | |
| 1997 | 1.492 | | |
| 1998 | 1.261 | | |
| 1999 | 1.056 | | |
| 2000 | 0.948 | | |
| 2001 | 0.884 | | |
| 2002 | 0.901 | | |

| | | | |
|---|---|---|---|
| 2003 | 1.042 | | |
| 2004 | 0.842 | | |
| 2005 | 0.858 | 0.82 | 1.03989135822954 |
| 2006 | 0.98 | 1.01 | 1.12468795858844 |
| 2007 | 1.205 | 1.21 | 1.02985235084254 |
| 2008 | 1.097 | 0.98 | 1.17114485213001 |
| 2009 | 1.08 | 1.09 | 1.08466643890384 |
| 2010 | 1.06 | 1.11 | 1.26656597339895 |
| 2011 | 1.038 | 0.84 | 1.22791768513029 |
| 2012 | 0.991 | 0.95 | 1.01477845464695 |
| 2013 | 0.871 | | 0.796529607653123 |
| 2014 | 0.953 | | 0.822876485381297 |
| 2015 | 1.12 | | 0.758448019109625 |
| 2016 | 0.993 | | 0.823645829051002 |
| 2017 | 0.793 | | 0.838994986934385 |
| 2018 | 0.877 | | |
| 2019 | 0.684 | | |
| 2020 | 0.628 | | |